Final Master's Project
Master's Degree in Industrial Engineering

Intervención en avenida de Cruz Roja: Impacto de estrategias de “Outdoor Comfort” y mitigación de UHI

Autor: Valentine Lopez

Tutor: Servando Álvarez Domínguez

Departamento de Ingeniería Energética
Escuela Técnica Superior de Ingeniería
Universidad de Sevilla

Sevilla, 2023

Final Master's Project
Master's Degree in Industrial Engineering

Intervención en avenida de Cruz Roja: Impacto de estrategias de “Outdoor Comfort” y mitigación de UHI

Autor:
Valentine Lopez

Tutor:
Servando Álvarez Domínguez

Departamento de Ingeniería Energética
Escuela Técnica Superior de Ingeniería
Universidad de Sevilla

Sevilla, 2023

Acknowledgment

First of all, I would like to thank my tutor, Servando Álvarez Domínguez, for his attentive supervision and invaluable help, which he could sometimes provide it in French. To Teresa Rocío Palomo Amore and José Sánchez Ramos, for their dedication. To Maria de la Paz, for her boundless patience, the time she devoted to this project, and her answers to my repeated doubts.

Thank you to my parents, who have supported me unfailingly and unconditionally from the start, as well as during the final stage of my studies.

Thank you to my grandparents, with whom I spent the last few days of the redaction.

Thanks to Malo, who, despite the difficult times, supports me whatever the cost.

Thank you to my friends who travelled kilometres to visit me in Spain, and those I met in Seville, who always gave me the energy I needed to move forward with this project.

Thanks to my 11 girl roommates in Seville, now my friends, who have put up with my mood swings, between the stress of university and the moments of joy I've shared with them.

Valentine Lopez

Sevilla, 2023

Resumen

Además del efecto del cambio climático, la isla de calor urbana (UHI, Urban Heat Island en inglés) tiene un impacto significativo en el confort exterior de las ciudades. Este fenómeno se caracteriza por un aumento significativo de la temperatura del aire en el centro de la ciudad en comparación con las afueras, tanto de día como de noche. Está estrechamente relacionado con las condiciones climáticas, la actividad humana, la urbanización y el diseño urbano. Así, la modificación del espacio público podría mejorar el uso y el confort de los espacios exteriores.

En esta tesis de fin de máster, el objetivo es observar los efectos de estos cambios en la forma urbana sobre el UHI, así como las consecuencias para el confort de los ciudadanos. El estudio se centrará en la avenida de la Cruz Roja, en el marco de un proyecto cofinanciado por la Unión Europea. En esta avenida se han realizado obras de rehabilitación para reducir los efectos de la isla de calor.

La tesis se estructura en tres partes diferenciadas: una introducción y el desarrollo del modelo de confort humano, que se utilizará para evaluar el confort del individuo con las condiciones externas. A continuación, se introduce un primer estudio de sensibilidad térmica general, para analizar de la mejor manera posible, en la última sección, el confort térmico y los efectos UHI en la Avenida de la Cruz Roja, antes y después de las obras de rehabilitación.

Para la realización de esta tesis se ha utilizado CartujaQanat, un software del grupo de termotecnia de la Universidad de Sevilla. En concreto, ha sido a través de ENERKEA, el motor de cálculo, como se ha podido introducir la geometría del problema, así como los datos climáticos de Sevilla, obteniendo de esta forma datos climáticos y físicos para la geometría dada.

Abstract

In addition to climate change effect, the Urban Heat Island (UHI) has a significant impact on outdoor comfort in cities. This phenomenon is characterised by a significant rise in air temperatures in the city centre compared with the suburbs, this applies both during the day and at night. It is strongly connected to climate conditions, human activity, urbanization and urban design. Thus, modifying the public space could improve the use and comfort of outdoor spaces.

In this master's thesis, the aim is to observe the effects of these changes in urban forms on the UHI, as well as the consequences for citizens' comfort. The study will focus on the Avenue de la Cruz Roja as part of a project co-funded by the European Union. In this avenue, rehabilitation works has been carried out to reduce the effects of the heat island.

The thesis is structured in three distinct parts: an introduction and the development of the human comfort model, which will be used to evaluate the individual's comfort with external conditions. Then, an initial, general thermal sensitivity study is introduced, to provide, in the last part, the best possible analysis of thermal comfort and UHI effects in the Avenue de la Cruz Roja, before and after rehabilitation works.

To carry out this thesis, CartujaQanat, a software of the Thermotechnic group of the University of Seville was used. More specifically, it was through ENERKEA, the calculation engine, that it has been possible to introduce the geometry of the problem as well as climate data of Seville, thus obtaining climate and physical data for the given geometry.

Index

Contents

Index of Tables

Index of Figures

Notation

Q	Heat load (W/m²)
T_{ext}	Ambient temperature (°C)
P_{ext}	Ambient pressure (kPa)
%RH	Relative humidity (%)
V	Outside air velocity (m/s)
M	Metabolic rate (W/m²)
met	Metabolic rate according to a person's activity level (met)
I_{clo}	Level of clothing (clo)
α	Clothing absorptivity (dimensionless)
fcl	Increased area due to clothing (dimensionless)
W	Mechanical work (W/m²)
R_{SW}	Solar radiation absorbed on the surface of the body (W/m²)
R_{LW}	Long wavelength radiant exchange with surrounding surfaces (W/m²)
C	Convective exchange (W/m²)
q_{res}	Respiratory sensible heat losses (W/m²)
E_{sk}	Heat losses by sweating and diffusion of water vapor through skin (W/m²)
E_{dif}	Natural diffusion of water through the skin (W/m²)
E_{rsw}	Thermoregulatory control mechanism (W/m²)
q_{sk}	Total rate of heat loss from skin (W/m²)
R	Radiative heat loss (W/m²)
S	Body heat storage rate (W/m²)
A_D	Dubois surface area (m²)
m	Mass (kg)
l	Height (m)
A_{cl}	Area of the clothed body (m²)
R_{cl}	Thermal resistance of the clothing (m²K/W)

T_{MR}	Mean radiant temperature (°C)
α	Albedo (dimensionless)
R_D	Total direct radiation (W/m²)
R_d	Diffuse radiation (W/m²)
R_r	Reflected radiation (W/m²)
U	Radiation heating efficiency (dimensionless)
I_a	Insulation of the air layer
h_r	Radiative heat transfer coefficient (W/m²K)
ε	Skin emissivity (dimensionless)
T_{sk}	Skin temperature (°C)
T_{cl}	Temperature of the clothing (°C)
h_c	Convective transfer coefficient (W/m²K)
T_a	Air temperature (°C)
P_a	Water vapor pressure of air (kpa)
$P_{a,sat}$	Saturation vapor pressure of water (kpa)
$T_{s,i}$	Superficial temperature of the cell i (°C)
$\dot{m}$	Mass flow (kg/s)
ρ_{aire}	Air density (kg/m^3)
$ACHd$	Dimensionless flow rate
A_{street}	Total street area (m²)
$Q_{anthropogenic}$	Anthropogenic generation (W/m²)
u	Air velocity near the outside surface (m/s)
Q_{h}	Metabolic heat produced by the presence of humans (W/m²)
$\mathrm{Q_b}$	Heat emitted by air-conditioning systems in buildings (W/m²)
$\mathrm{Q_t}$	Heat generated by traffic (W)
E_{factor}	Heat emission factor (J/m)
N_{lanes}	Average number of lanes
T_{min}	Minimum air temperature (°C)
T_{max}	Maximum air temperature (°C)
NDI	Normal Direct Intensity (W/m²)

BI	Brightness index
dHI	Diffuse Horizontal Irradiance (W/m²)
DHI	Direct Horizontal Irradiance (W/m²)
THI	Total Horizontal Irradiance (W/m²)
A	Extra-terrestrial radiation (W/m²)
B	Extinction coefficient (dimensionless)
C	Diffuse sky factor (dimensionless)
β	Solar height
w	Humidity level (g/kg)

1 INTRODUCTION

1.1 The growing necessity of studying comfort

Habitability today is accompanied by a challenge affecting the well-being and quality of life of its inhabitants: the climate change. The frequency and intensity of heatwaves are constantly escalating, increasing surface air temperatures on Earth. In summer 2022, Europe reached its hottest record in temperature, due to the severe heat waves. This summer, more than 61,000 people died from heat-related illness in the continent. Scientifics warn that this numbers could continue to increase, up to 120 000 in 2050. Governments are trying to implement efforts to limit consequences of prolonged heat waves such as warning systems or creating urban planning strategies [1].

In addition to this, there is a local phenomenon in cities: the Urban Heat Island (UHI). This is characterised by a significant rise in air temperatures in the city centre compared with the suburbs. UHI result from the accumulation of controllable and not controllable factors. The last one is about climate factors such as exposure, air speed or cloud cover. The controllable factors are linked to human activity and urban design due to urbanization. The density and proximity of buildings disrupt air circulation and limits natural ventilation. However, a high-rise building provides more shade and less sunlight for example. Adding to this morphological factor, buildings materials play a key role. They are characterized by the albedo, which is a percentage indicating the capacity of a surface to reflect incident sunlight. The closer this value is to 0, the easier it is for the material to absorb heat. This is the case for stone, brick, or concrete. This adsorbed heat is stored and then re-emitted into the surrounding air during the night, resulting in a high temperature difference between urban and rural areas. Buildings and pavements are also impermeable surfaces, meaning materials that do not absorb rainwater. It therefore runs off and evaporates quickly, reducing the evapo-transpiration and the capacity of rainwater to cool the atmosphere. Moreover, anthropogenic heat is a critical variable in the heat island effect. It includes heat produced by the presence of humans, heat emitted by air-conditioning systems in buildings, and heat generated by traffic. Finally, the lack of vegetation in public spaces contributes to the UHI since vegetations absorb solar radiation, provide shade, and participate in the evapo-transpiration.

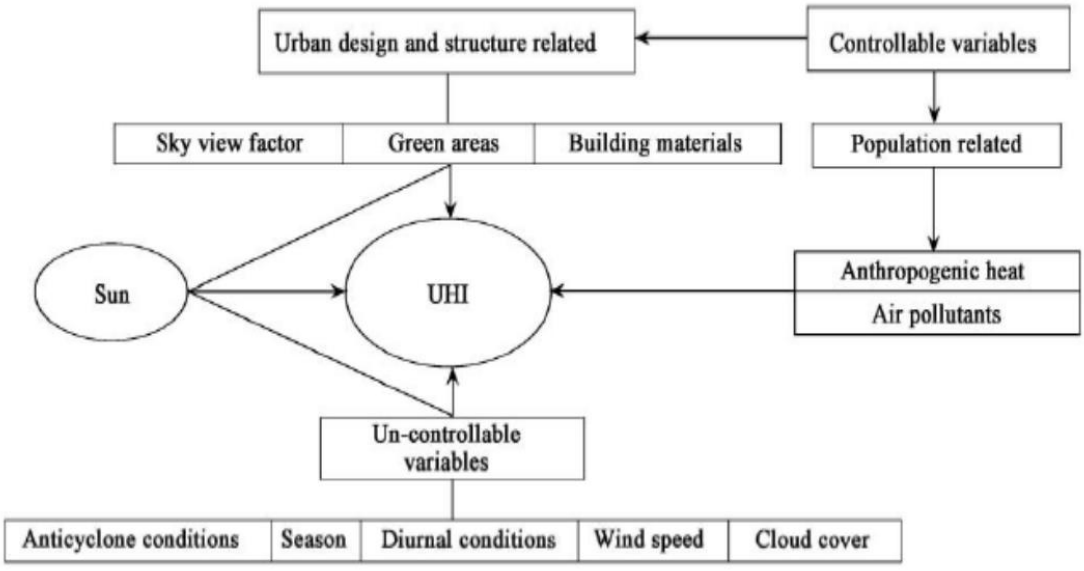

Figure 1 - Generation of Urban Heat Island (UHI) [2]

Urban heat islands are particularly severe during heatwaves. Moreover, waves of poor air quality often occur at the same time as heat problems. The simultaneous presence of a high-intensity UHI and a pollution peak and can lead to public health issues. These phenomena are particularly devastating on people having outdoor physical activities such as physical labour or sport training. UHI cause thermal ailments such as heat exhaustion and muscle cramps. Moreover, when the body is subjected to prolonged extreme temperature conditions, it is unable to regulate its internal temperature. This might lead to heat stroke, potentially lethal if not treated quickly enough [2].

Modifying the public space could improve the use and comfort of outdoor space. There are several solutions to combat UHI. It is possible to modify the urban form to build large breathing spaces and create wind corridors. Then, decreasing impermeable surfaces is mainly achieved through presence of water and vegetation, which also has climate advantages. The use of reflective materials also is promoted. It means increasing the albedo value of buildings and pavement, in order to decrease the heat absorption.

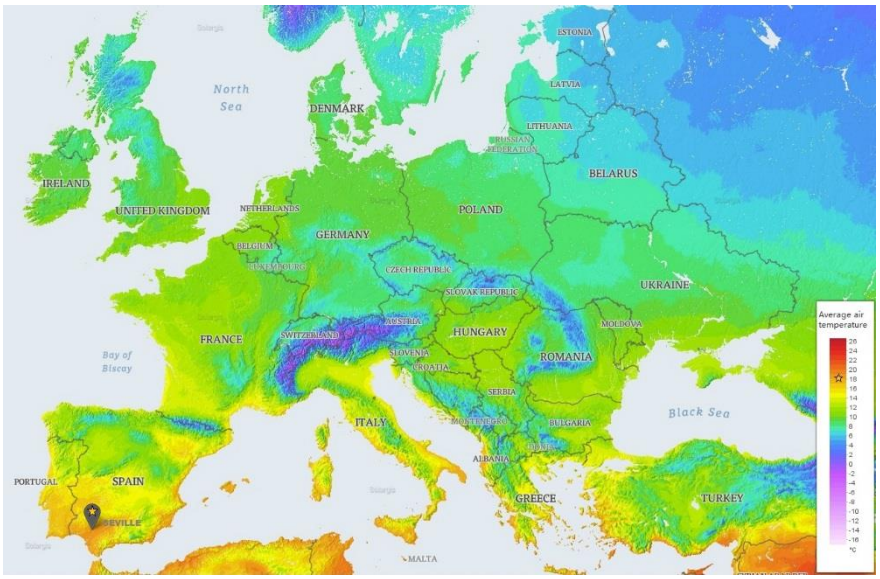

Figure 2 - Location of Seville and average air temperatures in Europe [3].

These phenomena are even more true in Seville where the city faces unique climate conditions with torrid summer temperatures, and long periods of intense heat, reaching over 40 degrees Celsius. Seville is the city that tops the charts in all continental Europe (see *Figure 2*).

To improve thermal comfort, rehabilitation works have been completed and are still in progress, such as the installation of coverings, shadows, and trees. This is the case of the Avenue de la Cruz Roja which is the focus of the study.

1.2 Objective

The Master's thesis initiative is connected to a project called Life Watercool, co-funded by the European Union. This collaborative effort involves entities such as Seville City Council, the Seville Metropolitan Water and Sewerage Company (Emasesa), and the engineering school ETSI of the University of Seville. The project's objective is promoting climate adaptation and water conservation throughout Sevilla, as a response to the climate change. A key aspect of the project involves the redevelopment of the Avenue de la Cruz Roja, which will not only benefit the immediate area but also adjacent streets.

This master's thesis is a continuation of a master's thesis written two years ago by the Energy Engineering Department at the ETSI (University of Seville) [4]. The focus of this study was to conduct a comprehensive climate analysis of the actual outdoor space under consideration. It highlights the necessity of having a reliable comfort algorithm to inform decision-making during the design phase of open space conditioning systems.

Considering the models developed in the previous study, the aim of this present master thesis is to study the impact of mitigation strategies on outdoor comfort, particularly in the Avenue de la Cruz Roka.

1.3 Plan

First, the definitions essential to the overall understanding of the study will be developed (**Chapter 2 – Definitions and background**). This introduces the study of thermal comfort outdoors, which is covered in **Chapter 3**. The study of the equilibrium equation is detailed there, with all the details of its terms.

Before discussing thermal comfort in the avenue de la Cruz Roja, it is important to carry out general heat load calculations, called sensitivity study. This will show the factors influencing the heat load experienced by the occupant (**Chapter 4**).

Then, a study will be carried out using actual geometric data of the avenue de la Cruz Roja (**Chapter 5).**

The **Conclusion** is developed in a final section.

2 DEFINITIONS AND BACKGROUND

2.1 Outdoor thermal comfort

Outdoor thermal comfort is a cognitive process that depends on many factors such as air temperature, humidity, wind speed and personal factors such as physical, physiological, and psychological. (ASHRAE Fundamental 2017. SI Edition [5]). It is therefore a subjective experience, varying between individuals, experiences and cultures. Some people will prefer cooler or warmer environments depending on their personal comfort preferences.

However, it is not an aberration to say that people feel comfortable when body temperatures are kept within a narrow range, skin humidity levels are low and the physiological effort required for thermoregulation is minimised (ASHRAE, 2017 [5]).

The human body needs to maintain an internal temperature of around 37ºC to ensure correct functioning. To do this, it manages heat gains and losses due to metabolism and the external environment. These heat exchanges are described by the heat balance equation, which describes the heat exchanges between the human body and its environment.

This balance is based on a single-node comfort model: the human body is considered to be at a single temperature, that of the skin. The *Figure 3* shows the heat flows involved in the interaction of the human body with its environment.

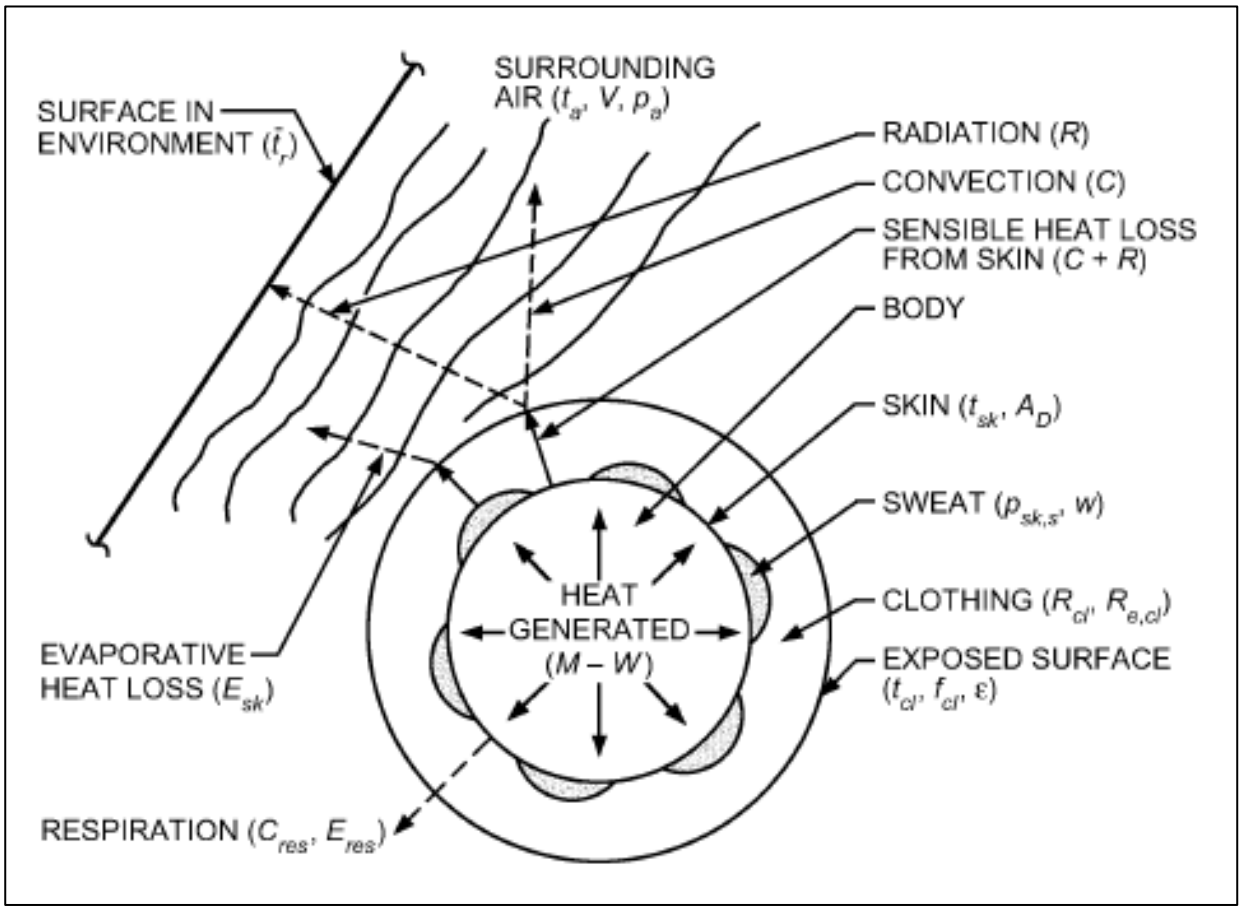

Figure 3 - Human interaction with the environment. (ASHRAE Handbook – Fundamentals (SI)) [5]

2.2 Thermal comfort models and indices

Comfort models are used to predict the comfort that a person develops under certain climate conditions, by studying the body response or thermal sensations produced. This will be reflected in certain variables, called comfort indices, which will help to determine whether an individual is suffering thermal stress or not.

Although most studies on thermal comfort consider only indoor situations, significant research have been carried out on the outdoors. The biggest difference between the indoor and outdoor environments lies in average radiant temperature and wind speed, that must be considered for outdoor comfort studies. Each index has its own scale where energy is expressed in a thermal sensation scale.

2.2.1 Heat load (Q)

This comfort index is defined as the heat that must be extracted or supplied to the body to be in comfort. It is the difference between internal heat production and heat losses through the mechanisms discussed in this document, for a person who is hypothetically in comfort. It means the following hypothesis:

- A skin temperature within acceptable values
- A comfortable core body temperature
- The sweating within acceptable values
- An energy budget close to zero

Brown and Gillespie (1986) developed the COMFA model that calculates the heat load [6]. An improvement of this model has been made considering other parameters, among them: gender, age, weight, activity intensity, clothing insulation, vapour resistance, air temperature, radiation temperature, relative humidity, wind speed, metabolic rate.

2.2.2 Heat stress index (HSI)

The heat stress index is a parameter that evaluates the necessary amount of sweat that a person must secrete to maintain a thermal balance and cooling efficiency of the human body (Urban Climate 18, 2016 [7]). It was defined by Givoni (1963) and later adopted by Pearlmutter. Its formula does not depend on the energy balance formula but on the evaporative heat loss needed to sustain thermal equilibrium in the body, and the maximum evaporative capacity. It is calculated with typical human characteristics, clothings, and the following conditions:

- A skin temperature of 35°C
- A uniform sweating over the entire body

2.2.3 PET (Physiologycal Equivalent Temperature).

The concept of physiological equivalent temperature was introduced by Höppe and Mayer in 1987. It is an outside air temperature at which the heat balance of the human body is maintained. It is defined as "the air temperature at which, in a typical indoor setting (without wind and solar radiation), the energy budget of the human body is balanced with the same core and skin temperature as under the complex outdoor conditions to be assessed" [8].

The energy gain or loss in the actual environment is compared to that of a virtual indoor environment with the following conditions:

- Mean radiant temperature equal to the outside air temperatures
- Outside calm air velocity of 0.1 m/s
- Water vapor pressure equivalent to the air having 50% relative humidity
- Metabolic heat of 80 W, i.e. performing light activity (met 1.5)
- Clothing level of 0.9 clo (office attire)

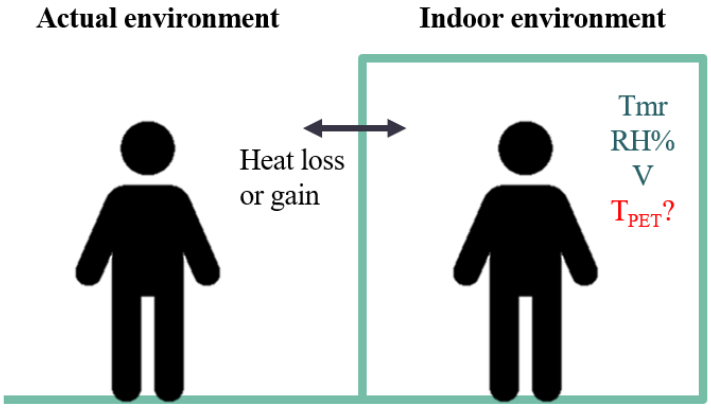

Figure 4 – Schema of PET environment

The great advantage of this comfort index is that it is highly customizable, since it does not refer to specific locations, but can be used in any case, both indoors and outdoors, and has its own rating scale for each and every type of climate. This is why it is one of the most widely used thermal indexes in this field of study.

2.2.4 Comparison heat load and PET.

PET depends on other factors such as psychological and physiological and makes the calculations more difficult than the other indices. The heat load index is more intuitive and easier to implement. This is the reason why the COMFA model will be used in this paper, since it depends on quantitative parameters that are easier to calculate.

3 OUTDOOR THERMAL COMFORT MODEL

As seen in the chapter 2, outdoor thermal comfort and in general thermal comfort are a subjective experience encompassing various factors. Several indices have been developed to predict whether a person, under certain external conditions, is thermally in a comfort zone or not. The majority of these indices are based on the physics of the heat balance equation, describing the thermal exchange between the human body and its environment.

It is thus necessary to develop this model, based on an understanding of climatological information and an understanding of the physiological responses of the human body.

3.1 Input data

The following variables are used as input data for the application of the comfort model:

- The geometry of the studied case.
- Climate conditions, untreated: ambient temperature and pressure, and relative humidity, which will be referred to as T_{ext} and P_{ext} and %RH.
- The radiations: direct over occupant, diffuse from sky over occupant, diffuse from cover over occupant, diffuse reflected from covered ground over occupant, diffuse reflected from adjacent ground over occupant.
- Temperatures of the elements that make up the surroundings, to evaluate the influence of these surfaces on the above climate conditions. As an example, the heating of surfaces such as soil or coverings would increase the temperature of the surroundings.
- Outside air velocity (V). It is expressed in m/s and affects the calculation of convective heat loss.
- Metabolic rate (M), more specifically the evaluation of the metabolic rate depending on the activity being performed. It will be possible to evaluate the metabolic heat that this activity would generate, in the met unity.
- Level of clothing (I_{clo}). The higher the level of clothing, the greater the resistance to heat conduction through the clothing, depending on whether it is beneficial or not.
- Clothing absorptivity (α).
- Increased area due to clothing (fcl).

3.2 Hypotheses

Initial hypotheses

a) The heat storage rate, both in the core and in the skin will be considered null.

b) The energy balance discussed above is understood as a single-node comfort model by considering that the human body is at a single temperature, this being the skin temperature. However, there are other comfort models, such as the two-node model of Pierce (1970), and later the double-node model of KSU developed by the University of Kansas, in which the human body is conceived as two isothermal compartments: the nucleus (or core) where metabolic heat is generated, and the skin. This model, by differentiating two zones, would

require two energy balances, which exchange heat between them by passive conduction from the core to the skin, varying as a function of blood flow. In this case, the present paper will develop the single-node comfort model, the use of which becomes more academic as it is characterized by greater simplicity.

c) In this part only, a general case with a squared geometry with a coverage is studied. Thus, it is possible to identify 3 zones: the coverage; the covered ground, which is the ground under the coverage; the adjacent ground, which is the whole ground except the covered ground.

3.3 Energy balance

3.3.1 Metabolic rate

The metabolic rate measures the energy expenditure that a person experiences when performing a task. Most of this energy is converted into heat (M), while the remainder is used to perform work (W). The metabolic rate depends on the type of activity being performed. As shown in *Table 1*, the difference between the estimated values for a light activity such as "Standing relaxed" and a more intense physical activity such as "Walking 6.4 km/h" is quite remarkable. The harder the work, the greater the metabolic heat and the more effort the body will have to make to maintain a constant body temperature.

The unit used to express the metabolic rate is the **met** (*metabolic equivalent of task*), and one unit is defined as the metabolic rate of a sedentary person, equivalent to 58.1 W/m² [5]. Its value can be calculated in a more exact way, since the equivalence mentioned is based on a body of height 1.73 m and weight of 70 kg, male gender.

$$M = 58{,}1 * met\ [W/m^2] \quad (1)$$

Activity	W/m2	met
Resting		
Sleeping	40	0,7
Laying down	45	0,8
Sitting	60	1,0
Standing, relaxed	70	1,2
Walking		
3,2 km/h	115	2,0
4,3 km/h	150	2,6
6,4 km/h	220	3,8
Office activity		
Reading, sitting	55	0,9
Writing	60	1,0
Typing	65	1,1
Presenting, standing	80	1,4
Elevando/Embalando	120	2,1

Table 1 - Heat generated in each physical activity [5]

3.3.2 Energy balance

The energy balance says that the net heat production $M - W$ must be dissipated by other heat transfer mechanisms through the skin surface (q_{sk}) and respiratory tract (q_{res}), considering there are surplus or deficit stored (S). These mechanisms are:

- Solar radiation absorbed on the surface of the body (direct, diffuse and reflected by other surfaces) (R_{SW})
- Long wavelength radiant exchange with surrounding surfaces (R_{LW})
- Convective exchange between the body surface and the ambient air (C)
- Respiratory sensible heat losses (q_{res})
- Heat losses by sweating and by diffusion of water vapor through the skin (E_{sk})

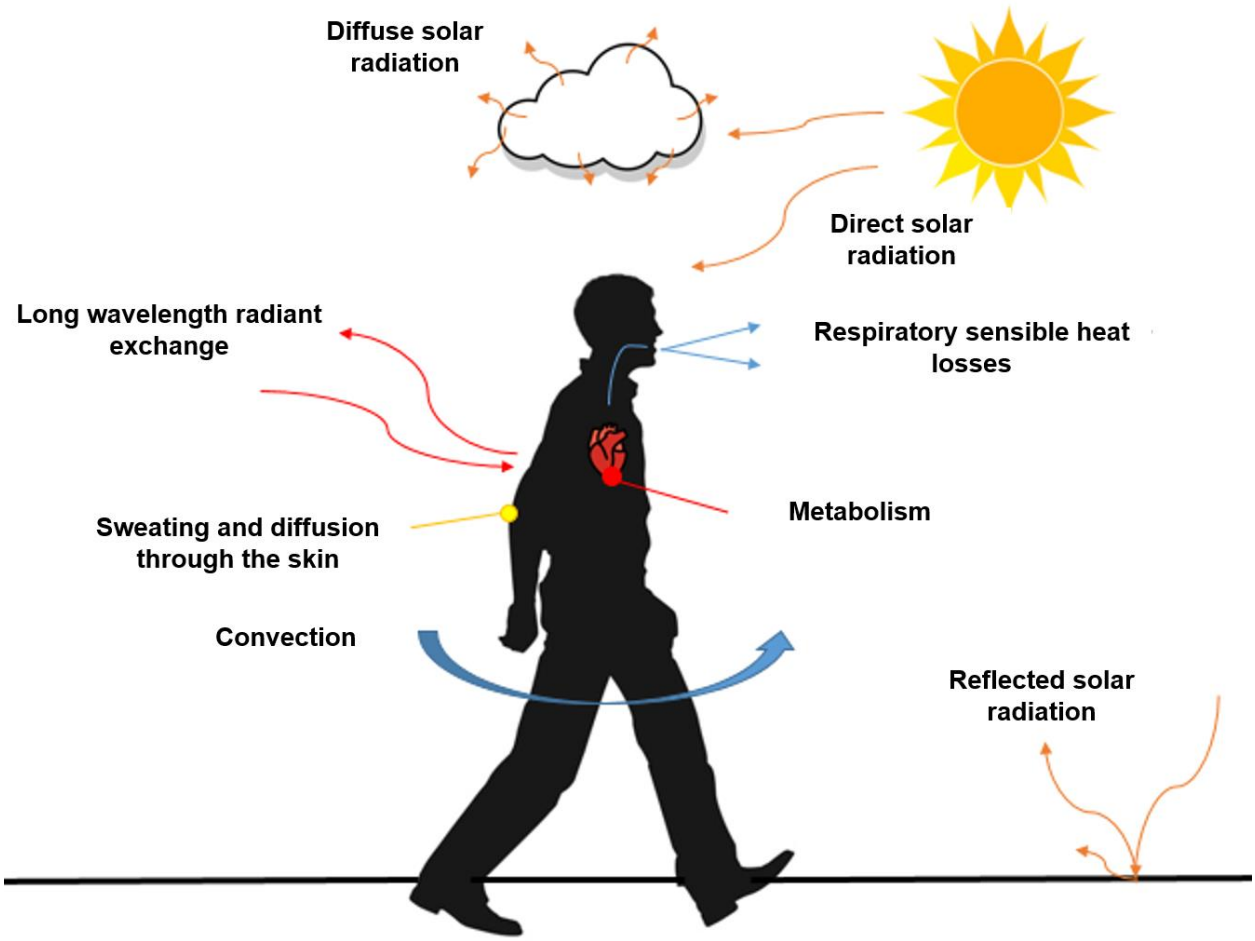

Figure 5 - Representation of heat exchange flows

The energy balance is written:

$$M - W = q_{sk} + q_{res} + S = (C + R + E_{sk}) + (C_{res} + E_{res}) + (S_k + S_{cr}) \quad (2)$$

Where:

- q_{sk} is the total rate of heat loss from skin. It is the sum of the convective heat loss C, the radiative heat loss R, and the evaporative heat loss E_{sk}.

- The radiative heat loss R is the sum of short and long wavelengths.

$$R = R_{SW} + R_{LW}\ [W/m^2] \quad (3)$$

  Where R_{SW} is the shortwave radiation and R_{LW} the longwave radiation.

- q_{res} is the total rate of heat loss through respiration. It is the sum of the sensible (C_{res}) and latent (E_{res}) loses from respiration.

- In most activities, values close to 0 can be taken for mechanical efficiency (μ), since the mechanical work W is quite small compared to the metabolic rate.

$$\mu = \frac{W}{M} \sim 0 \quad (X) \quad \rightarrow \quad W \sim 0\ W/m2 \quad (4)$$

- S represents the body heat storage rate, which is the variation of the heat content in the body when there is a disequilibrium, differentiating between the amount stored in the skin and in the core. However, as mentioned at the beginning, a single node model that does not store heat will be developed, so the storage term will be neglected.

3.3.3 Type of radiation

As explained in 3.3.2, objects and humans can be affected by two types of solar radiation:

- **Shortwave radiation** is radiation received directly or indirectly from the sun.
- **Longwave radiation**, also known as terrestrial radiation. Contrary to shortwave radiation, this is emitted by the earth, objects and substances that have previously absorbed shortwave radiation.

The term R is therefore the sum of these two radiations (equation (3)).

3.3.3.1 Short wavelength radiation R_{SW}

The term R_{SW} is itself the sum of different radiations. Of all the radiations a person receives, some is absorbed, some is reflected, and some is transmitted directly to the skin.

Direct radiation reaches our bodies directly without any significant scattering or reflection. This is the case when we are exposed to direct sunlight without any obstacles.

Diffuse radiation propagates in different directions after interacting with particles in the atmosphere or other objects. For example, when sunlight reaches the Earth's atmosphere, it is scattered in different directions by air molecules, creating a general luminosity in the sky.

Radiation reflected rebounds on reflective surfaces, depending on the optical properties of that surface. For example, incident light can be reflected off the roofs or facades of buildings.

In the case of a general geometry, there are 5 different short wavelength radiation:

- Direct on occupant
- Diffuse from the sky over the occupant
- Diffuse from cover over occupant
- Reflected from ground cover on occupant
- Reflected from adjacent ground onto occupant

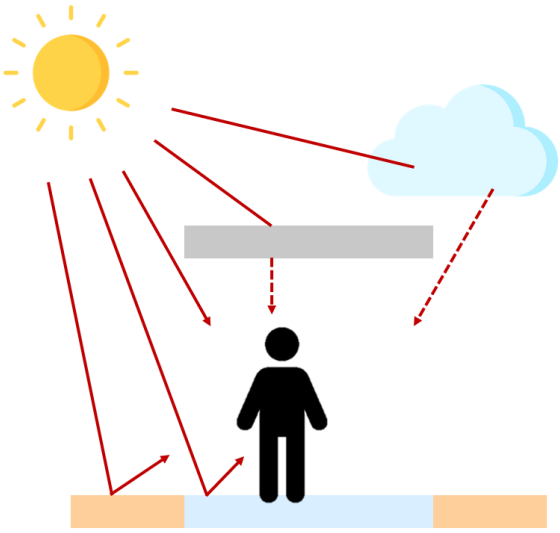

Figure 6 – Short wavelength radiations

3.3.3.2 Longwave radiation R_{LW}

The longwave radiative heat R_{LW} is exchanged between the human body and its environment. When we are outside, our body not only receives short waves from the sun, but also exchanges long waves with surrounding surfaces and the sky.

During the day, if the surrounding surfaces are warmer than our body temperature, they emit long waves that can be absorbed by our bodies, contributing to a feeling of heat or discomfort, particularly in hot climates or on sunny days.

In the case of initial geometry, there are 5 different long wavelength radiations:

- From the sky over the occupant
- From cover over occupant
- From ground cover on occupant
- From adjacent ground onto occupant
- From imaginary closed superficies. Indeed, it is necessary to define the geometry of the enclosure where the occupant is. However, geometries are not always closed. The occupant is not only surrounded by physical surfaces such as cover, ground, trees or buildings. There are also not physical surfaces, called imaginary superficies that help to close the enclosure, for the calculations. They are superficies that face the sky or the walls.

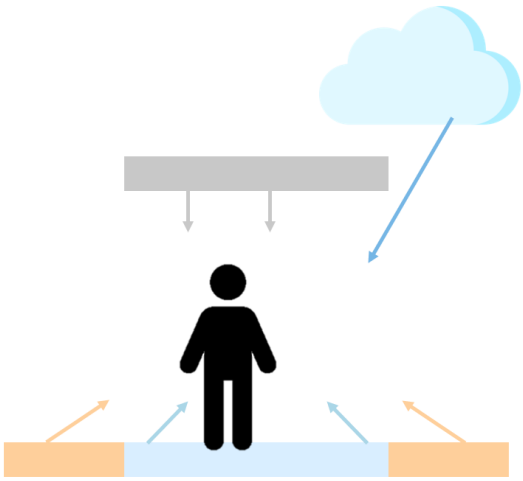

Figure 7 – Long wavelength radiations (physical surfaces)

3.4 Useful parameters and variables

3.4.1 Body surface area

Each term of the energy balance equation is in W/m². It has been necessary to define which area is considered. The used surface is the nude body surface calculated by Dubois and Dubois (1916), knowing height and weight:

$$A_D = 0{,}007184 m^{0{,}425} l^{0{,}725} \; [m^2] \qquad (5)$$

Where:

- A_D is DuBois surface area (m²)
- m the mass (kg)
- l the height (m)

Since the surface of human body is covered by a certain percentage of clothes, a **correction factor fcl** is introduced. It represents the ratio of the area of clothing covering the body to the area of skin.

This correction factor is equal to the ratio A_{cl}/A_D where A_{cl} is the area of the clothed body.

3.4.2 The level of clothing I_{clo} and clothing resistance R_{cl}

The factor fcl is not enough to describe how clothed humans are, hence the need to introduce the **level of clothing (I_{clo})**. When the level of clothing increases, the resistance to heat conduction through the clothing also increases. Values of I_{clo} close to zero correspond to a naked person. The more someone wears clothes are wearing, the higher the value of this parameter (*Table 2*).

The **thermal resistance of the clothing** (R_{cl}) is a function of this parameter:

$$R_{cl} = 0{,}155 I_{clo} \quad [m^2 K/W] \qquad (6)$$

Description of clothing	Iclo
Shorts, short sleeve shirt	0,36
Pants, short sleeve shirt	0,57
Pants, long sleeve shirt	0,61
Pants, long sleeve shirt + suit jacket	0,96
Long sleeve pajamas, long pants pajamas, 3/4 sleeve robe and slippers.	0,96
Knee-length skirt, short-sleeved shirt, stockings and sandals	0,54
Knee-length skirt, long-sleeved shirt, stockings	0,67
Knee-length skirt, long-sleeved shirt, stockings, long-sleeved sweater	1,1

Table 2 – Iclo for different examples of clothings

3.4.3 Mean radiant temperature T_{MR} and absorbed radiation

The **mean radiant temperature** (T_{MR}) is introduced, to quantify the exchanges of thermal radiations between a human and its surrounding environment. It is defined as an "imaginary" temperature that an enclosure must have so that the same amount of heat can be exchanged by radiation alone as in the initial situation. According to J.Pickup and R. de Dear in their paper [9] (An Outdoor Thermal Comfort Index OUT_SET*, 2019), at a certain point in time, the mean radiant temperature can be used as an outdoor comfort index.

The mean radiant temperature can be considered as the sum of both radiant temperatures: short wavelength and long wavelength. As a first approximation, it is possible to calculate the short wavelength radiation as if it were absorbed solely by the skin, contributing directly to heat gain on the individual.

Thus, the first step is to calculate the total radiation absorbed, which is the sum of direct, diffuse and reflected radiation. To do this, the **albedo** (α) is introduced. It is defined as the percentage of incoming radiation reflected by a surface. The remaining value to unity would be the amount absorbed. Therefore, the amount of direct, diffuse and reflected radiation that is absorbed is multiplied by this factor.

$$R_{D,a} = (1-\alpha)R_D \quad (7)$$

$$R_{d,a} = (1-\alpha)R_d \quad (8)$$

$$R_{r,a} = (1-\alpha)R_r \quad (9)$$

Where R_D, R_d and R_r are respectively the total direct, diffuse and reflected radiation in W/m². Thus, the sum of this absorbed radiations gives the total absorbed radiation R_a, also known as the shortwave absorbed radiation.

$$R_a = (1-\alpha)(R_D + R_d + R_r)\ [W/m^2] \quad (10)$$

The first approximation was calculating radiation as if it were absorbed solely by the skin. However, this gain is reduced by the fact that there is an air chamber between the clothing and the skin, inducing air movement that dissipates some of this heat (*Figure 8*). This phenomenon is represented by a factor called solar **radiation heating efficiency** (*U*).

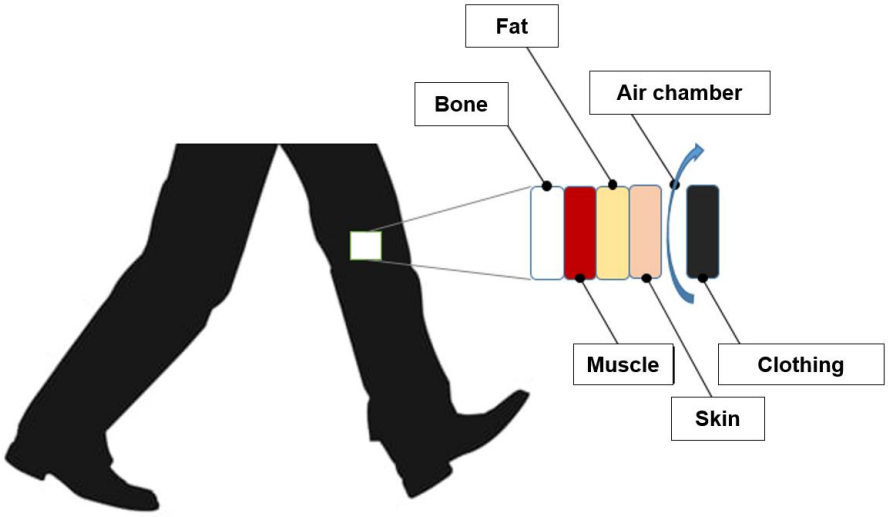

Figure 8 – Representation of the different layers

This efficiency is calculated as a function of the level of clothing (I_{clo}), the increased area due to clothing (f_{cl}) and the **insulation of the air layer** (I_a).

$$U = \frac{I_a}{f_{cl}\left(I_{clo} + \frac{I_a}{f_{cl}}\right)} \tag{11}$$

Tanabe et al [10] determined, by exposing a naked mannequin to air velocities in the range of 0.1 to 1.4 m/s, that the insulation of the air layer decreases by increasing air velocity, as air movement in the chamber between the clothing and the skin partially dissipates heat. The variation of insulation is expressed as:

$$I_a = 0{,}3767 - 0{,}3225 \log(V) \tag{12}$$

Once the radiation heating efficiency (U) is known, the amount of solar radiation absorbed by the skin is known, by multiplying equation (10) by U. This gives the solar radiation, i.e. the shortwave radiation. With a division with the radiative heat transfer coefficient (h_r), the solar radiant temperature is obtained.

$$T_{rsolar} = \frac{(R_D + R_d + R_r)(1-\alpha)U}{h_r}\ [W/m^2] \tag{13}$$

This temperature, added to the radiant temperature characterising the longwave radiations gives the total mean radiant temperature T_{MR}. The longwave radiation temperature is calculated using surface temperatures and form factors. This will be seen in part 5.4.1.

ASHRAE gives an approximation of the linearization of the radiative heat transfer coefficient since skin emissivity (ε) has values close to unity (typically 0.95):

$$h_r = 4{,}7\varepsilon\ [W/m^2K] \tag{14}$$

In this paper, it is supposed that h_r is nearly constant and has the value of 4,7 W/m²K.

3.4.4 Skin temperature

There is a skin temperature T_{sk} that is obtained from empirical formulas, constant and uniform throughout the human body. The average skin temperature can be calculated, as explained in the UNE-EN ISO 7933:2004 standard [11], based on certain parameters that determine the situation in which a person is. For example, it can depend on the level of clothing I_{clo} , the metabolism and some climate parameters such as air temperature or water vapor pressure in air.

This paper does not go into detail about the skin temperature, because in the heat load model, the formula values of T_{sk} and E_{sk} are provided in the situation of thermal comfort (see 3.7).

3.5 Heat transfer with the environment

Now that all the terms necessary for understanding and calculation have been introduced, it's time to detail the terms of the equilibrium equation.

3.5.1 Sensible heat loss

3.5.1.1 Convective heat loss C

Convective exchange is an exchange that occurs between the body and the air surrounding the individual. It is mainly influenced by air temperature and air velocity, in fact, the magnitude of the exchange will increase as the air velocity increases. As shown in equation (15), the heat flow, which depends on the temperature difference, can have both directions, i.e., if the temperature of the clothing (T_{cl}) is higher than that of the air, heat is lost, while if the air temperature is higher, heat is gained.

$$C = f_{cl} h_c (T_{cl} - T_a) \left[\frac{W}{m^2}\right] \tag{15}$$

The convective transfer coefficient h_c can be calculated by various correlations, depending on what activity the individual is doing (*Table 3*). This coefficient is calculated as a function of air velocity.

Equation	Limits	Conditions	Source
$\boldsymbol{h_c = 8,6V^{0,6}}$ $\boldsymbol{h_c = 3,1}$	$0.2 < V < 4.0$ $0 < V < 0.2$	Seated with moving air	Mitchell (1974)
$\boldsymbol{h_c = 5.7(M - 0.8)^{0,39}}$	1.1 < M < 3.0	Active in stationnary air	Gagge et al. (1976)
$\boldsymbol{h_c = 6.5V^{0,39}}$	0.5 < V < 2.0	Walking in stationnary air	Nishi and Gagge (1970)
$\boldsymbol{h_c = 14.8V^{0,69}}$	0.15 < V < 1.5	Standing with air in movement	Seppänen et al. (1972)

Table 3 – Convective transfer coefficient h_c

In this paper, the condition seated with air in movement will be considered. Therefore:

- If $0.2 < V < 4.0$:

$$h_c = 8{,}6V^{0{,}6}$$

- If $0 < V < 0.2$:

$$h_c = 3{,}1 \qquad (16)$$

3.5.1.2 Radiative heat loss R

Radiative heat is the exchange that takes place between the person and the surrounding objects, since all bodies, by the simple fact of being at a certain temperature, emit radiation. In this case, radiation is taken into account with the mean radiant temperature. If the body temperature is higher than the mean radiant temperature, heat is lost and vice versa.

$$R = f_{cl} h_r (T_{cl} - T_{MR}) \ [W/m^2] \qquad (17)$$

3.5.2 Evaporative heat loss E_{sk}

In addition to the two previous losses, there is also a latent heat loss when water vapor evaporates in the skin. By the process of secretion, the human body expels water, which requires a certain amount of energy to evaporate. This heat is extracted from the human body, so that, because of this heat subtraction, the body temperature is reduced.

This loss is related to the saturation of the air, so that if the saturation pressure decreases, the amount evaporated will increase, proportionally to the humidity of the skin.

Evaporative heat loss from is the sum of the evaporation of sweat secreted because of thermoregulatory control mechanism E_{rsw} and the natural diffusion of water through the skin E_{dif}.

$$E_{sk} = E_{rsw} + E_{dif} \ [W/m^2] \qquad (18)$$

The formula is not developed in this paper since studying the total heat load implies using a constant and given value E_{sk}.

3.5.3 Respiratory losses q_{res}

The respiratory losses are the human body heat losses through the respiratory tract, both sensible (Cres) and latent (Eres). Sensible losses are produced by exhaling hot air contained in the human body and latent losses by evaporating the water vapor particles contained in the air we breathe. Both terms can be calculated in a more complex way, however, it will be done in an approximate way because, comparing the order of magnitude of these losses with respect to the others, they are relatively small.

Both expressions are a function of metabolism M since oxygen consumption in the lungs is directly related to the type of physical activity being performed.

$$C_{res} = 00014M(34 - T_a) \qquad (19)$$

$$E_{res} = 0{,}0173M(5{,}87 - P_a) \qquad (20)$$

Where the air temperature T_a (°C) and water vapor pressure of air P_a (kPa) are at standard conditions of 20°C, 50% of relative humidity at sea level.

3.5.3.1 Relative humidity

The formulas developed in the previous paragraph use humidity expressed as the water vapor pressure of air (P_a). This is the pressure exerted by the vapor pressure of water in the gas mixture under consideration, in this case the air. The more this pressure increases, the more humid the air becomes. Humidity can therefore be expressed in kPa, and not just as a percentage as relative humidity.

The partial pressure of water is calculated using the saturation vapor pressure of water ($P_{a,sat}$) and relative humidity. They are given with the formulas:

$$P_{a,sat} = e^{\frac{C_1}{T_a(K)}+C_2+(C_3 \cdot T_a(K))+C_4 \cdot (T_a(K))^2+C_5 \cdot (T_a(K))^3+(C_6 \cdot ln(T_a(K)))} \quad (21)$$

$$P_a = \frac{RH\% * P_{a,sat}}{100} \ [kPa] \quad (22)$$

With the value constants:

C1	-5,80E+03
C2	-5,52E+00
C3	-4,86E-02
C4	4,18E-05
C5	-1,45E-08
C6	6,5459673

Table 4 – Value of the constants for the partial pressure of water calculation

3.6 Temperature of clothing

Like all heat transfer phenomena, the sensible heat loss through the environment can also be expressed as a temperature difference between the skin (T_{sk}) and the clothing (T_{cl}), between the thermal resistance exerted by the clothing.

$$C + R = \frac{T_{sk} - T_{cl}}{R_{cl}} \quad (23)$$

With formulas of the convective and radiative heat loss C and R, it can be written:

$$f_{cl} h_c (T_{cl} - T_a) + f_{cl} h_r (T_{cl} - T_{MR}) = \frac{T_{sk} - T_{cl}}{R_{cl}} \quad (24)$$

This gives a formula for the clothing temperature, which will be used for the calculations of the convective and radiative heat loss:

$$T_{cl} = \frac{\frac{T_{sk}}{R_{cl}} + \frac{T_a}{1/f_{cl}h_c} + \frac{T_{MR}}{1/f_{cl}h_r}}{\frac{1}{R_{cl}} + f_{cl}h_c + f_{cl}h_r} \quad (25)$$

3.7 COMFA : heat load model

The calculation of the heat load is done using the COMFA model. This comfort index is defined as the heat that must be extracted or supplied to the body to be in comfort. It is the difference between internal heat production and heat losses through the mechanisms discussed in this document. The calculations are made for a person who is hypothetically in comfort, i.e., with a skin temperature $T_{sk,comfort}$ and sweating $E_{sk,comfort}$ within acceptable values at the actual activity level. At a given level of metabolic activity M, and when the body is not far from thermal neutrality, these two parameters are the only physiological ones influencing the heat balance.

The following linear regression equations based on data from Rohles and Nevins (1971) [5] indicate values of T_{sk} and E_{rsw} that provide thermal comfort.

$$T_{sk,comfort} = 35{,}7 - 0{,}0275(M - W) \quad (26)$$

$$E_{rsw,comfort} = 0{,}42(M - W - 58{,}15) \quad (27)$$

The heat load is then:

$$Q = M - W - q_{res} - ((C + R)_{confort} + E_{sk,confort}) \; [W/m^2] \quad (28)$$

Where:

- The values of first three terms M, W and q_{res} calculated with the actual conditions are those calculated earlier in the development of the comfort model.
- In the case of sweating, its value in comfort conditions corresponds to the thermoregulatory component in comfort. It means $E_{rsw,comfort} = E_{sk,comfort}$, the diffusion component (E_{dif}) being zero.
- In the case of sensible losses in comfort, they must be recalculated considering the new skin temperature $T_{sk,comfort}$.

The heat load calculated is expressed in a thermal sensation scale ranging from -150W/m² to +150 W/m² (*Table 5*).

5	Sweltering (S)	**> 150 W/m^2**
4	Very Hot (VH)	
3	Hot (H)	50 ÷ 150 W/m^2
2	Warm (W)	
1	Slightly Warm (SW)	
0	**Comfortable (Cm)**	**-50 ÷ 50 W/m^2**
-1	Slightly Cool (SC)	-150 ÷ -50 W/m^2
-2	Cool (C)	
-3	Cold (Co)	
-4	Very Cold (VC)	< -150 W/m^2

Table 5 – Thermal sensation scale for the COMFA index

4 PRELIMINARY STUDY OF SENSITIVITY

Before studying the real street, it is necessary to carry out some general calculations of the heat load. The aim is to identify combinations of environmental variables that lead to a comfort situation. This is called the study of sensitivity.

4.1 Input data

The input data is the following:

- Climate data outside for a typical day: air temperature, temperature of the sky, humid temperature, relative humidity, wind speed and local solar radiations (direct and diffuse)
- Level of clothing: I_{clo} = 0,57 clo
- Metabolic rate: met = 1 (person at rest) or met = 2 (person walking), meaning respectively M = 60 W/m² and M = 116.3 W/m²
- Clothing absorptivity α = 0,3 (light-coloured clothing)
- Increased area due to clothing fcl = 1,171

4.2 Heat load for a typical day without coverage

Initial heat load calculations have been carried out for a simple, square geometry with no cover, for a typical day. It is then possible to generate the evolution of the thermal load over the day (*Figure 9*), as well as all the terms that make it up (*Figure 10*).

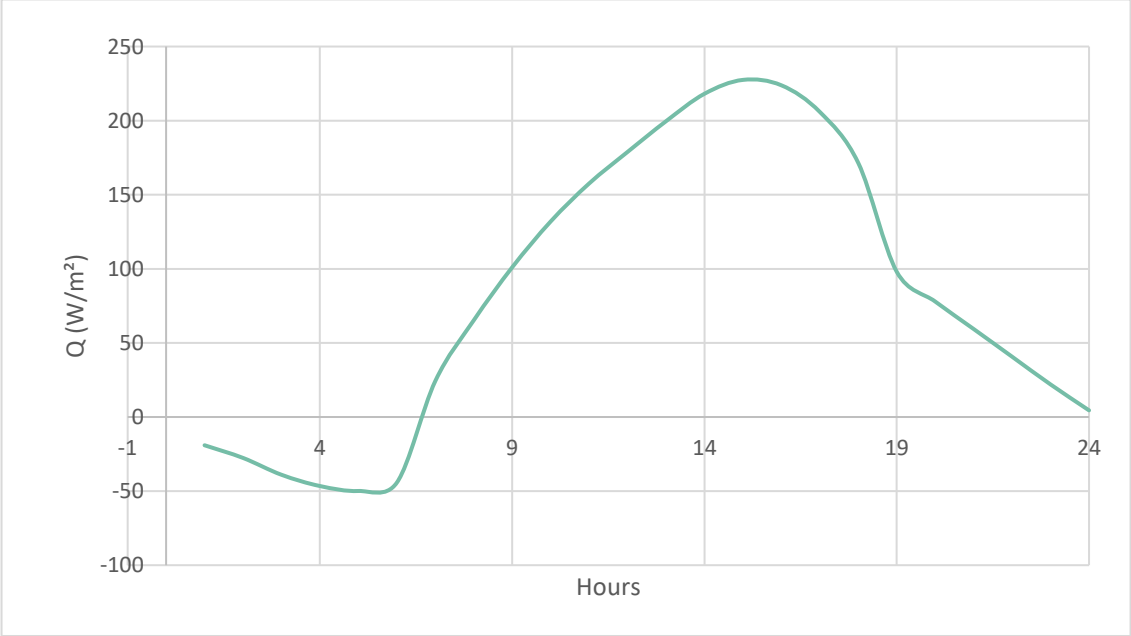

Figure 9 – Heat load evolution

What is important to observe in *Figure 9* is not whether the heat load value is negative or positive. Rather, it should be observed in relation to the zones on the comfort scale. At night, the heat load is

included in the interval -50/+50 W/m², meaning that the occupant is in comfort. From 6h, it increases with the radiation and air temperature, until entering the sweltering zone (greater than 150W/m²) after 10h. The curve remains in this zone for 8 hours until 18h. Moreover, it should be noted that at 16h, the heat load reaches its maximum value and starts to decrease. This is explained by the fact that the convection and longwave radiation heats are maximum at that time. They are shown in the next graph.

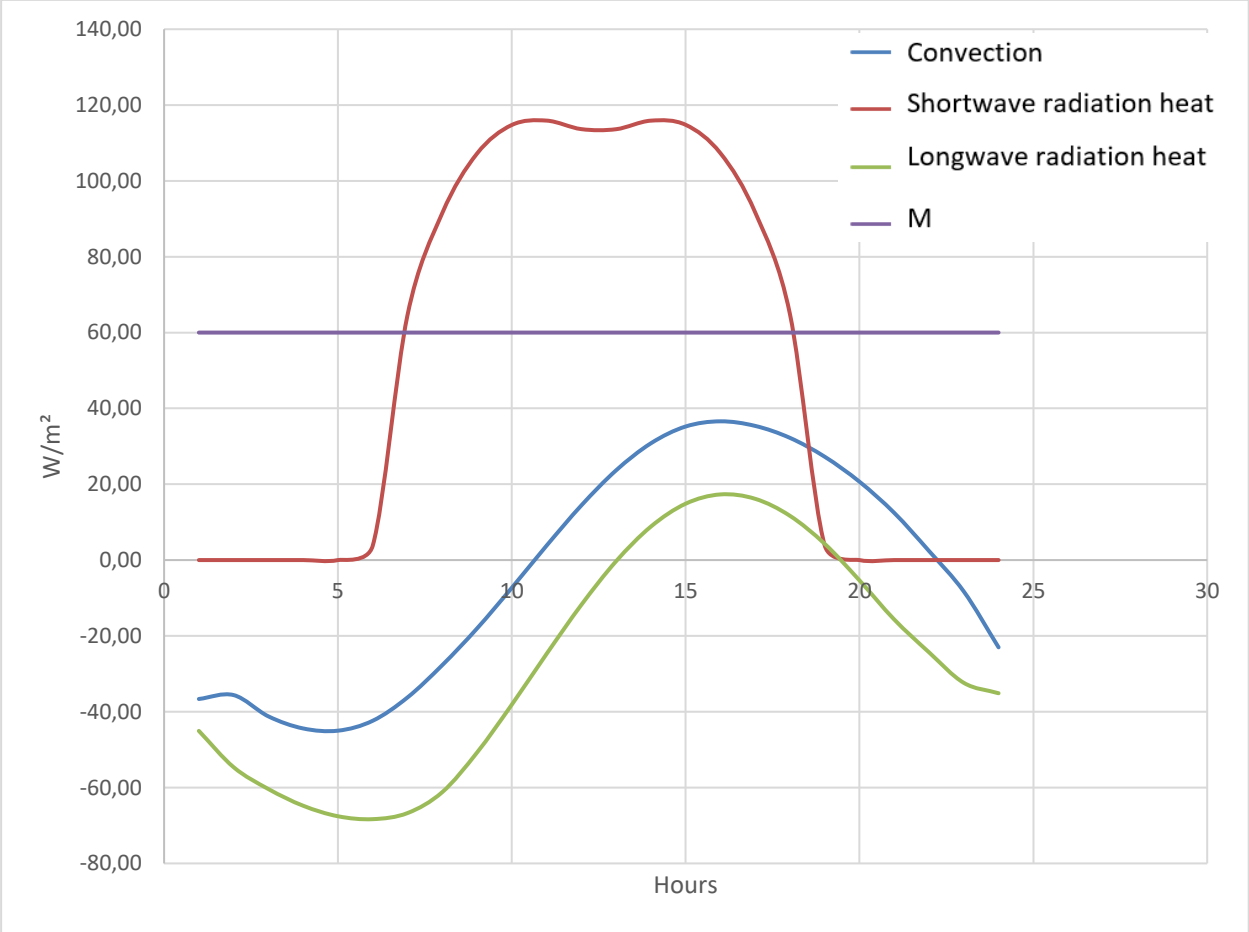

Figure 10 – Evolution of all heat mechanisms involved in the heat load equation

At night, shortwave radiation heat is equal to zero because there is no sun. Around 6h, when the sun appears, this heat increases until around 11h. Thereafter, it decreases slightly and then increases until it reaches its maximum which it had at 11h, but now at 14h.

When the long wavelength and convective term are negative, it means that the occupant is warmer than the surroundings. Thus, there is a heat transfer from the occupant to the surroundings. The convective term is negative at night and positive during the day, as the ambient temperature increases during the day. In addition, it is common for wind speed to be higher during the day compared to the night, encouraging convection in the street.

The long wavelength radiation heat is not a gain, except between 13h and 19h. Indeed, this period corresponds to the highest temperatures: in a warmer environment, long wavelength radiations from surrounding hot surfaces contribute to the body heat gain.

4.3 Study of sensibility

4.3.1 Introduction

The aim of this paragraph is not to represent a typical day, with a typical air temperature, relative humidity, wind speed and solar radiations. The aim is to present tables of heat load in which the air temperature and solar radiations can vary, for example, with a fixed air speed, humidity and met. In this way, several reference tables are generated, in which it will later be possible to position and compare the results obtained for a representative day.

The aim is to obtain a 2D matrix. This table must be obtained with only 2 variables that are allowed to change: the air temperature, and a parameter representing solar radiation. However, the solar radiation is subdivided into 2 parts: the shortwave radiations (R_{SW}) and the longwave radiations (R_{LW}). This gives 3 input variables for the table.

The median radiant temperature includes radiations from surfaces as a consequence of their increased temperature added to direct, diffuse and reflected solar radiation. Indeed, as seen in section 3.4.3, the mean radiant temperature is the sum of the long and short radiant temperature. A mean radiant temperature of 40°C can be achieved, for example, with 35°C due to surface temperatures (long wavelength radiation). The rest is the increase due to solar radiation (short wavelength radiation). This is why it is now possible to study both short and long radiations at the same time, thanks to the mean radiant temperature.

It is therefore possible to analyse the influence of air temperature and radiation parameters, through the associated temperature T_{MR}, on the heat load.

4.3.2 Tables of sensibility

The tables can now be generated:

- For different level of humidity (w). Three levels are considered: low (8g/kg), medium (10g/kg) and high (12g/kg)
- For met 1 and met 2
- For air speed equals to 0,2 or 1 m/s
- T_a varies between 26°C and 40°C
- T_{MR} varies between 28°C and 42°C

The colours for the heat load value Q obtained represent the following comfort scale:

	Q (W/m^2)
Comfortable	-50/50
Slightly Warm	50/85
Warm	85/120
Hot	120/150
Sweltering	>150

Table 6 – Heat load scale

The tables are shown in annex (7.1). As an example, the heat load table for the low humidity, the wind speed of 1m/s and met 2 is shown below.

V= 1 m/s w=8 g/kg	Tmr							
Tair	28	30	32	34	36	38	40	42
26	47,01	51,71	56,40	61,10	65,79	70,48	75,18	79,87
28	54,94	59,63	64,32	69,02	73,71	78,41	83,10	87,79
30	63,56	68,26	72,95	77,64	82,34	87,03	91,73	96,42
32	72,19	76,88	81,58	86,27	90,96	95,66	100,35	105,05
34	80,81	85,51	90,20	94,89	99,59	104,28	108,98	113,67
36	89,44	94,13	98,83	103,52	108,21	112,91	117,60	122,30
38	98,06	102,76	107,45	112,15	116,84	121,53	126,23	130,92
40	106,69	111,38	116,08	120,77	125,47	130,16	134,85	139,55

Table 7 – Heat load table (W/m²) for the low humidity, the wind speed of 1m/s and met 2

These tables will be commented in the following parts. The purpose of this paragraph is to help understand the table. Under the conditions of wind, humidity and metabolism set out below, it is possible to read the heat load for the climate parameters of our choice. For example, at an air temperature of 32°C and a mean radiant temperature of 36°C, the heat load is 90.96 W/m². It can also be seen that as the temperatures T_a and T_{MR} increase, the further the heat load moves away from comfort.

As expected, if there is less physical activity, for the same wind and humidity conditions, the heat load values decrease and the table shifts towards the green colours, i.e. the comfort zone (*Table 8*).

V= 1 m/s w=8 g/kg	Tmr							
Tair	28	30	32	34	36	38	40	42
26	6,23	10,92	15,62	20,31	25,00	29,70	34,39	39,09
28	14,69	19,38	24,07	28,77	33,46	38,16	42,85	47,54
30	23,14	27,84	32,53	37,23	41,92	46,61	51,31	56,00
32	31,60	36,30	40,99	45,68	50,38	55,07	59,77	64,46
34	40,06	44,75	49,45	54,14	58,83	63,53	68,22	72,92
36	48,52	53,21	57,90	62,60	67,29	71,99	76,68	81,37
38	56,97	61,67	66,36	71,06	75,75	80,44	85,14	89,83
40	65,43	70,13	74,82	79,51	84,21	88,90	93,60	98,29

Table 8 – Heat load table (W/m²) for the low humidity, the wind speed of 1m/s and met 1

5 STUDY OF THE REAL STREET

5.1 Project presentation

LIFE Watercool is a project co-funded by the European Union's Life initiative. LIFE Watercool consists in improving the use and comfort to cope with high temperatures in different spaces and situations.

The first phase of the project is centred on the Avenue de la Cruz Roja, which becomes pedestrianised, with the paving and installation of water supply and drainage services, and the creation of sustainable urban drainage systems. Then, other phases are carried out in the areas adjacent to this street.

The street is located in the city centre of Seville, in a densely populated area. The project is divided into two activities called C-1 (new urban design of the avenue) and C-2 (bioclimatic adaptation).

The C-1 project aim is transforming a completely urbanised street to decrease the impact of urban heat island. The partners involved in this project are EMASESA (Project Coordinator), Seville City Council, the University of Seville, the University of Seville, the Pyme SDOS and the EFE Verde Agency.

Techniques known as Sustainable Urban Drainage Systems techniques (SUDS) have been implemented through rehabilitation works:

- Structural tree surrounds
- Permeable paving
- Floodable flowerbeds
- Infiltration wells

The C-2 project is a series of microclimatic actions, including water cooling installations, new materials, and bioclimatic spaces. The partners involved in this project are the Seville City Council and the University of Seville. The drafting of this Project has been supervised by EMASESA (Seville City Council), with the collaboration of the Thermotechnic Group of the engineering school ETSI of the University of Seville, under the direction of the technician of the City Council Cesar Gallardo Soler.

More specifically, the aim is to demonstrate the efficiency of urban water management to improve the quality of life in the street, by reducing the impact of urban heat island. It is first tested on a small scale, here the studied street. As seen in introdution, facing this UHI means decreasing impermeable surfaces. It is mainly achieved through presence of water and vegetation. In the C-2 project, the existing urban water system has been reinforced with elements to accumulate, drain, and interconnect untreated water (from rain and river water).

5.2 Objective

The objective of this part is to compare the thermal comfort of the initial situation of the Avenue de la

Cruz Roja with the final situation, after the rehabilitation works.

An analyse of the initial and final case of the avenue is carried out, considering a person at rest and a person walking. The comparison is done for four typical days for the months of June, July, August and September.

5.3 Input data and hypotheses

5.3.1 Input data

The input data is the following:

- Climate data outside of the street: air temperature, temperature of the sky, humid temperature, relative humidity, wind speed and local solar radiations (direct and diffuse)
- Level of clothing: I_{clo} = 0,57 clo
- Metabolic rate: met =1 (person at rest) or met = 2 (person walking), meaning respectively M = 60 W/m² and M = 116.3 W/m²
- Clothing absorptivity α = 0,3 (light-coloured clothing)
- Increased area due to clothing fcl = 1,171
- Geometry of the street that is detailed in the next sections
- Traffic evolution in Sevilla

5.3.2 Avenue description

Located in the northeast of the city, the avenue de la Cruz Roja and the surrounding streets have a total length of 900 meters, between Ronda de Capuchinos and Jorge de Montemayor, Manuel Villalobos (*Figure 11*).

There are 4 sections of sewage collectors, one supply under the sidewalk and there is no irrigation network.

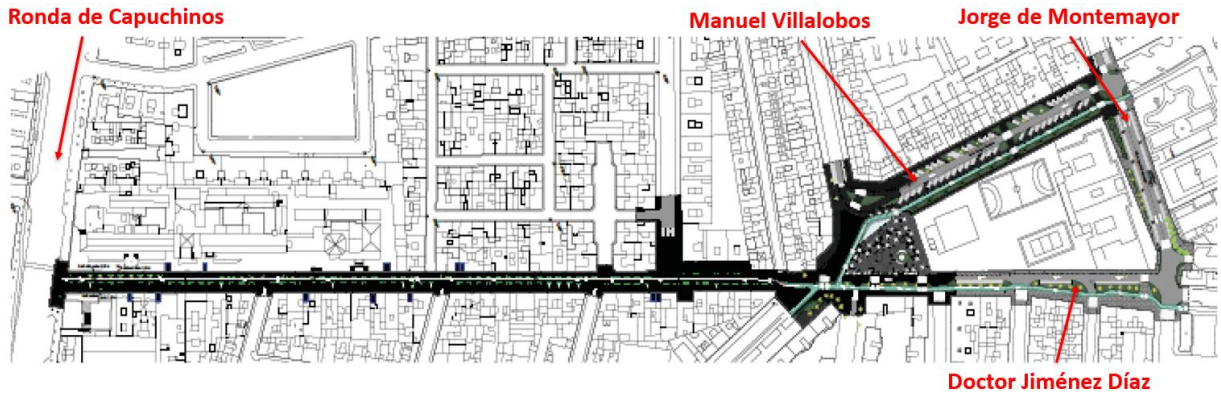

Figure 11 – Map of the street

5.3.3 Initial situation

Initially, the avenue is formed by two sidewalks, a green bike lane and a vehicle lane. Trees and buildings are present, delimiting a clear geometry on both sides of the street. There are very old, damaged or diseased trees, so it has been deemed appropriate to replace these specimens and add new ones for the final situation.

Even if there are some trees, there are few shaded areas at the time when the solar height is maximum. Moreover, there is a lot of anthropogenic generation with traffic from the road. The albedo of the ground is low: the sidewalk and bicycle lane are done with concrete of reflectivity equals to 0,5; the car lane is asphalt with 0,1 reflectivity. All this makes the effects of the UHI more remarkable. The comfort of citizens must be improved through rehabilitation works.

Figure 12 – Satellite view and zoom on a section of the street

5.3.4 Final situation

After the rehabilitation work, the avenue changes drastically in order to improve its habitability during the summer months. Buildings are maintained, however numerous activities are carried out, the main ones stand out:

- Introduction of SUDS (Sustainable Urban Drainage Systems) to recover part of the rainwater such as structural flowerbeds, permeable pavements, floodable flowerbeds and infiltration wells.
- Demolition of the car lane and creation of a pedestrian area, reducing anthropogenic generation. The bicycle lane is maintained.
- Change of the pavement with a clearer material. The reflectivity increases, which helps in part to decrease the UHI effects.
- Modification of the water supply, drainage and irrigation network.
- Maintenance of existing trees and planting of new species to create more shade in the street.

Figure 13 – Street before (left) and after (right) rehabilitation works

All these data are known. In particular, trees and SUDS can be easily observed on plans. For example, the *Figure 14* shows an area of the street where the different types of pavement and floodable flowerbeds are described in the legend.

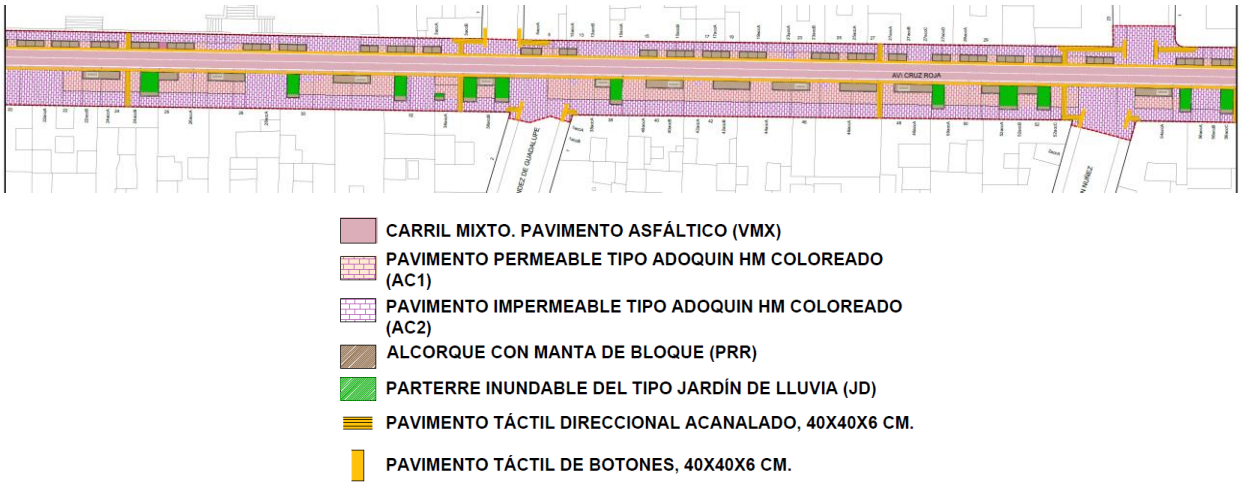

Figure 14 – Rehabilitation works plan

The types of pavements used in this project are the following ones:

- Permeable pavement of prefabricated concrete pavers
- Impermeable pavement of prefabricated concrete pavers
- Permeable pavement of large format prefabricated concrete plaques
- Impermeable pavement of large format prefabricated concrete plaques
- Colored precast concrete pavers
- Bituminous pavement in car lane
- Bituminous pavement in bicycle lane
- Flowerbeds covered with concrete block covering
- Flowerbeds
- Landscaped flowerbeds and rain gardens
- Structural flooring

5.3.5 Hypothesis

The following considerations will be taken into account:

- The area of the street alongside the school is not considered since there are no buildings on one side of the street.
- Only the forced convection of the wind is considered.
- The ground is assumed to be adiabatic. This assumption means that heat transfers to the ground are lower than other transfers that occur in the street.

5.4 CartujaQanat and ENERKEA

The CartujaQanat software was developed by the thermotechnology group of the University of Seville to mitigate the heat in Seville or other areas where high temperatures prevail. ENERKEA is a calculation engine that belongs to CartujaQanat software. It is the tool that has been used in this master thesis. It designs outdoor spaces and helps taking decisions to achieve thermal comfort.

First, the initial situation of the project is defined: the user selects the intervention area and designs the geometry of it. Based on satellite images from Google Maps, it creates a mesh and defines the nature of the cells in this mesh (bicycle lane, car lane, sidewalk,..) and its material. The user also has to characterise the trees, the shadows, the buildings and their properties.

Finally, the user also selects solutions in a catalogue so that they can be evaluated, climatically and economically. For example, it underlines in which areas the paving needs to be replaced, or where shade need to be implemented.

More specifically, the calculation engine first calculates data such as radiation and view factors (see 5.4.1). It raises a surface balance and solve it. Therefore, for a predefined geometry and a set of climate data ($T_a, T_{sky}, T_{humidity}, RH\%, R_D, R_d, V$, azimuth, solar height), ENERKEA can determines:

- The temporal evolution of solar radiation on each cell of the considered geometry, differentiating direct and diffuse onto occupant.
- The temporal evolution of surface temperatures of each cell and elements making up the surroundings.
- The view factors for every cell of the geometry.

5.4.1 View factors

According to Wien's law, every object emits its own thermal radiation. In each environment, shapes and objects interact with each other, receiving and emitting thermal radiation. It is possible to quantify the proportion of thermal radiation emitted by one surface that is received by another. This is what the view factor does. It is used to determine the amount of radiative heat exchanged between the surfaces. It only depends on the geometry of the environment.

To determine the long wavelength radiant temperature of a given situation it is necessary to take into account the considered geometry through this view factors. The software gives this different factor in the form of a matrix, showing the interaction of a single cell with every other cells. The aim of this part is to study the comfort of a person located in the given geometry. This requires a study of the radiation received and exchanged with the environment. By taking the view factors of the cell where the person is, it is possible to calculate the long wavelength radiant temperature (T_{LW}).

$$T_{LW} = \frac{\sum F_{individual-i} \cdot T_{s,i}}{\sum F_{individual-i}} \quad (29)$$

Where $T_{s,i}$ is the superficial temperature of the cell i.

5.5 Air modelization in the street

5.5.1 Natural and forced convection

As the sun heats the buildings and walls, the air near the surfaces heats up and decreases in density, creating a low-pressure zone. Cooler and denser air from outside the street flows into this zone. In this way, air circulates naturally: this is natural convection.

On the other hand, when there's wind, it acts like an external force influencing air movement in the street. As the wind blows down the street, it collides with buildings and obstacles, creating zones of high and low pressure. These pressure differences generate a flow of air in the street, known as forced convection.

In a street, the force of the wind is the main mechanism of air movement. Thus, in this study, only the force of the wind will be considered, meaning only the forced convection is considered.

5.5.2 Air changed per hour (ACH)

The air coming from outside enters in the interior space of the street, the space formed by the buildings. It enters with a certain velocity, a certain flow rate, and then leaves after a time that depends on the geometry. The higher the buildings are, the less the interior air is renewed. Thus, it is necessary to enter the equivalent hourly renewals which is the number of times that the total volume of air in a space is completely replaced in one hour. It is noted ACH (Air Changed per Hour).

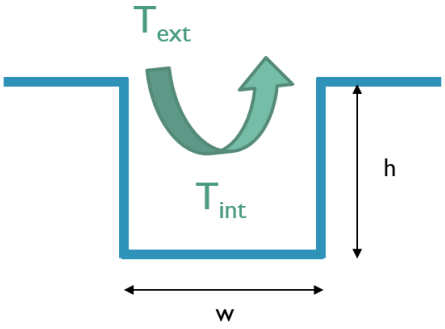

Figure 15 – Schema of the street

The Avenue de la Cruz Roja is surrounded by buildings whose height (h) is equal to the width (w) of the street, on average (*Figure 15*). Then the h/w ratio is approximately equal to 1. With this geometry, it is shown that there is only one vortex, a whirling mass of air.

Modelling these vortexes is complex. This is done with specialized fluid dynamics programs. The Energy Engineering Department at the ETSI (University of Seville) carried out a study in parallel which produced different graphs. Specifically, the graph below (*Figure 16*) shows the streamlines in a street that is of the same typical dimensions as Avenue de la Cruz Roja.

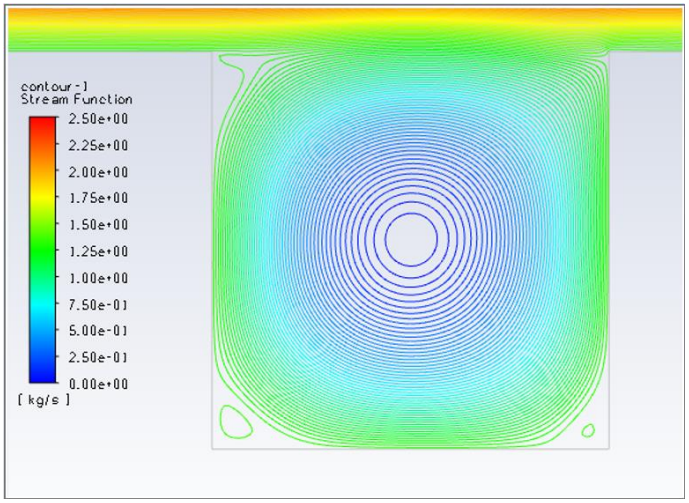

Figure 16 – Modelling of air vortex

The conclusion of the simulations of this study showed that for an outside air inlet velocity of 1m/s, the dimensionless flow rate $ACHd$ is 0,0141, for h/w ratio approximately equals to 1. From this number, we get the mass flow needed to solve the equations that will be introduced in the next parts.

The mass flow $\dot{m}$ [kg/s] is defined as follow:

$$\frac{\dot{m}}{A_{street} \cdot V \cdot \rho_{aire}} = ACHd \tag{30}$$

It is important to keep in mind that this dimensionless parameter varies proportionally with the air flow rate, which changes every hour of the day. Using a proportional calculation, it is simple to calculate its evolution.

The *Table 9* shows the different values of the mass flow, depending on the air velocity. Calculations are done for a street width and depth of 15 m, with $\rho_{aire} = 1{,}225\ kg/m^3$.

V	ACHd	$\dot{m}$	ACH
0,2	0,0028	0,7773	0,00019
0,4	0,0056	1,5545	0,00038
0,6	0,0085	2,3318	0,00056
0,8	0,0113	3,1091	0,00075
1,0	0,0141	3,8863	0,00094
1,2	0,0169	4,6636	0,00113
1,4	0,0197	5,4408	0,00132
1,6	0,0226	6,2181	0,00150
1,8	0,0254	6,9954	0,00169
2,0	0,0282	7,7726	0,00188
2,2	0,0310	8,5499	0,00207
2,4	0,0338	9,3272	0,00226

Table 9 – Values of mass flow depending on air velocity

5.5.3 Balance on air

In this paragraph, the air temperature inside the street enclosure will be referred as the "indoor temperature". The air temperature at roof level will be referred as the "outdoor temperature".

The outside air that enters the street, in the zone defined above, participates in the renewal of the air in the street (indoor). It must be considered that this outside air does not have the same temperature as the inside air. The outside temperature always has the same value (it is the temperature undisturbed by what happens in the street). In contrast, the indoor temperature is unknown.

To determine this indoor temperature, a balance is made on this indoor air. Heat exchanges between this indoor air and the outdoor air is equal to the anthropogenic generation plus the sum of the convection from the surrounding areas (ground, buildings and trees).

$$\dot{m} \cdot C_p \cdot (T_{int} - T_{ext}) = Q_{anthropogenic} + \sum_i h_i \cdot A_i \cdot (T_{sup,i} - T_{int}) \quad (31)$$

Where $Q_{anthropogenic}$ is the anthropogenic generation. The mass flow $\dot{m}$ is obtained thanks to the air changed per hour calculated in the previous part.

Some details of the terms of the equation (31) are given in the following paragraphs.

5.5.3.1 Heat transfer coefficient

As stated in the hypotheses, only the forced convection is considered. The heat transfer coefficient is given thanks to correlations established for forced convection [12], [13].

$$h = 3{,}5 + 5{,}6 \cdot u \quad (32)$$

Where u is the air velocity near the outside surface and depends on the surface exposition of the wind.

- On the exposed surface (windward):

If the speed of the wind is greater than 2 m/s:

$$u = 0{,}25 \cdot V \quad (33)$$

Otherwise:

$$u = 0{,}5\ m/s \quad (34)$$

- On the surface no exposed (leeward):

$$u = 0{,}3 + 0{,}05 \cdot V \quad (35)$$

In this specific street, the west façade is considered as leeward since the prevailing wind in Seville is southwest. The ground is exposed to the wind, so it is windward.

5.5.3.2 Anthropogenic heat

Anthropogenic heat is the heat released due to human activities. It is a critical variable in the heat island effect. To study it, it is necessary to quantify the parameters related to pavements, buildings, population density, traffic and green or water masses existing. It also depends on the hour, the day and the radiation over the studied localization. A previous study has been done by the Thermotechnic Group of the University of Sevilla to calculate the anthropogenic heat in Sevilla. The modeling is first based on the available geophysical information, statistical data available on the web, information from the city council cameras and a correction made by counting on site.

The anthropogenic heat is the sum of the metabolic heat produced by the presence of humans (Q_{h}), heat emitted by air-conditioning systems in buildings ($\mathrm{Q_t}$) and heat generated by traffic ($\mathrm{Q_t}$). It is thus expressed as:

$$Q_{anthropogenic} = Q_{\mathrm{h}} + \mathrm{Q_b} + \mathrm{Q_t} \quad [W/m^2] \tag{36}$$

In this paper, the first two terms are not considered in the anthropogenic heat because their interaction is taken into account in the geometry defined in the software.

Determining the contribution of the heat released by traffic requires data about traffic density, types of vehicles, fuel types and fuel consumption, which can be seen from the formula:

$$\mathrm{Q_t} = \frac{E_{factor} \cdot N_{lanes} \cdot \left(L_{moderate} \cdot D_{moderate} + L_{high} \cdot D_{high}\right)}{A_{street}} \; [W/m^2] \tag{37}$$

Where:

- E_{factor} is the heat emission factor in $[J/m]$, which depends on the types of vehicles and fuel consumption assumptions. It is smaller by night than by day.
- N_{lanes} is the average number of lanes. ($N_{lanes} = 1$)
- $L_{moderate}$ and L_{high} $[m]$ are the total lengths of streets with moderate and high density of traffic respectively, in the studied localization. In the Avenue de la Cruz Roja, $L = 900\ m$.
- $D_{moderate}$ and D_{high} are the number of vehicles per hour of each traffic type.
- A_{street} is the total street area [m^2].

5.5.3.2.1 Number of vehicles per hour (D)

The evolution of the traffic was taken from the City Council of Seville. This is a global profile used for all streets with traffic (*Figure 17*).

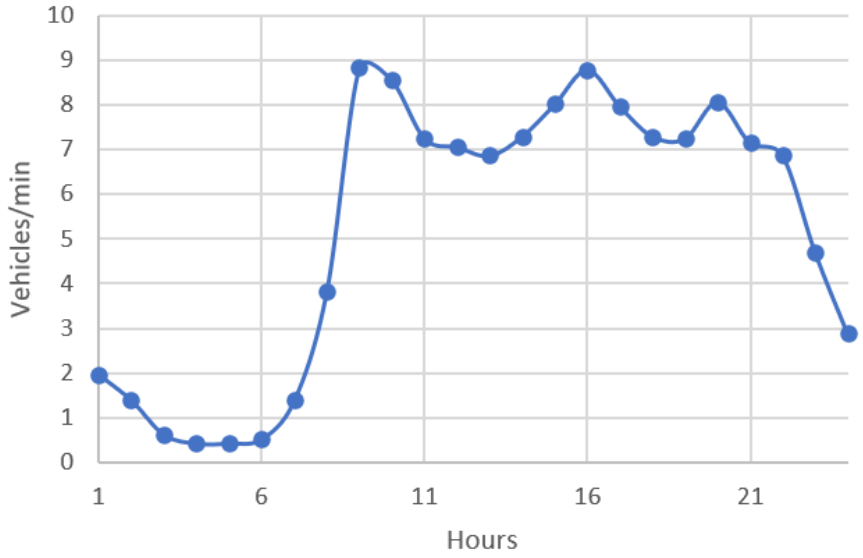

Figure 17 – Daily distribution of traffic

5.5.3.2.2 Heat emission factor E_{factor}

As explained, the heat emission factors of vehicles depends on the type of vehicle and fuel consumption rates. The National Department of Traffic in Spain provides statistics that the study used for the *Table 10* giving the fleet of vehicles in Seville.

For each type of vehicle, the study calculated the heat emission factor E_{factor}, considering the fuel consumption, the density of the fuel and the Net Heat Combustion of the fuel.

Type of vehicle	Heat emission factor [J/m]
Petrol motorbike	1427
Petrol car	4461
Diesel car	3929
LPG bus	8531
Diesel medium size truck	10005
Others	3511

Table 10 – Heat emission factor E_{factor} depending on the type of vehicle

To simplify the calculations in the Avenue de la Cruz Roja, the percentage considered is 85% combustion vehicles and 15% buses. This is also justified by the fact that the percentage of trucks passing through that street is very small.

At night, the number of car passing is low, so the E_{factor} is at its minimum and only due to combustion vehicles. Apart from this time slot, as in the case of Seville, buses pass very regularly, so we consider a high E_{factor}.

5.5.3.2.3 Anthropogenic heat

The evolution curve of anthropogenic heat follows the same daily curve as the vehicle flow (*Figure 18*).

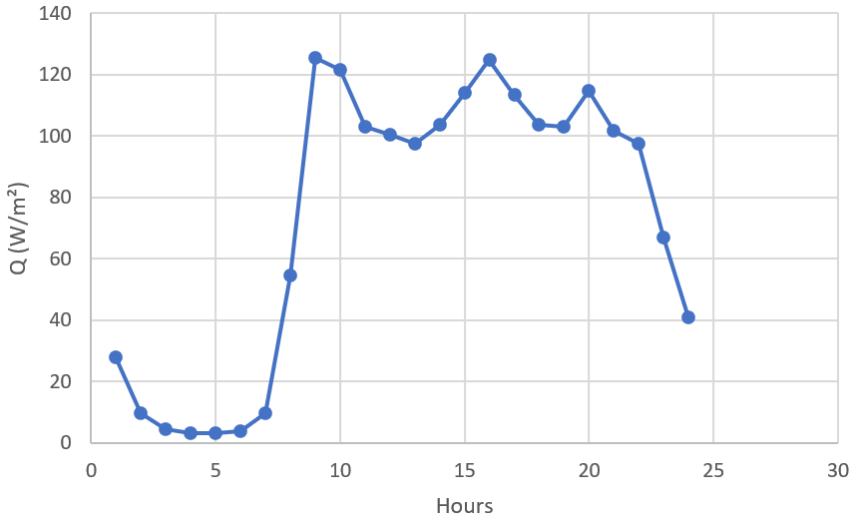

Figure 18 – Daily evolution of the anthropogenic heat

5.6 Methodology

Now that we have the theoretical foundations and data needed to begin the study, the time comes to follow some steps in order to compare the thermal comfort the initial and final situation.

It is important to note that many calculations will be made using ENERKEA outputs. There are therefore two main levels. The first one is implementing the geometry in the program and obtaining the outputs (see 5.6.1); and at the same time there is the selection of representative days for each month of June, July, August and September (see 5.6.2). The second level is the use of these data, which consists of:

1. Carry out the balance on air with iterations to obtain stable results for the interior temperature (see 5.6.3).
2. Realise last calculations with ENERKEA with these results and make an integration with the outputs (see 5.6.4)

5.6.1 Implementation of the geometry and studied section

5.6.1.1 Implementation of the geometry in CartujaQanat

The mesh is done with square cells of 2 meters wide and high, differentiating the nature of the cells (bicycle lane, car lane, sidewalk) and its material. Then the software gives an urban geometry file which will be used as the geometry basis for calculations.

5.6.1.2 Studied section

In the street, there are benches, trees, buildings of different heights... To make the calculations easier and faster, a partition of the avenue is made, with different sections of street. It is supposed that the study of one section of the street is enough to study the whole street. It means that the results obtain for one section are the same for the whole street.

Since there are zones with road, pedestrian sidewalk or bike path, it is necessary to divide the section with different subzones. The geometry is explained in the following paragraphs.

5.6.1.3 Surrounding boundaries

When a street is partitioned to isolate a section, the surrounding boundary conditions are modified. This phenomenon is known as the side effect and has an impact on the study results.

Radiation and temperature calculations will be carried out for the entire section, but only cells far from the edge will be studied. The section is divided into 3 parts, and only the central part will be studied for thermal comfort and temperatures.

5.6.2 Selection of the representative days

Once the geometry is known, it is necessary to add meteorological data in the software. To represent one day for each month (June, July, August, September), a meteorological data is created. This climate data comes from 2 different sources. The first is the Typical Meteorological Year (TMY). This is not a meteorological set of data for a specific year, but meteorological data with values given for each hour of the year for Sevilla. The second source is the set of data measured by the Energy Engineering Department at the ETSI (University of Seville) [14].

It has been noted that the TMY air temperature is lower than that measured, as the heat island effect is not taken into account. Moreover, the wind speed measured is very high and the solar radiation measurements carried out by the Energy Department were considered unreliable.

It was therefore decided:

- For air temperature, to take the data from the measurements carried out by the Energy Department.
- For the rest of the data, to use the TMY data.
- For solar position, the calculations have been carried out by the Energy Department.

The data which is taken into account to create a representative day is:

- Aire temperature
- Wind speed
- Radiations

5.6.2.1 Aire temperature

For each month, the maximum temperature of each day is searched. Then the 85th percentile is searched. This is a classic percentile for design. It is not the hottest day of the considered month, but the 85th percentile.

As for the maximum, the minimum temperature of each day is searched, and an average of each minimum is done. The average T_{min} time (t_{min}) is calculated so that the minimum temperature of the generated day will be at its minimum at the average T_{min} time.

As a result, the maximum and minimum temperatures of the typical day are generated from:

- 85th percentile of T_{max} that reaches its maximum at 16h.
- The average minimum of T_{min} that reaches its minimum at average T_{min} time.

Then, the data for the rest of the day are generated as follows. Two different temperatures are introduced:

$$T_{range} = \frac{T_{max} - T_{min}}{2} \tag{38}$$

$$T_{average} = \frac{T_{max} + T_{min}}{2} \tag{39}$$

Moreover, two times are also introduced in order to define the air temperature.

$$t_{range1} = \frac{\pi}{24 - (t_{max} - t_{min})} \tag{40}$$

$$t_{range2} = \frac{\pi}{(t_{max} - t_{min})} \tag{41}$$

Then, depending on the considered hour, the air temperature is defined:

- If $hour \leq t_{min} \Rightarrow \quad T_a = T_{average} + T_{range} \cdot \cos\{t_{range1}(hour - t_{max} + 24)\}$
- If $hour > t_{max} \Rightarrow \quad T_a = T_{average} + T_{range} \cdot \cos\{t_{range1}(hour - t_{max})\}$
- If $hour > t_{max} \Rightarrow \quad T_a = T_{average} + T_{range} \cdot \cos\{t_{range1}(hour - t_{max})\}$

The daily air temperature obtained for the representative day of each month is the following one.

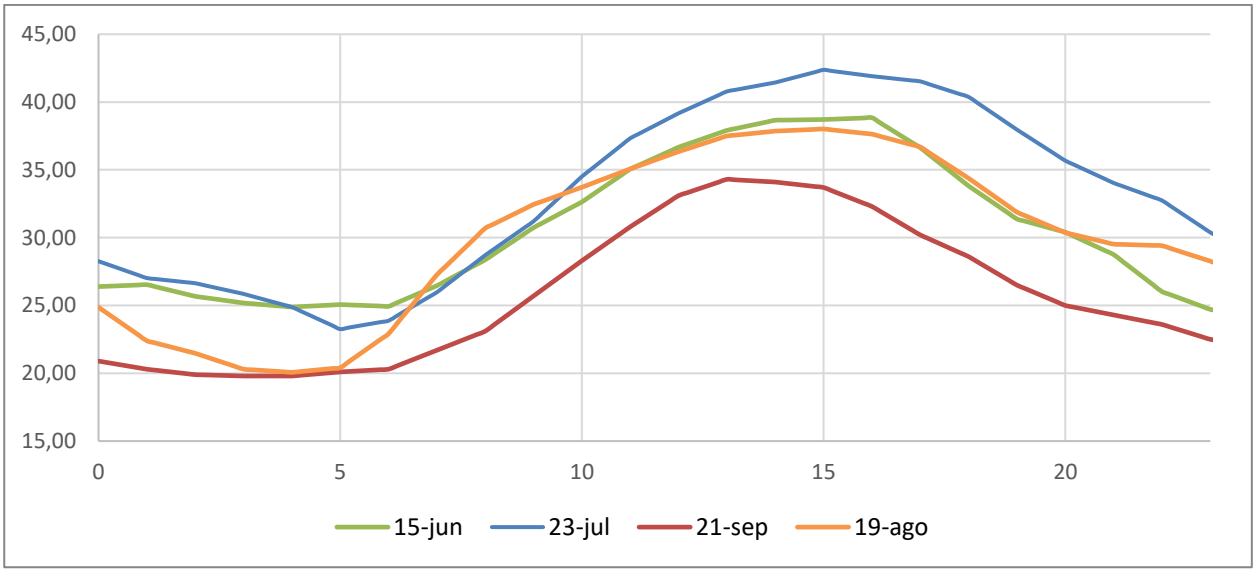

Figure 19 – Air temperature of the representative days (°C)

5.6.2.2 Wind speed

For the wind speed, an average is made for each instant of the month. For example, it means that for 00h, the average of the speed at that time for each day is made.

The daily wind speed obtained for the representative day of each month is the following one.

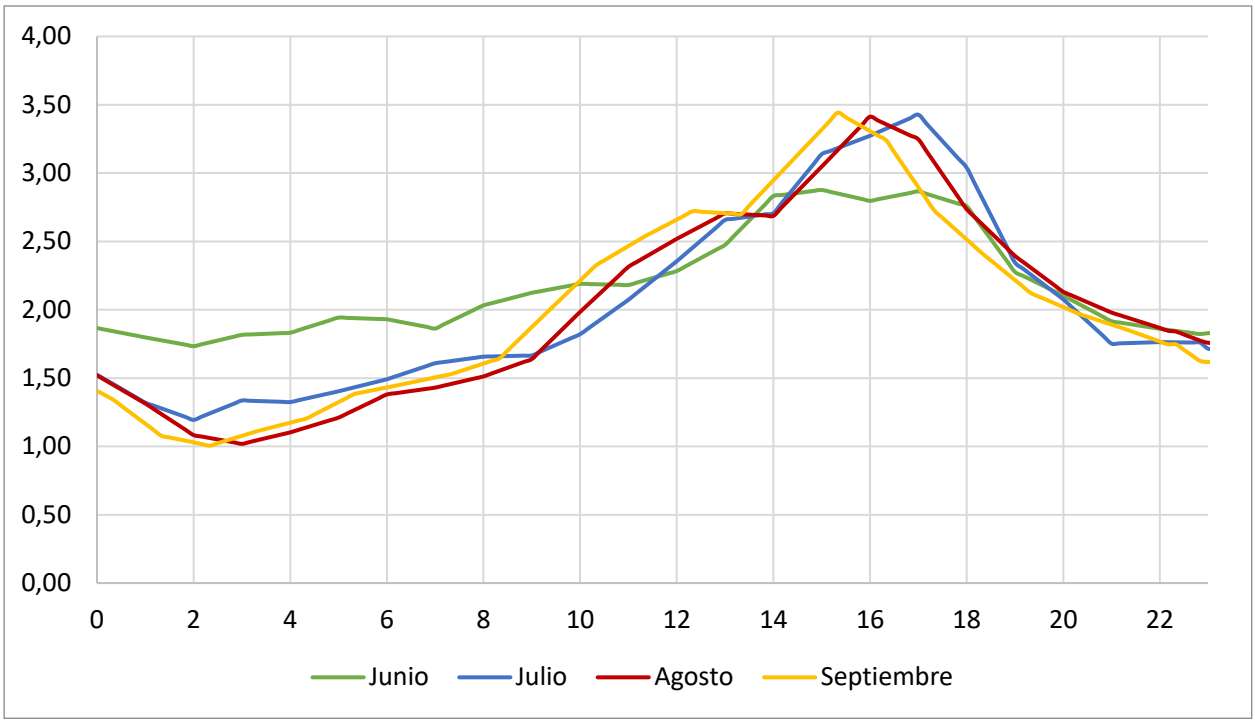

Figure 20 – Wind speed of the representative days (m/s)

5.6.2.3 Radiations

To calculate solar radiations, it had been assumed that there were no clouds. The representative day is a clear day, to assume that the radiations are at their highest.

The Energy Engineering Department previously calculated the data associated with the representative day of each month. The main steps of the calculations for a clear day are shown in the following paragraphs [15]. It can be resumed as the calculation of:

1. Extra-terrestrial radiation each day of the year
2. Normal Direct Intensity on clear days (Hourly), (NDI), and calculation of the brightness index, (BI)
3. Diffuse Horizontal Irradiance on clear days (Hourly), (dHI)
4. Direct Horizontal Irradiance on clear days (Hourly), (DHI)
5. Total Horizontal Irradiance on clear days (Hourly), (THI)

Values of extraterrestrial solar irradiance and its related data widely used in the literature have been employed for the calculations in this section. It gives general values that will be use, for each month. Using the monthly values of the extra-terrestrial radiation (A), the extinction coefficient (B), and the diffuse sky factor (C), the Energy Department calculated the extra-terrestrial radiation each day of the year.

Then, for the second step, the theorical normal direct intensity is given by the formula:

$$NDI_{th} = A \cdot e^{-B/sen(\beta)} \ [W/m^2] \qquad (42)$$

Where β is the solar height, A and B are calculated from the table above.

It has been demonstrated by the that for Seville, the brightness index BI on clear days is 1. The real normal direct intensity is thus:

$$NDI = IDN_{th} \cdot BI \ [W/m^2] \tag{43}$$

It means that the theorical normal direct intensity is equal to the measured one for a clear day in Sevilla.

The steps 3, 4 and 5 then follow. The diffuse Horizontal Irradiance on clear days is calculated according to the following equation:

$$dHI = C \cdot \frac{DNI_{th}}{BI^2} \ [W/m^2] \tag{44}$$

Then the Direct Horizontal Irradiance on clear days is calculated:

$$DHI = DNI_{th} \cdot \cos(zenith) = DNI_{th} \cdot \text{sen}(altura\ solar) \tag{45}$$

Finally, the Total Horizontal Irradiance on clear days comes with the equation:

$$\text{THI} = dHI + DHI \ [W/m^2] \tag{46}$$

This gives the radiation for each representative day of each month. These daily radiations obtained are represented in the *Figure 21*, where highest values are the direct radiations and lower ones are the diffuse radiations.

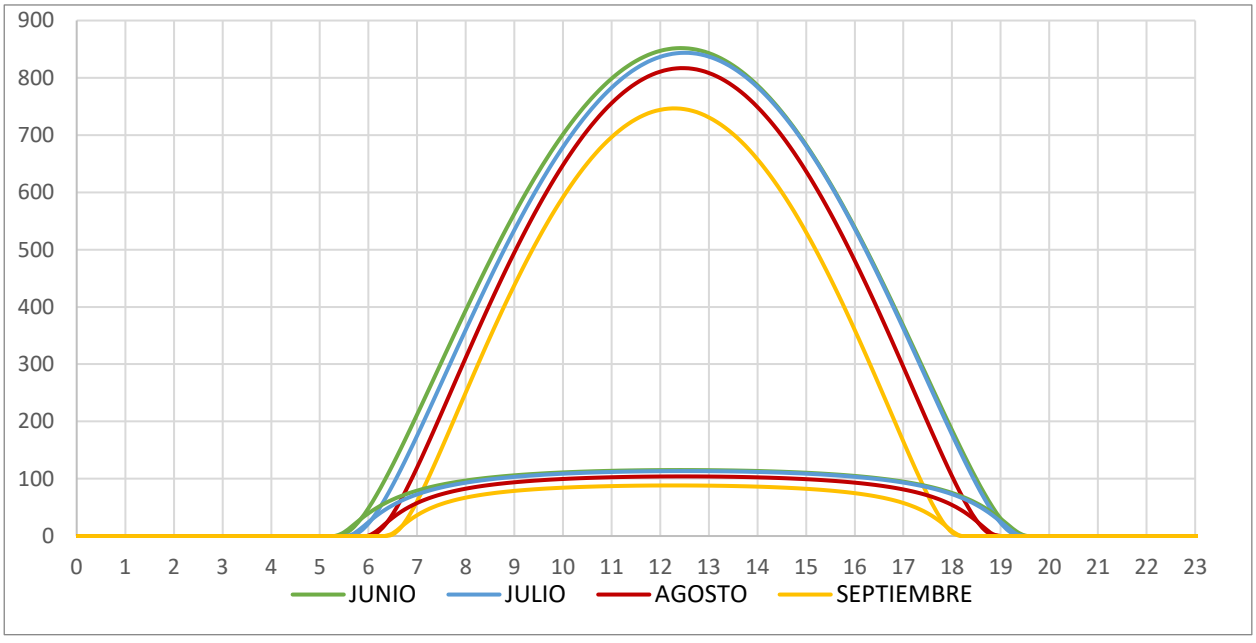

Figure 21 – Solar radiations of the representative days (W/m²)

5.6.3 Model coupling (air/surfaces) from one day to periodic established

Once geometric and climate data is known, the calculation programs RAD3D and MCKEA can give the surface temperature of every cell for each geometry. It also gives the radiations received.

In order to realise the sensitivity study, it is possible to run only this single calculation and to use the surface temperatures provided by these calculations. But it is important to bear in mind that these calculations are made using outdoor climatological data of the representative days. In this data, the temperature of the air which is used is always the one outside the street, instead of using the temperature inside the street enclosure, which is for now an unknown.

Since the initial conditions of T_{int} are not known, it is necessary to use the balance equation on air to calculate this interior temperature, as seen in 5.5.3. In total, 3 iterations are made over 3 following days, to erase the initial climate effects and reach a convergence point (*Figure 22*).

For the second and third iteration, the initial conditions are taken as follows: $T_{int} = T_{a,ext}$, for each hour.

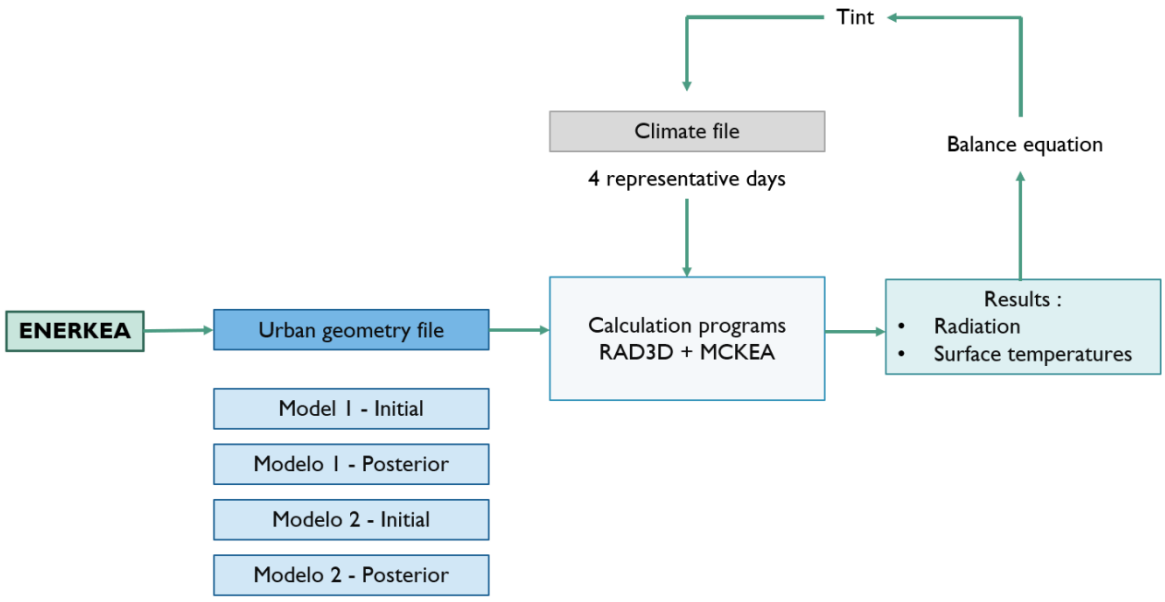

Figure 22 – Schematic view of the iterations

5.6.4 Integration values

In this part, ENERKEA outputs give values every 10 minutes. For the exploitation and presentation of the results for the initial and final situation, it is preferable to have data every hour. Thus, a time integration is carried out for each hour, for each situation, and each met (met 1 or met 2).

5.7 Study of the section

5.7.1 Description initial and final situation

The section is located between the Juan Manuel Rodríguez Correa and Antonio Machín intersections. The two side facades are 15 meters high. The living area is 30 m length and 15 m width.

5.7.1.1 Initial situation

Figure 23 – Initial situation of the section

From left to right in the image:

- Left sidewalk: Concrete on resistant structure. Reflectivity = 0,5. Occupancy = 0,45.
- Bicycle lane (green): Concrete on resistant structure. Reflectivity = 0,5. Occupancy = 0,1.
- Car lane (grey): Asphalt on resistant structure. Reflectivity = 0,1. Occupancy = 0.
- Right sidewalk: Concrete on resistant structure. Reflectivity = 0,5. Occupancy = 0,45.

There are 3 Sophora-Japonica trees 10 meters high according to OpenTrees.org.

It was considered more likely that there would be more people on the sidewalk than on the cycle lane. Throughout the study, the percentage of occupancy is 90% for the sidewalk and 10% for the cycle lane. These factors of occupancy must be entered into the calculation software at the same time as the surface properties. They will also be used to generate integrals to calculate averages for future calculations. They will be used as weighting factors.

5.7.1.2 Final situation

Figure 24 – Final situation of the section

In the image:

- Red sidewalk: Cobblestone (stone on resistant structure). Reflectivity = 0,75 (light color). Occupancy = 0,90.
- Green pavement: Tree surrounds or permeable pieces with 20% vegetation, and bike path. Possibility of a planter for seating. Reflectivity = 0,75. Occupancy = 0,10.

Five more trees are added according to plans. In total, there are 8 sophora-Japonica 10 meters high.

The following figure shows photos taken in July 2023, showing the current state of the section after rehabilitation works.

Figure 25 – Pictures of the section after rehabilitation works

5.7.2 Results

5.7.2.1 Air temperature

The balance on air was used to calculate the air temperature evolution in the street enclosure, for each representative day and each state (initial, final). It is compared to the temperature outside the street enclosure. The latter is the temperature of the air before entering the street, which will be heated inside, due to the various heat phenomena taking place there.

In this paragraph, the air temperature inside the street enclosure will be referred as the "indoor temperature". The air temperature at roof level will be referred as the "outdoor temperature". The graph for July is shown in *Figure 26*. The graphs for the other 3 months are shown in annex (7.2.1).

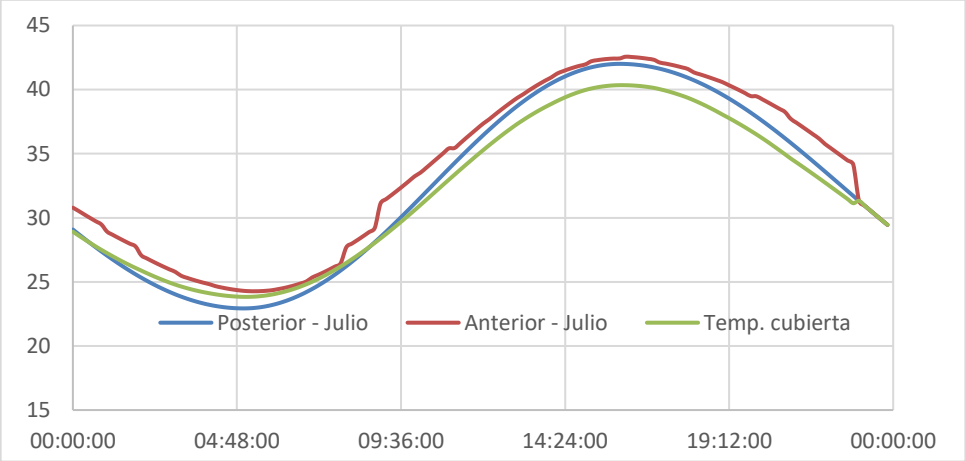

Figure 26 – Indoor air temperature evolution (°C) for July, for initial case (Posterior), final case (Posterior), and the outdoor temperature ("Temp.cubierta")

On the graph, indoor temperatures for initial case are always higher than the outside temperature *("Temp.cubierta")*. This difference is even more remarkable when the sun is at its maximum height. On the other hand, in the final case, the indoor temperature becomes lower than the temperature outside the street. For example, this is the case for July, between 1h and 9h. The graphs also show that after the rehabilitation works, the indoor air temperature is lower than it was in the initial situation.

Moreover, with elimination of traffic, anthropogenic heat has been eliminated compared to initial case. The influence of anthropogenic heat can be seen on the graphs because it has a constant value every hour, which is added to the balance equation of air (see 5.5.3). In the initial case, several temperature jumps are observed, particularly at 8h and 9h, when traffic picks up compared with the night. During the night, the jumps are less noticeable because there is less traffic.

5.7.2.2 COMFA study

In this section, the COMFA heat load (see 3.7) is calculated as a function of:

- The situation (initial or final)
- The representative day
- The met (1 or 2)
- The humidity. Three humidity levels (w) are considered: low (8 g/kg), medium (10 g/kg) and high (12 g/kg)

It is important to keep in mind that the following results have been done with the integration values (see 5.6.4).

5.7.2.2.1 Heat load evolution

For each representative day, each level of humidity and each met, the evolution of the heat load for both situations was calculated. The results showed that varying the humidity did not affect the curves so significantly. It has been decided to do the study with the high humidity. In the following graphs, only the results with met 2 are shown, since they reach the higher heat load: in average, the maximum for the met 1 is 40 W/m² below. The graphs with met 1 are shown in annex (7.2.2).

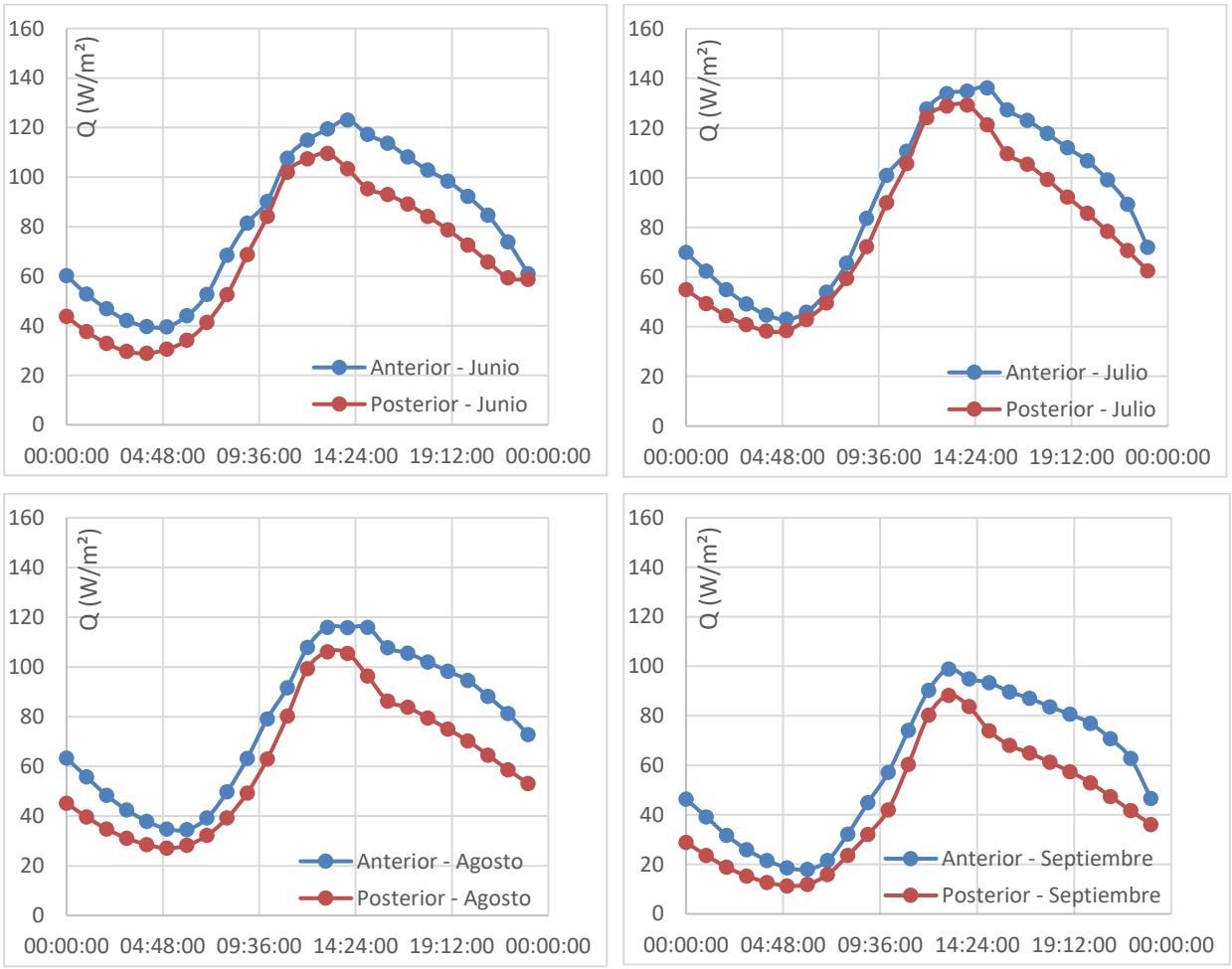

Figure 27 – Daily variation in heat load, for the initial (anterior) and final (posterior) states. From left to right, top to bottom: June, July, August, September

On the graphs, it is clear that heat load of the initial case is always higher than the case after rehabilitation works.

Between the end of the night and the beginning of the morning, the gap between the heat loads of the initial and final cases becomes narrower. For July, for example, these two heat loads are almost identical from 5h to 12h. However, during the rest of the day, this gap widens and becomes more substantial. On average, it is around 20 W/m² difference from 3pm to 8pm, the lowest load being that of the final case.

5.7.2.2.2 Heat load tables

For each representative day, each level of humidity and each met, the heat load values are calculated for four different times: 12h, 14h, 16h and 18h. To compare the initial and final states in a visual way, the heat load tables introduced in 4.3.2 are used. For a given hour, the values of the air temperature, the mean radiant temperature and the heat load are collected. The next step is to localise this set of data in the corresponding table. In this section, only tables with a velocity v = 0.2m/s will be studied. The results showed that varying the humidity did not affect the curves so significantly. It has been decided to do the study with the high humidity.

In this part, only the met 2, for 16h is represented. All other tables are given in the annex.

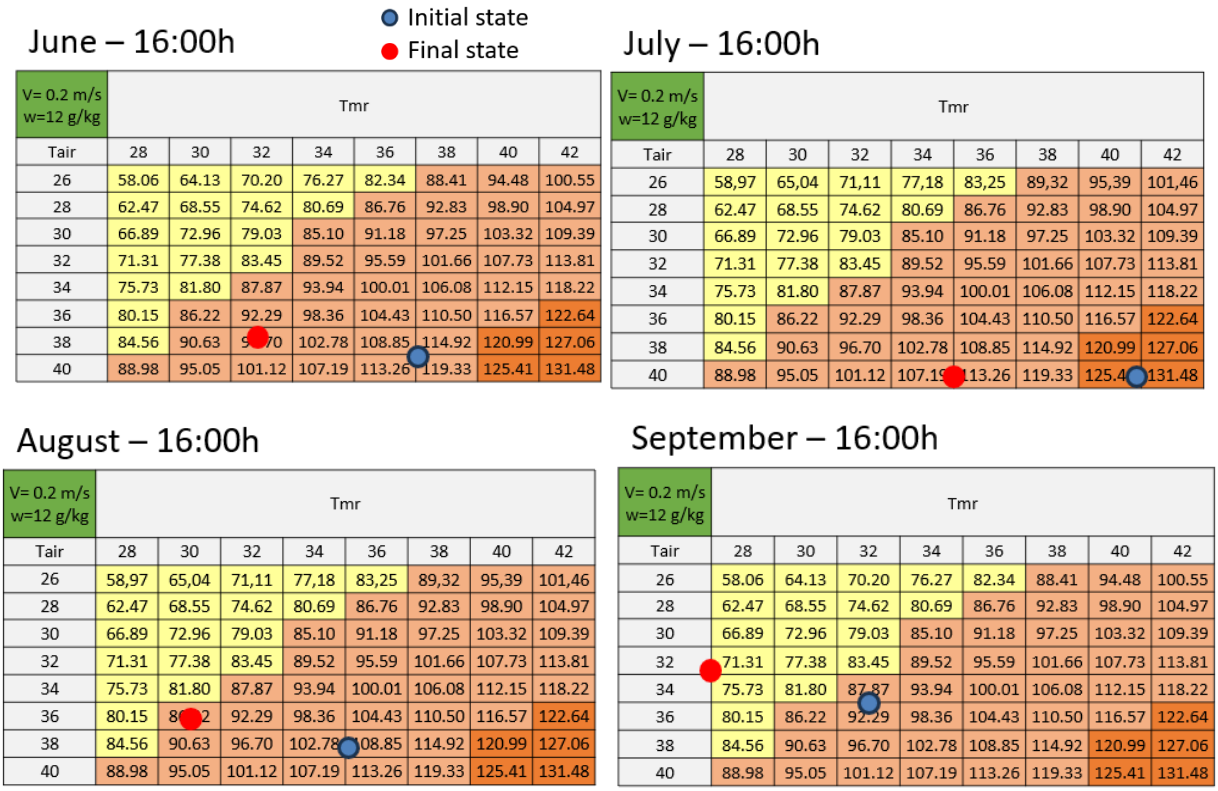

June – 16:00h

V= 0.2 m/s w=12 g/kg	Tmr							
Tair	28	30	32	34	36	38	40	42
26	58.06	64.13	70.20	76.27	82.34	88.41	94.48	100.55
28	62.47	68.55	74.62	80.69	86.76	92.83	98.90	104.97
30	66.89	72.96	79.03	85.10	91.18	97.25	103.32	109.39
32	71.31	77.38	83.45	89.52	95.59	101.66	107.73	113.81
34	75.73	81.80	87.87	93.94	100.01	106.08	112.15	118.22
36	80.15	86.22	92.29	98.36	104.43	110.50	116.57	122.64
38	84.56	90.63	96.70	102.78	108.85	114.92	120.99	127.06
40	88.98	95.05	101.12	107.19	113.26	119.33	125.41	131.48

July – 16:00h

V= 0.2 m/s w=12 g/kg	Tmr							
Tair	28	30	32	34	36	38	40	42
26	58,97	65,04	71,11	77,18	83,25	89,32	95,39	101,46
28	62.47	68.55	74.62	80.69	86.76	92.83	98.90	104.97
30	66.89	72.96	79.03	85.10	91.18	97.25	103.32	109.39
32	71.31	77.38	83.45	89.52	95.59	101.66	107.73	113.81
34	75.73	81.80	87.87	93.94	100.01	106.08	112.15	118.22
36	80.15	86.22	92.29	98.36	104.43	110.50	116.57	122.64
38	84.56	90.63	96.70	102.78	108.85	114.92	120.99	127.06
40	88.98	95.05	101.12	107.19	113.26	119.33	125.41	131.48

August – 16:00h

V= 0.2 m/s w=12 g/kg	Tmr							
Tair	28	30	32	34	36	38	40	42
26	58,97	65,04	71,11	77,18	83,25	89,32	95,39	101,46
28	62.47	68.55	74.62	80.69	86.76	92.83	98.90	104.97
30	66.89	72.96	79.03	85.10	91.18	97.25	103.32	109.39
32	71.31	77.38	83.45	89.52	95.59	101.66	107.73	113.81
34	75.73	81.80	87.87	93.94	100.01	106.08	112.15	118.22
36	80.15	86.22	92.29	98.36	104.43	110.50	116.57	122.64
38	84.56	90.63	96.70	102.78	108.85	114.92	120.99	127.06
40	88.98	95.05	101.12	107.19	113.26	119.33	125.41	131.48

September – 16:00h

V= 0.2 m/s w=12 g/kg	Tmr							
Tair	28	30	32	34	36	38	40	42
26	58.06	64.13	70.20	76.27	82.34	88.41	94.48	100.55
28	62.47	68.55	74.62	80.69	86.76	92.83	98.90	104.97
30	66.89	72.96	79.03	85.10	91.18	97.25	103.32	109.39
32	71.31	77.38	83.45	89.52	95.59	101.66	107.73	113.81
34	75.73	81.80	87.87	93.94	100.01	106.08	112.15	118.22
36	80.15	86.22	92.29	98.36	104.43	110.50	116.57	122.64
38	84.56	90.63	96.70	102.78	108.85	114.92	120.99	127.06
40	88.98	95.05	101.12	107.19	113.26	119.33	125.41	131.48

Figure 28 – Heat load table (W/m²) for initial and final state, for met 2, high humidity, v=0,2m/s and at 16h

On the heat load tables, the points always move to the left and upwards from the initial and final case. This means that after rehabilitation works, the air temperature and the mean radiant temperature decrease. The reduction in the mean radiant temperature means that there are less radiations: the greater number of trees blocks some of the incident radiation.

The most significant movements are always in radiant temperature, they are small for the air temperature. For example, in July at 16h, the radiant temperature fell from 41°C to 35°C, while the air temperature did not fall.

Over the day, even if the air temperature increases in each situation, the difference in air temperature remains almost unchanged. For example, for the month of September (met 1, see annex 7.2.3.1), there is a difference of 2°C at 12h, then 2°C, then 3°C and finally 3°C at 18h. On the other hand, the variation is not the same for radiant temperature. For the same month of September, the difference rises from 2°C at 12h, to 2°C, to 5°C and then to 4°C at 18h.

5.7.2.2.3 Heat load frequency

For each representative day, each level of humidity and each met, a frequency analyse is carried out for both situations. The results showed that varying the humidity did not affect the curves so significantly. It has been decided to do the study with the high humidity. First, the study is done with histograms done for the whole day, for each month. In a second part, an integral of the heat load frequencies for the full four months is generated, from 12h to 18h.

The table gives the frequency when the occupant is considered in the different zones in the comfort scale: comfortable (C), slightly warm (SW), warm (W), hot (H), or sweltering (S). Calculations are made for the whole day. From this tables, it is possible to generate a frequency histogram in order to compare the heat load in the initial and final situation (*Figure 29*).

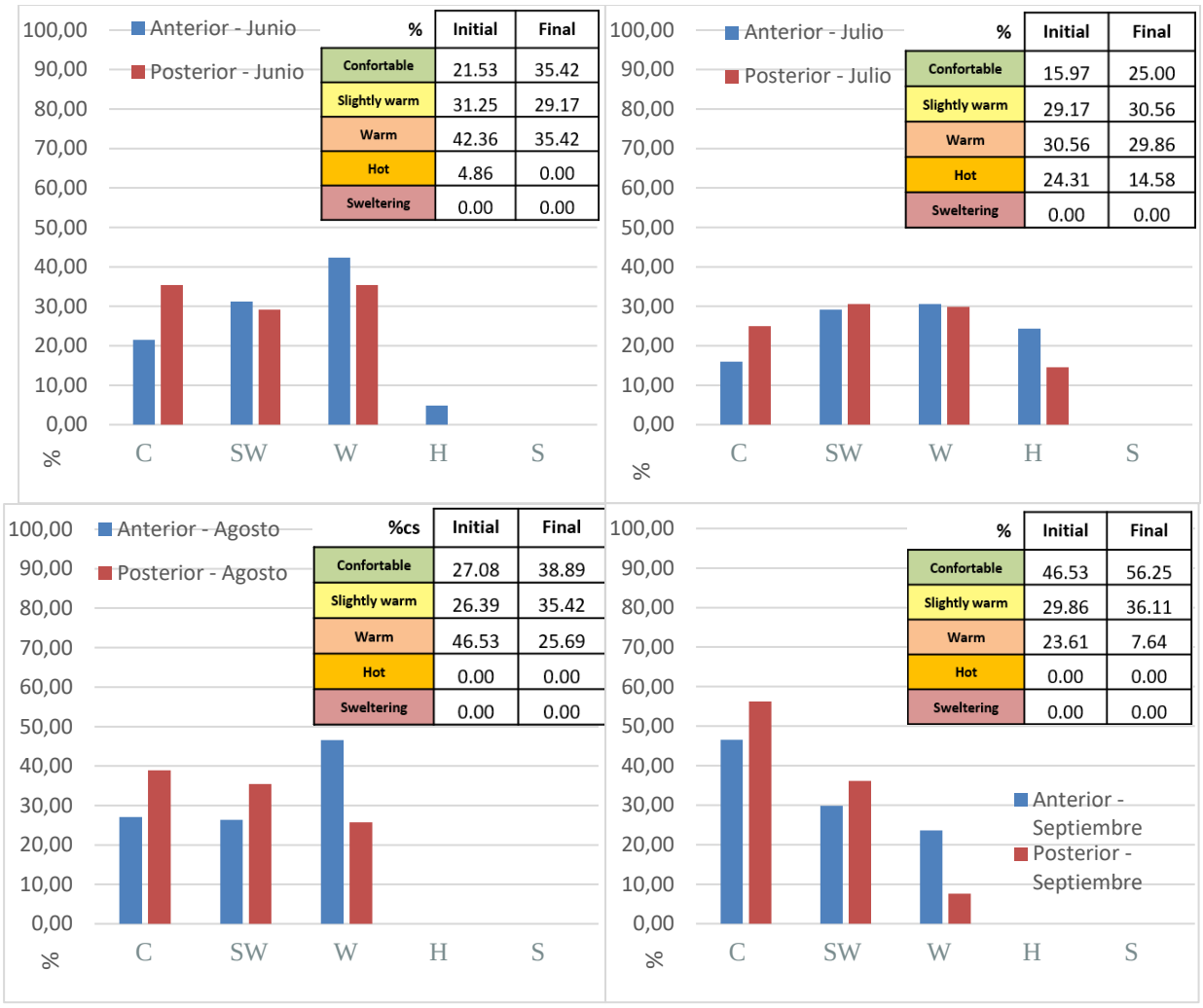

Figure 29 – Frequency of heat load, for the initial (anterior) and final (posterior) states. From left to right, top to bottom: June, July, August, September. Met 2

The histograms for met 2 show that heat load values are spread across the 4 zones of the comfort scale up to "Hot" for the months of June and July. In August and September, the heat load decreases, covering only 3 zones of the comfort scale, up to "Warm".

As we move from the initial state to the final state, the histograms shift to the left, indicating that there are fewer values in the high heat load range. In June, for example, there were 4.86% of heat load values in the "hot" zone in the initial state, and none in the final state.

It can be seen that the trends are the same, but more or less marked depending on the month. Compared with the initial situation:

- "Comfort" frequency increases (on average it is multiplied by 1.46).
- “Slightly warm" frequency increases slightly (on average multiplied by 1.13).
- “Warm" frequency decreases (on average multiplied by 0.67).
- “Hot” frequency decreases 100% for June and decreases with a 0,6 factor for July.

It is also interesting to compare the same month for the two different met. The following histograms compare the month of August.

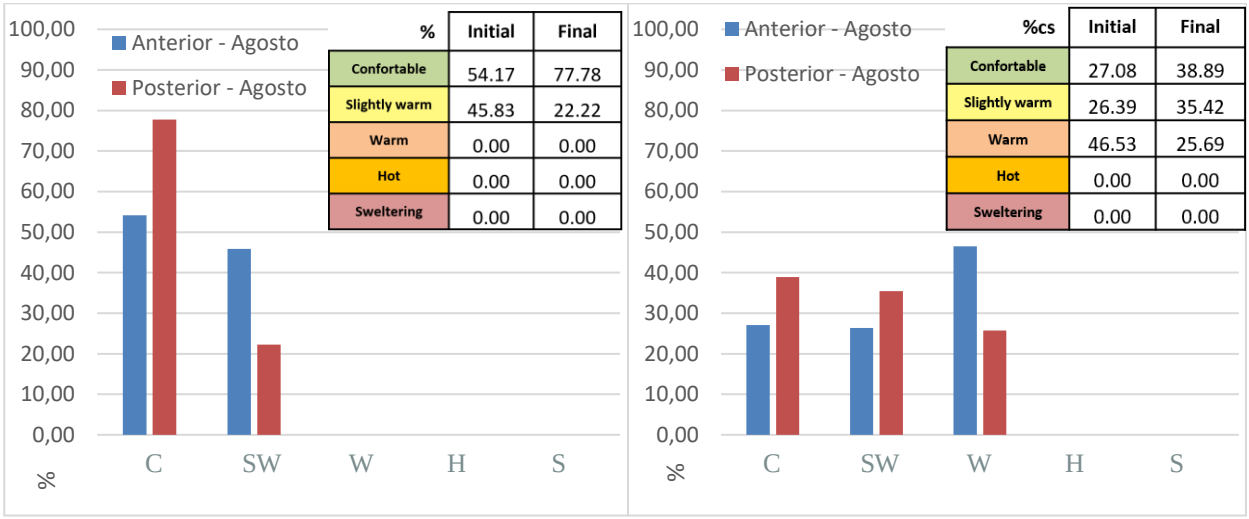

Figure 30 – Frequency of heat load, for the initial (anterior) and final (posterior) states for month of august. From left to right: met 1 and met 2.

The histograms for met 1 also shift to the left, indicating that comfort is better in the final situation. There are more heat load values at the lower level of the comfort scale for met 1. This is coherent since met 1 is a person at rest compared to met 2 which is a person walking. In the final state for met 1, "Comfortable" frequencies increase, while "Slightly warm" frequencies decrease, meaning the histogram is indeed shifting to the left, and is more concentrated around the comfortable.

Then, the values of heat load for the four months are studied, only from 12h to 18h. The reason is that this time slot represents the central hours of the day, where the sun hits the more pavement and temperatures are at the maximum (see the air temperature evolution in 5.7.2.1). This provides the number of occurrences of the heat load. This is done for the 4 representative days, from 12h to 18h, with values integrated every 10 minutes, giving a total of 148 values. With this, a continuous integral of the heat load apparition is generated, for this period of time. The next 2 graphs show this integral for met 1 and met 2.

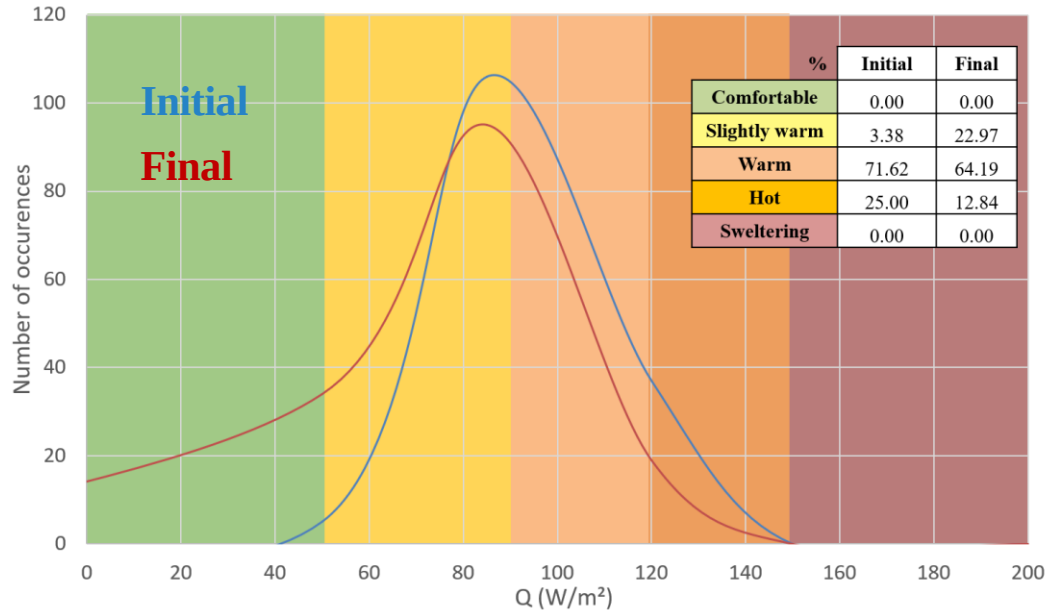

%	Initial	Final
Comfortable	0.00	0.00
Slightly warm	3.38	22.97
Warm	71.62	64.19
Hot	25.00	12.84
Sweltering	0.00	0.00

Figure 31 – Heat load frequency for the four months, met 1

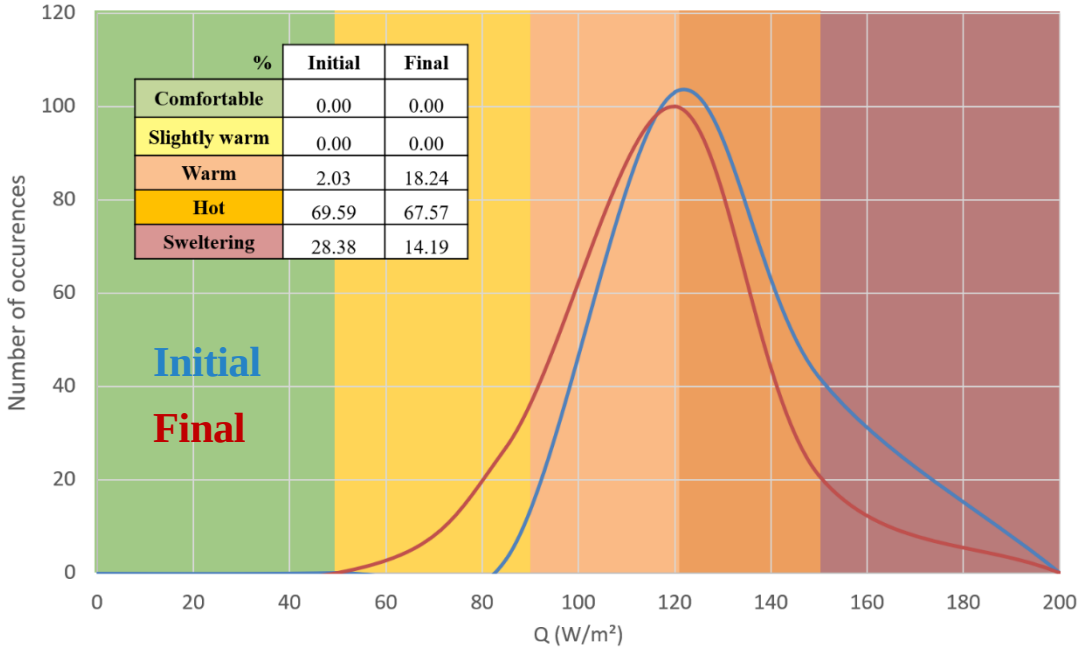

%	Initial	Final
Comfortable	0.00	0.00
Slightly warm	0.00	0.00
Warm	2.03	18.24
Hot	69.59	67.57
Sweltering	28.38	14.19

Figure 32 – Heat load frequency for the four months, met 2

The major difference between met 1 and met 2 is that the curves are more to the left for met 1. There are more values in comfort zone. This is logical, as commented before because met 1 corresponds to less physical activity than met 2.

For each met, the trends are the same: the curves of the final state are more spread out, shifting to the left in relation to the initial state. For example, the maximum frequency goes down from the "hot" state to the "warm" state in the case of met 2.

It has been noticed that running the same calculations but at early hours, the graph is mostly in the green zone. Indeed, the more the graph is on the left, the more the number of hours the occupants are in comfort. This is the case in the morning where radiations and temperatures are not too hight.

5.7.3 Justification

In an attempt to explain the results obtained above and to justify that the rehabilitation work does indeed help to mitigate the UHI effect, other complementary studies are carried out:

- The superficial temperatures of the pavement.
- The radiations absorbed by pavement.

5.7.3.1 Superficial temperatures of the pavement

To study the surface temperature of the pavement, a spatial integral is performed on all the cells making up the pavement. This gives a single surface temperature for the pavement. The integration takes into account the geometry defined in the software and the weighting factors representing the occupancy rate of the pavement (see 5.7.1).

The graph for August is shown below. See the appendix for the other months.

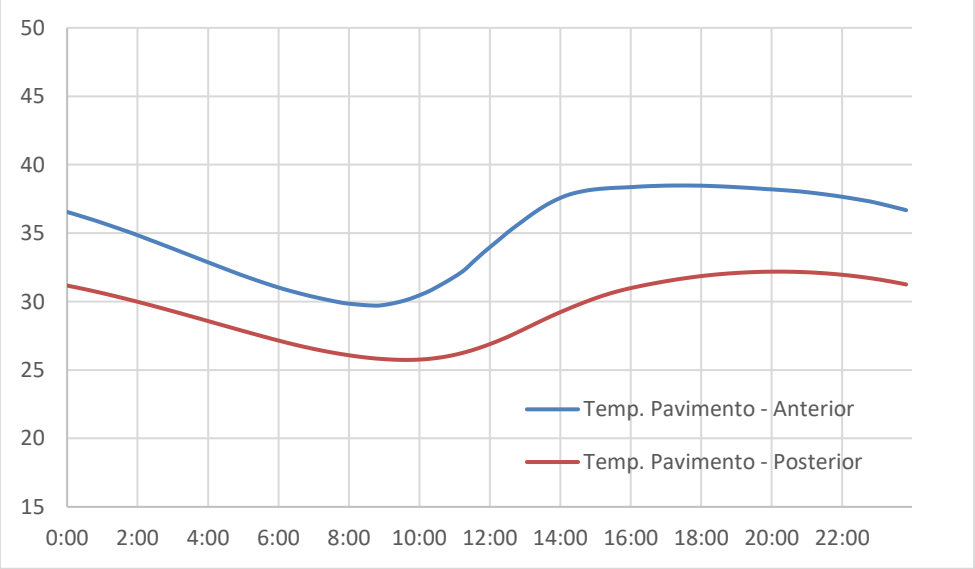

Figure 33 – Superficial temperature evolution of the pavement (°C), August

For July, August and September, the temperature gap between each situation is varying between 3.5 and 8°C. In the month of June, the difference is less noticeable than for the other months. There is generally a difference of 1.5 or 2°C between the two situations.

The rehabilitation works therefore help to reduce the surface temperature of the pavements. The effect on temperature reduction is as significant during the day as at night.

5.7.3.2 Radiations absorbed by the pavement

Finally, the radiations absorbed by the ground is interesting to study. This is the incident radiation on the ground (direct and diffuse radiation), taking into account the multiplicative factor of absorptivity. The graphs for August are shown here, the other ones are in annex.

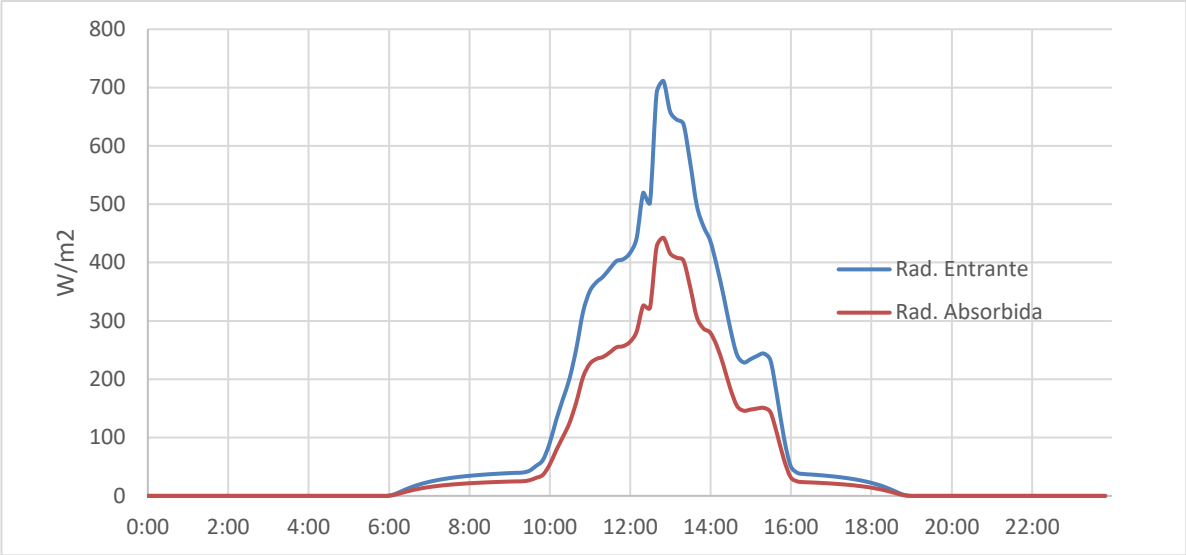

Figure 34 –Evolution of absorbed and incoming radiations in the street (W/m²), Initial case, August

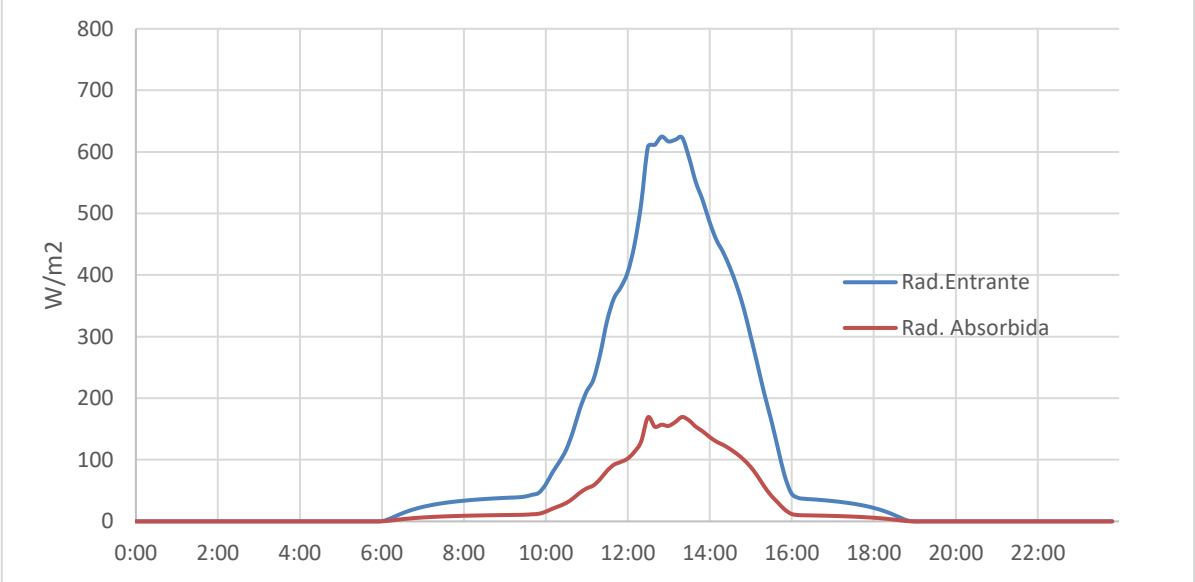

Figure 35 – Evolution of absorbed and incoming radiations in the street (W/m²), Final case, August

On these graphs, the red curve is the radiations absorbed by the pavement and the facades. The blue curve is all the radiations that enters the street, which is the sum of diffuse and direct radiations. The radiation absorbed decreases considerably in the final state. The maximum drops from 442 to 154 W/m². The difference is explained by the fact that the reflectivity changes between the two states, so has the absorptivity. This result is closely linked to the surface temperature of the pavement, which is also reduced. The same conclusions can be drawn for incoming radiation, although it is declining more slowly: from 711 W/m² to 623 W/m².

5.7.4 Conclusions

The heat due to the solar radiations that reach the ground stays in the street environment since the ground is supposed to be adiabatic. The part absorbed by the ground is transferred to the air and surrounding objects by convection. Since the surface temperature of the ground is increased by the action of the incident rays, it releases a certain amount of radiant energy in the form of longwave radiation. It thus heats up the street. For the radiations reaching the buildings, one part of the heat is absorbed by the building and the other part stays in the street environment. It increases the air temperature inside the street.

The radiations on the ground and buildings therefore raises the temperature in the street. This justifies the fact that when air enters the street, it heats up, due to convection. The air comes out of the street with at a higher temperature. This explains the shape of the street air temperature curves, which increase over the day.

As the ground is made of more reflective materials, more incident rays are reflected, so fewer are absorbed. Added to this phenomenon, the radiation absorption of the trees has slightly increased because more trees have been put up, decreasing the absorption of the pavement and the surrounding surfaces. To sum up, the addition of trees and the modification of ground reflection play a major role in absorbed radiation. This has been demonstrated by the study of the radiation absorbed by the pavement which shows that the maximum decreases by 53% on average. This major reduction in incident radiation explains the movements in the heat load tables (see 5.7.2.2.2), where the most significant movements between the two states are in radiant temperature, not ambient temperature. Radiations that used to be absorbed by the pavement are now much less so. They contribute less to longwave radiation and convection from the pavement.

All this has a major influence on the superficial temperatures, which can be reduced between 1,5°C and 8°C compared with what they might have been before the rehabilitation works were carried out. As a result, the air temperature inside the street enclosure decreases.

Moreover, the effect of the anthropogenic generation contributed to the high temperature in the initial case. After rehabilitation works, the anthropogenic generation decreased because there is no traffic anymore, contributing to the reduction of the air temperature.

The rehabilitation works does contribute to reducing the urban heat island effect. In addition, by reducing the surface temperatures and air temperature in the street, it has shown that pedestrian comfort has been increased. Among all the heat load tables calculated to observe comfort zone shifts, there is one case where the initial situation was already in the comfort zone, 14 cases that remained in the same zone in the final state, and 17 that changed category, moving closer to the comfort zones. These movements are due to the combined effect of the decrease in surface temperature, the decrease in air temperature and the decrease in radiation on the occupant. This has resulted in a reduction in the median temperature ranging from 1 to 8°C, with an average of 3°C.

6 CONCLUSION

Initially, this study planted the equations needed to introduce outdoor thermal comfort. Among the various ways of quantifying and calculating comfort, heat load was chosen through COMFA calculations. This comfort, which is difficult to qualify because it is subjective, was assessed using a thermal comfort scale that indicates five zones in which a pedestrian can feel from comfortable to suffocating.

Thanks to this theoretical study, it was possible to carry out a preliminary analysis before doing it on the real avenue. By analysing the climate effects on the thermal comfort perceived by the occupant through the heat load, it has been shown that it is possible to analyse this heat load as a function of air temperature and mean radiant temperature.

Finally, the heart of this master thesis is the last part, the study of the impact of the rehabilitation works in the Avenue de la Cruz Roja on perceived thermal comfort. The idea was to compare different data between the initial state and the final state. To achieve this, a few additional theoretical studies were carried out. Firstly, it was necessary to determine the air temperature inside the street, which is different from that outside, given that the street can be compared to an urban canyon where the buildings, air circulation and traffic create a completely different environment. Then, the anthropogenic heat released by traffic had to be modelled. After defining the climate conditions on representative days for the four hottest months of the year, calculations were carried out on a section of the street, including the air temperature, surface temperatures, radiation absorbed by the pavement, and the heat load perceived by pedestrians, whether sitting or walking.

The study showed that the change in pavement reflection means that more of the incident rays are returned to the atmosphere, reducing absorption by the pavement and surrounding surfaces. With the removal of the car lane, the anthropogenic generation decreased because there is no traffic anymore, contributing to the reduction of the air temperature. The greater number of trees prevents some of the incident rays from reaching the surfaces, thereby reducing the radiation absorbed and the surface temperature. The interaction between the reduction in surface temperature, in air temperature and in radiation has improved pedestrian comfort.

In conclusion, this study has shown that the UHI mitigation measures taken in the Avenue de la Cruz Roja have been beneficial. The actions that had the greatest impact on this reduction were the addition of greenery, the increase in the reflectivity of the ground, and the absence of traffic. The solutions to combat UHI, by modifying public spaces can improve the use and comfort of outdoor space.

7 ANNEX

7.1 Sensitivity study

7.1.1 Met 1

V= 0.2 m/s w=8 g/kg	Tmr							
Taire	28	30	32	34	36	38	40	42
26	19,00	25,07	31,14	37,21	43,28	49,35	55,43	61,50
28	23,25	29,32	35,39	41,46	47,53	53,60	59,67	65,75
30	27,50	33,57	39,64	45,71	51,78	57,85	63,92	70,00
32	31,75	37,82	43,89	49,96	56,03	62,10	68,17	74,24
34	36,00	42,07	48,14	54,21	60,28	66,35	72,42	78,49
36	40,25	46,32	52,39	58,46	64,53	70,60	76,67	82,74
38	44,50	50,57	56,64	62,71	68,78	74,85	80,92	86,99
40	48,75	54,82	60,89	66,96	73,03	79,10	85,17	91,24

V= 1 m/s w=8 g/kg	Tmr							
Taire	28	30	32	34	36	38	40	42
26	6,23	10,92	15,62	20,31	25,00	29,70	34,39	39,09
28	14,69	19,38	24,07	28,77	33,46	38,16	42,85	47,54
30	23,14	27,84	32,53	37,23	41,92	46,61	51,31	56,00
32	31,60	36,30	40,99	45,68	50,38	55,07	59,77	64,46
34	40,06	44,75	49,45	54,14	58,83	63,53	68,22	72,92
36	48,52	53,21	57,90	62,60	67,29	71,99	76,68	81,37
38	56,97	61,67	66,36	71,06	75,75	80,44	85,14	89,83
40	65,43	70,13	74,82	79,51	84,21	88,90	93,60	98,29

V= 0.2 m/s w=10 g/kg	Tmr							
Taire	28	30	32	34	36	38	40	42
26	19,33	25,40	31,47	37,54	43,61	49,68	55,75	61,82
28	23,58	29,65	35,72	41,79	47,86	53,93	60,00	66,07
30	27,83	33,90	39,97	46,04	52,11	58,18	64,25	70,32
32	32,08	38,15	44,22	50,29	56,36	62,43	68,50	74,57
34	36,33	42,40	48,47	54,54	60,61	66,68	72,75	78,82
36	40,58	46,65	52,72	58,79	64,86	70,93	77,00	83,07
38	44,83	50,90	56,97	63,04	69,11	75,18	81,25	87,32
40	49,08	55,15	61,22	67,29	73,36	79,43	85,50	91,57

V= 1 m/s w=10 g/kg	Tmr							
Taire	28	30	32	34	36	38	40	42
26	6,56	11,25	15,95	20,64	25,33	30,03	34,72	39,42
28	15,01	19,71	24,40	29,10	33,79	38,48	43,18	47,87
30	23,47	28,17	32,86	37,55	42,25	46,94	51,64	56,33
32	31,93	36,62	41,32	46,01	50,71	55,40	60,09	64,79
34	40,39	45,08	49,78	54,47	59,16	63,86	68,55	73,25
36	48,84	53,54	58,23	62,93	67,62	72,32	77,01	81,70
38	57,30	62,00	66,69	71,38	76,08	80,77	85,47	90,16
40	65,76	70,45	75,15	79,84	84,54	89,23	93,92	98,62

V= 0.2 m/s w=12 g/kg	Tmr							
Taire	28	30	32	34	36	38	40	42
26	19,66	25,73	31,80	37,87	43,94	50,01	56,08	62,15
28	23,91	29,98	36,05	42,12	48,19	54,26	60,33	66,40
30	28,16	34,23	40,30	46,37	52,44	58,51	64,58	70,65
32	32,40	38,48	44,55	50,62	56,69	62,76	68,83	74,90
34	36,65	42,73	48,80	54,87	60,94	67,01	73,08	79,15
36	40,90	46,97	53,05	59,12	65,19	71,26	77,33	83,40
38	45,15	51,22	57,30	63,37	69,44	75,51	81,58	87,65
40	49,40	55,47	61,55	67,62	73,69	79,76	85,83	91,90

V= 1 m/s w=12 g/kg	Tmr							
Taire	28	30	32	34	36	38	40	42
26	6,88	11,58	16,27	20,97	25,66	30,35	35,05	39,74
28	15,34	20,04	24,73	29,42	34,12	38,81	43,51	48,20
30	23,80	28,49	33,19	37,88	42,57	47,27	51,96	56,66
32	32,26	36,95	41,64	46,34	51,03	55,73	60,42	65,11
34	40,71	45,41	50,10	54,80	59,49	64,18	68,88	73,57
36	49,17	53,87	58,56	63,25	67,95	72,64	77,34	82,03
38	57,63	62,32	67,02	71,71	76,41	81,10	85,79	90,49
40	66,09	70,78	75,47	80,17	84,86	89,56	94,25	98,94

7.1.2 Met 2

V= 0.2 m/s w=8 g/kg	Tmr							
Tair	28	30	32	34	36	38	40	42
26	57,66	63,73	69,80	75,87	81,94	88,01	94,08	100,15
28	61,16	67,24	73,31	79,38	85,45	91,52	97,59	103,66
30	65,58	71,65	77,72	83,79	89,87	95,94	102,01	108,08
32	70,00	76,07	82,14	88,21	94,28	100,35	106,42	112,50
34	74,42	80,49	86,56	92,63	98,70	104,77	110,84	116,91
36	78,84	84,91	90,98	97,05	103,12	109,19	115,26	121,33
38	83,25	89,32	95,39	101,47	107,54	113,61	119,68	125,75
40	87,67	93,74	99,81	105,88	111,95	118,02	124,10	130,17

V= 1 m/s w=8 g/kg	Tmr							
Tair	28	30	32	34	36	38	40	42
26	47,01	51,71	56,40	61,10	65,79	70,48	75,18	79,87
28	54,94	59,63	64,32	69,02	73,71	78,41	83,10	87,79
30	63,56	68,26	72,95	77,64	82,34	87,03	91,73	96,42
32	72,19	76,88	81,58	86,27	90,96	95,66	100,35	105,05
34	80,81	85,51	90,20	94,89	99,59	104,28	108,98	113,67
36	89,44	94,13	98,83	103,52	108,21	112,91	117,60	122,30
38	98,06	102,76	107,45	112,15	116,84	121,53	126,23	130,92
40	106,69	111,38	116,08	120,77	125,47	130,16	134,85	139,55

V= 0.2 m/s w=10 g/kg	Tmr							
Tair	28	30	32	34	36	38	40	42
26	58,31	64,39	70,46	76,53	82,60	88,67	94,74	100,81
28	61,82	67,89	73,96	80,03	86,10	92,18	98,25	104,32
30	66,24	72,31	78,38	84,45	90,52	96,59	102,66	108,73
32	70,66	76,73	82,80	88,87	94,94	101,01	107,08	113,15
34	75,07	81,15	87,22	93,29	99,36	105,43	111,50	117,57
36	79,49	85,56	91,63	97,70	103,78	109,85	115,92	121,99
38	83,91	89,98	96,05	102,12	108,19	114,26	120,33	126,41
40	88,33	94,40	100,47	106,54	112,61	118,68	124,75	130,82

V= 1 m/s w=10 g/kg	Tmr							
Tair	28	30	32	34	36	38	40	42
26	47,67	52,37	57,06	61,75	66,45	71,14	75,84	80,53
28	55,59	60,29	64,98	69,68	74,37	79,06	83,76	88,45
30	64,22	68,91	73,61	78,30	82,99	87,69	92,38	97,08
32	72,84	77,54	82,23	86,93	91,62	96,31	101,01	105,70
34	81,47	86,16	90,86	95,55	100,25	104,94	109,63	114,33
36	90,10	94,79	99,48	104,18	108,87	113,57	118,26	122,95
38	98,72	103,41	108,11	112,80	117,50	122,19	126,89	131,58
40	107,35	112,04	116,73	121,43	126,12	130,82	135,51	140,20

V= 0.2 m/s w=12 g/kg	Tmr							
Tair	28	30	32	34	36	38	40	42
26	58,97	65,04	71,11	77,18	83,25	89,32	95,39	101,46
28	62,47	68,55	74,62	80,69	86,76	92,83	98,90	104,97
30	66,89	72,96	79,03	85,10	91,18	97,25	103,32	109,39
32	71,31	77,38	83,45	89,52	95,59	101,66	107,73	113,81
34	75,73	81,80	87,87	93,94	100,01	106,08	112,15	118,22
36	80,15	86,22	92,29	98,36	104,43	110,50	116,57	122,64
38	84,56	90,63	96,70	102,78	108,85	114,92	120,99	127,06
40	88,98	95,05	101,12	107,19	113,26	119,33	125,41	131,48

V= 1 m/s w=12 g/kg	Tmr							
Tair	28	30	32	34	36	38	40	42
26	48,32	53,02	57,71	62,41	67,10	71,79	76,49	81,18
28	56,25	60,94	65,63	70,33	75,02	79,72	84,41	89,10
30	64,87	69,57	74,26	78,95	83,65	88,34	93,04	97,73
32	73,50	78,19	82,89	87,58	92,27	96,97	101,66	106,36
34	82,12	86,82	91,51	96,20	100,90	105,59	110,29	114,98
36	90,75	95,44	100,14	104,83	109,52	114,22	118,91	123,61
38	99,37	104,07	108,76	113,46	118,15	122,84	127,54	132,23
40	108,00	112,69	117,39	122,08	126,78	131,47	136,16	140,86

7.2 Studied section

7.2.1 Air temperature

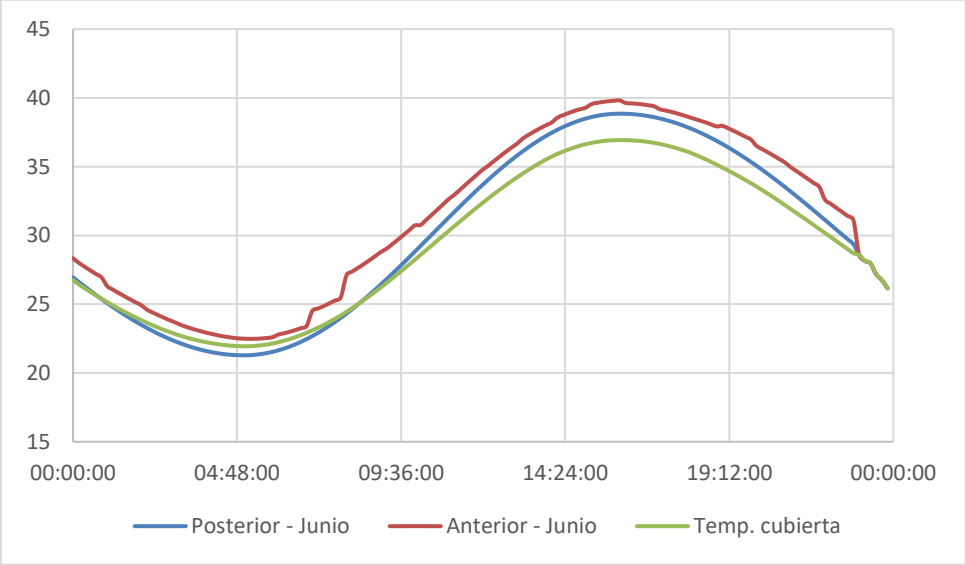

Indoor air temperature evolution (°C) for June, for initial case (posterior), final case (posterior), and the outdoor temperature (cubierta)

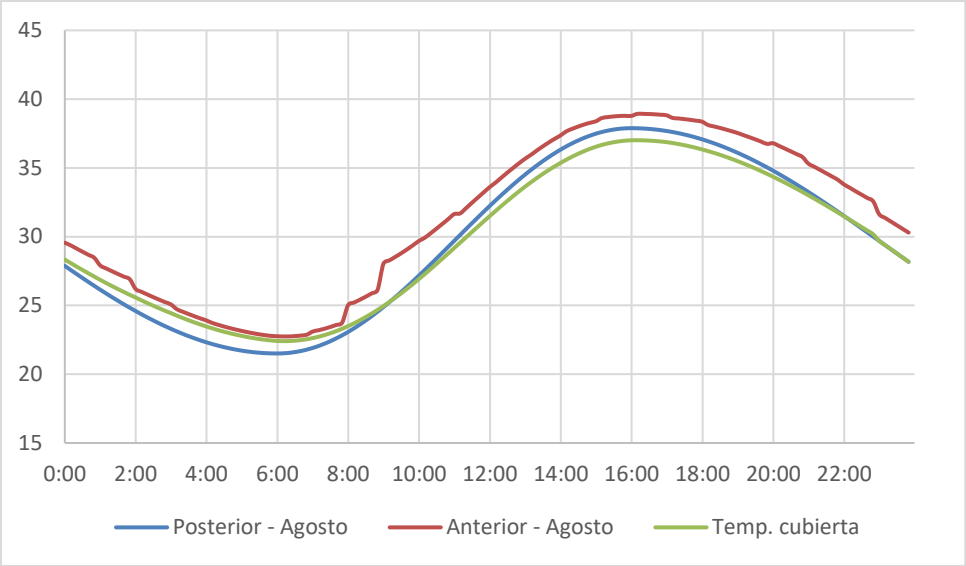

Indoor air temperature evolution (°C) for August, for initial case (posterior), final case (posterior), and the outdoor temperature (cubierta)

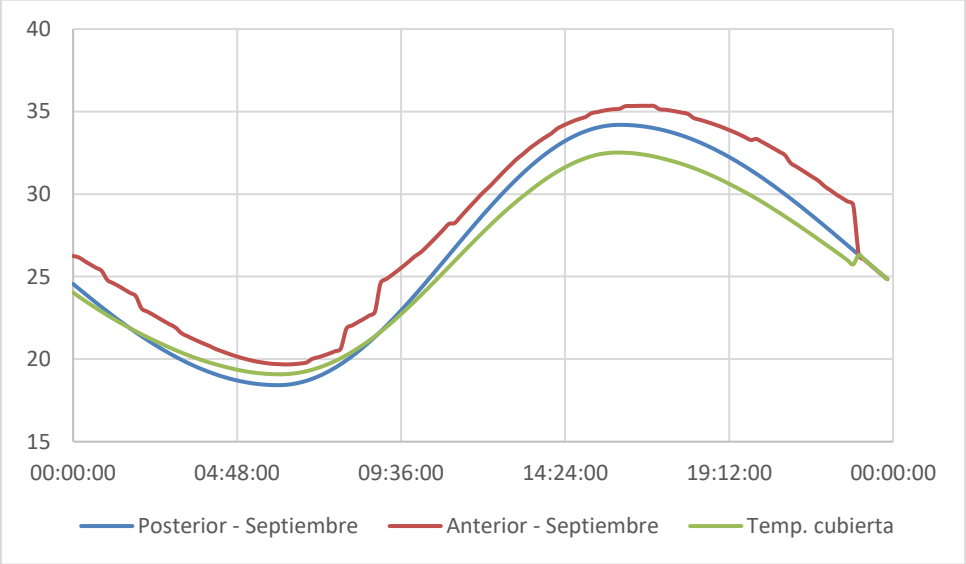

Indoor air temperature evolution (°C) for September, for initial case (posterior), final case (posterior), and the outdoor temperature (cubierta)MO

7.2.2 Heat load evolution

7.2.2.1 Met 1

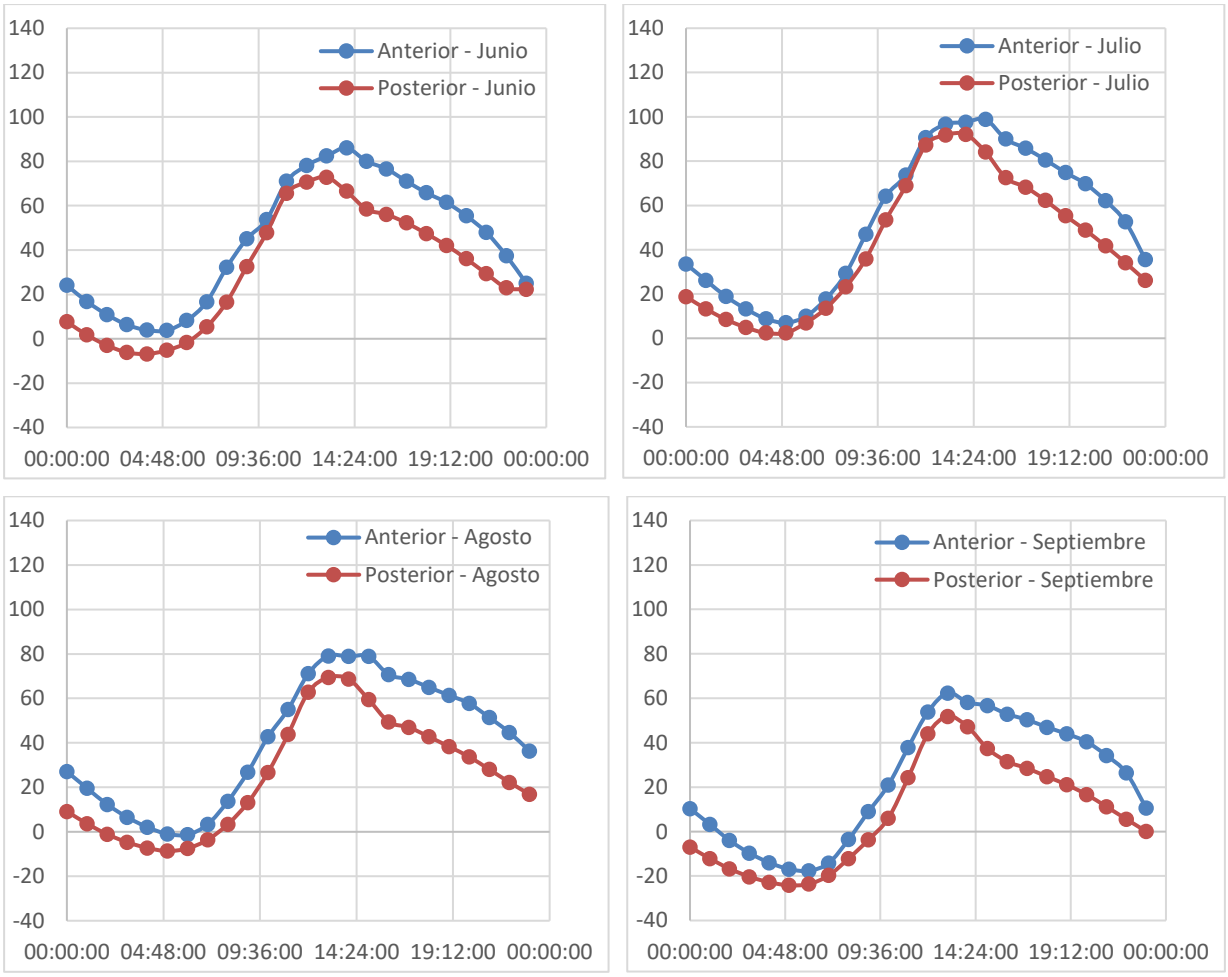

Daily variation in heat load, for the initial (anterior) and final (posterior) states, met 1. From left to right, top to bottom: June, July, August, September

7.2.2.2 Met 2

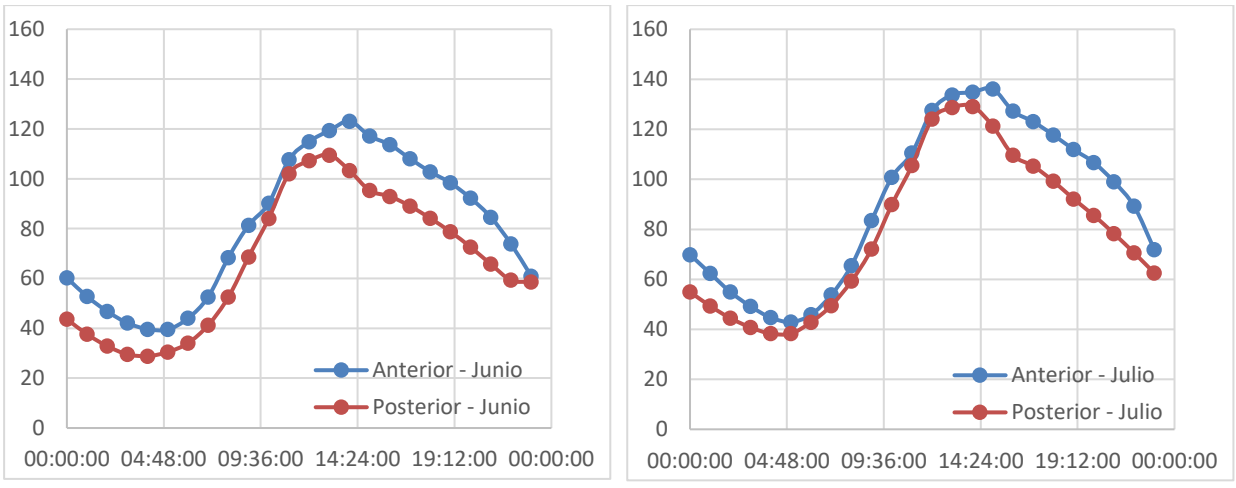

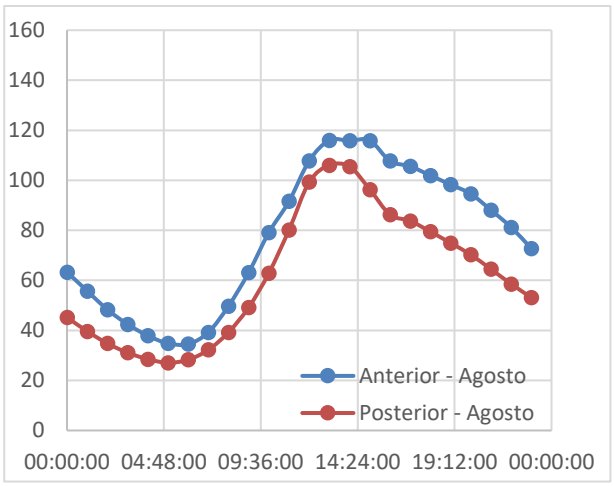

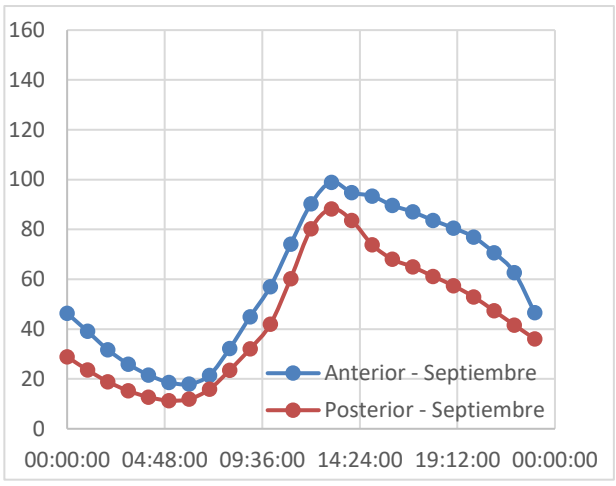

Daily variation in heat load, for the initial (anterior) and final (posterior) states, met 2. From left to right, top to bottom: June, July, August, September

7.2.3 Heat load tables

7.2.3.1 Met 1

June – 12:00h

V= 0.2 m/s w=12 g/kg	Tmr							
Tair	28	30	32	34	36	38	40	42
26	19,66	25,73	31,80	37,87	43,94	50,01	56,08	62,15
28	23,91	29,98	36,05	42,12	48,19	54,26	60,33	66,40
30	28,16	34,23	40,30	46,37	52,44	58,51	64,58	70,65
32	32,40	38,48	44,55	50,62	56,69	62,76	68,83	74,90
34	36,65	42,73	48,80	54,87	60,94	67,01	73,08	79,15
36	40,90	46,97	53,05	59,12	65,19	71,26	77,33	83,40
38	45,15	51,22	57,30	63,37	69,44	75,51	81,58	87,65
40	49,40	55,47	61,55	67,62	73,69	79,76	85,83	91,90

June – 14:00h

V= 0.2 m/s w=12 g/kg	Tmr							
Tair	28	30	32	34	36	38	40	42
26	19,66	25,73	31,80	37,87	43,94	50,01	56,08	62,15
28	23,91	29,98	36,05	42,12	48,19	54,26	60,33	66,40
30	28,16	34,23	40,30	46,37	52,44	58,51	64,58	70,65
32	32,40	38,48	44,55	50,62	56,69	62,76	68,83	74,90
34	36,65	42,73	48,80	54,87	60,94	67,01	73,08	79,15
36	40,90	46,97	53,05	59,12	65,19	71,26	77,33	83,40
38	45,15	51,22	57,30	63,37	69,44	75,51	81,58	87,65
40	49,40	55,47	61,55	67,62	73,69	79,76	85,83	91,90

June – 16:00h

V= 0.2 m/s w=12 g/kg	Tmr							
Tair	28	30	32	34	36	38	40	42
26	19,66	25,73	31,80	37,87	43,94	50,01	56,08	62,15
28	23,91	29,98	36,05	42,12	48,19	54,26	60,33	66,40
30	28,16	34,23	40,30	46,37	52,44	58,51	64,58	70,65
32	32,40	38,48	44,55	50,62	56,69	62,76	68,83	74,90
34	36,65	42,73	48,80	54,87	60,94	67,01	73,08	79,15
36	40,90	46,97	53,05	59,12	65,19	71,26	77,33	83,40
38	45,15	51,22	57,30	63,37	69,44	75,51	81,58	87,65
40	49,40	55,47	61,55	67,62	73,69	79,76	85,83	91,90

June – 18:00h

V= 0.2 m/s w=12 g/kg	Tmr							
Tair	28	30	32	34	36	38	40	42
26	19,66	25,73	31,80	37,87	43,94	50,01	56,08	62,15
28	23,91	29,98	36,05	42,12	48,19	54,26	60,33	66,40
30	28,16	34,23	40,30	46,37	52,44	58,51	64,58	70,65
32	32,40	38,48	44,55	50,62	56,69	62,76	68,83	74,90
34	36,65	42,73	48,80	54,87	60,94	67,01	73,08	79,15
36	40,90	46,97	53,05	59,12	65,19	71,26	77,33	83,40
38	45,15	51,22	57,30	63,37	69,44	75,51	81,58	87,65
40	49,40	55,47	61,55	67,62	73,69	79,76	85,83	91,90

July – 12:00h

V= 0.2 m/s w=12 g/kg	Tmr							
Taire	28	30	32	34	36	38	40	42
26	19.66	25.73	31.80	37.87	43.94	50.01	56.08	62.15
28	23.91	29.98	36.05	42.12	48.19	54.26	60.33	66.40
30	28.16	34.23	40.30	46.37	52.44	58.51	64.58	70.65
32	32.40	38.48	44.55	50.62	56.69	62.76	68.83	74.90
34	36.65	42.73	48.80	54.87	60.94	67.01	73.08	79.15
36	40.90	46.97	53.05	59.12	65.19	71.26	77.33	83.40
38	45.15	51.22	57.30	63.37	69.44	75.51	81.58	87.65
40	49.40	55.47	61.55	67.62	73.69	79.76	85.83	91.90

July – 14:00h

V= 0.2 m/s w=12 g/kg	Tmr							
Taire	28	30	32	34	36	38	40	42
26	19.66	25.73	31.80	37.87	43.94	50.01	56.08	62.15
28	23.91	29.98	36.05	42.12	48.19	54.26	60.33	66.40
30	28.16	34.23	40.30	46.37	52.44	58.51	64.58	70.65
32	32.40	38.48	44.55	50.62	56.69	62.76	68.83	74.90
34	36.65	42.73	48.80	54.87	60.94	67.01	73.08	79.15
36	40.90	46.97	53.05	59.12	65.19	71.26	77.33	83.40
38	45.15	51.22	57.30	63.37	69.44	75.51	81.58	87.65
40	49.40	55.47	61.55	67.62	73.69	79.76	85.83	91.90

July – 16:00h

V= 0.2 m/s w=12 g/kg	Tmr							
Taire	28	30	32	34	36	38	40	42
26	19.66	25.73	31.80	37.87	43.94	50.01	56.08	62.15
28	23.91	29.98	36.05	42.12	48.19	54.26	60.33	66.40
30	28.16	34.23	40.30	46.37	52.44	58.51	64.58	70.65
32	32.40	38.48	44.55	50.62	56.69	62.76	68.83	74.90
34	36.65	42.73	48.80	54.87	60.94	67.01	73.08	79.15
36	40.90	46.97	53.05	59.12	65.19	71.26	77.33	83.40
38	45.15	51.22	57.30	63.37	69.44	75.51	81.58	87.65
40	49.40	55.47	61.55	67.62	73.69	79.76	85.83	91.90

July – 18:00h

V= 0.2 m/s w=12 g/kg	Tmr							
Taire	28	30	32	34	36	38	40	42
26	19.66	25.73	31.80	37.87	43.94	50.01	56.08	62.15
28	23.91	29.98	36.05	42.12	48.19	54.26	60.33	66.40
30	28.16	34.23	40.30	46.37	52.44	58.51	64.58	70.65
32	32.40	38.48	44.55	50.62	56.69	62.76	68.83	74.90
34	36.65	42.73	48.80	54.87	60.94	67.01	73.08	79.15
36	40.90	46.97	53.05	59.12	65.19	71.26	77.33	83.40
38	45.15	51.22	57.30	63.37	69.44	75.51	81.58	87.65
40	49.40	55.47	61.55	67.62	73.69	79.76	85.83	91.90

August – 12:00h

V= 0.2 m/s w=12 g/kg	Tmr							
Taire	28	30	32	34	36	38	40	42
26	19.66	25.73	31.80	37.87	43.94	50.01	56.08	62.15
28	23.91	29.98	36.05	42.12	48.19	54.26	60.33	66.40
30	28.16	34.23	40.30	46.37	52.44	58.51	64.58	70.65
32	32.40	38.48	44.55	50.62	56.69	62.76	68.83	74.90
34	36.65	42.73	48.80	54.87	60.94	67.01	73.08	79.15
36	40.90	46.97	53.05	59.12	65.19	71.26	77.33	83.40
38	45.15	51.22	57.30	63.37	69.44	75.51	81.58	87.65
40	49.40	55.47	61.55	67.62	73.69	79.76	85.83	91.90

August – 14:00h

V= 0.2 m/s w=12 g/kg	Tmr							
Taire	28	30	32	34	36	38	40	42
26	19.66	25.73	31.80	37.87	43.94	50.01	56.08	62.15
28	23.91	29.98	36.05	42.12	48.19	54.26	60.33	66.40
30	28.16	34.23	40.30	46.37	52.44	58.51	64.58	70.65
32	32.40	38.48	44.55	50.62	56.69	62.76	68.83	74.90
34	36.65	42.73	48.80	54.87	60.94	67.01	73.08	79.15
36	40.90	46.97	53.05	59.12	65.19	71.26	77.33	83.40
38	45.15	51.22	57.30	63.37	69.44	75.51	81.58	87.65
40	49.40	55.47	61.55	67.62	73.69	79.76	85.83	91.90

August – 16:00h

V= 0.2 m/s w=12 g/kg	Tmr							
Taire	28	30	32	34	36	38	40	42
26	19.66	25.73	31.80	37.87	43.94	50.01	56.08	62.15
28	23.91	29.98	36.05	42.12	48.19	54.26	60.33	66.40
30	28.16	34.23	40.30	46.37	52.44	58.51	64.58	70.65
32	32.40	38.48	44.55	50.62	56.69	62.76	68.83	74.90
34	36.65	42.73	48.80	54.87	60.94	67.01	73.08	79.15
36	40.90	46.97	53.05	59.12	65.19	71.26	77.33	83.40
38	45.15	51.22	57.30	63.37	69.44	75.51	81.58	87.65
40	49.40	55.47	61.55	67.62	73.69	79.76	85.83	91.90

August – 18:00h

V= 0.2 m/s w=12 g/kg	Tmr							
Taire	28	30	32	34	36	38	40	42
26	19.66	25.73	31.80	37.87	43.94	50.01	56.08	62.15
28	23.91	29.98	36.05	42.12	48.19	54.26	60.33	66.40
30	28.16	34.23	40.30	46.37	52.44	58.51	64.58	70.65
32	32.40	38.48	44.55	50.62	56.69	62.76	68.83	74.90
34	36.65	42.73	48.80	54.87	60.94	67.01	73.08	79.15
36	40.90	46.97	53.05	59.12	65.19	71.26	77.33	83.40
38	45.15	51.22	57.30	63.37	69.44	75.51	81.58	87.65
40	49.40	55.47	61.55	67.62	73.69	79.76	85.83	91.90

September – 12:00h

V= 0.2 m/s w=12 g/kg	Tmr							
Taire	28	30	32	34	36	38	40	42
26	19.66	25.73	31.80	37.87	43.94	50.01	56.08	62.15
28	23.91	29.98	36.05	42.12	48.19	54.26	60.33	66.40
30	28.16	34.23	40.30	46.37	52.44	58.51	64.58	70.65
32	32.40	38.48	44.55	50.62	56.69	62.76	68.83	74.90
34	36.65	42.73	48.80	54.87	60.94	67.01	73.08	79.15
36	40.90	46.97	53.05	59.12	65.19	71.26	77.33	83.40
38	45.15	51.22	57.30	63.37	69.44	75.51	81.58	87.65
40	49.40	55.47	61.55	67.62	73.69	79.76	85.83	91.90

September – 14:00h

V= 0.2 m/s w=12 g/kg	Tmr							
Taire	28	30	32	34	36	38	40	42
26	19.66	25.73	31.80	37.87	43.94	50.01	56.08	62.15
28	23.91	29.98	36.05	42.12	48.19	54.26	60.33	66.40
30	28.16	34.23	40.30	46.37	52.44	58.51	64.58	70.65
32	32.40	38.48	44.55	50.62	56.69	62.76	68.83	74.90
34	36.65	42.73	48.80	54.87	60.94	67.01	73.08	79.15
36	40.90	46.97	53.05	59.12	65.19	71.26	77.33	83.40
38	45.15	51.22	57.30	63.37	69.44	75.51	81.58	87.65
40	49.40	55.47	61.55	67.62	73.69	79.76	85.83	91.90

September – 16:00h

V= 0.2 m/s w=12 g/kg	Tmr							
Taire	28	30	32	34	36	38	40	42
26	19.66	25.73	31.80	37.87	43.94	50.01	56.08	62.15
28	23.91	29.98	36.05	42.12	48.19	54.26	60.33	66.40
30	28.16	34.23	40.30	46.37	52.44	58.51	64.58	70.65
32	32.40	38.48	44.55	50.62	56.69	62.76	68.83	74.90
34	36.65	42.73	48.80	54.87	60.94	67.01	73.08	79.15
36	40.90	46.97	53.05	59.12	65.19	71.26	77.33	83.40
38	45.15	51.22	57.30	63.37	69.44	75.51	81.58	87.65
40	49.40	55.47	61.55	67.62	73.69	79.76	85.83	91.90

September – 18:00h

V= 0.2 m/s w=12 g/kg	Tmr							
Taire	28	30	32	34	36	38	40	42
26	19.66	25.73	31.80	37.87	43.94	50.01	56.08	62.15
28	23.91	29.98	36.05	42.12	48.19	54.26	60.33	66.40
30	28.16	34.23	40.30	46.37	52.44	58.51	64.58	70.65
32	32.40	38.48	44.55	50.62	56.69	62.76	68.83	74.90
34	36.65	42.73	48.80	54.87	60.94	67.01	73.08	79.15
36	40.90	46.97	53.05	59.12	65.19	71.26	77.33	83.40
38	45.15	51.22	57.30	63.37	69.44	75.51	81.58	87.65
40	49.40	55.47	61.55	67.62	73.69	79.76	85.83	91.90

7.2.3.2 Met 2

June – 12:00h

V= 0.2 m/s w=12 g/kg	Tmr							
Tair	28	30	32	34	36	38	40	42
26	58.06	64.13	70.20	76.27	82.34	88.41	94.48	100.55
28	62.47	68.55	74.62	80.69	86.76	92.83	98.90	104.97
30	66.89	72.96	79.03	85.10	91.18	97.25	103.32	109.39
32	71.31	77.38	83.45	89.52	95.59	101.66	107.73	113.81
34	75.73	81.80	87.87	93.94	100.01	106.08	112.15	118.22
36	80.15	86.22	92.29	98.36	104.43	110.50	116.57	122.64
38	84.56	90.63	96.70	102.78	108.85	114.92	120.99	127.06
40	88.98	95.05	101.12	107.19	113.26	119.33	125.41	131.48

June – 14:00h

V= 0.2 m/s w=12 g/kg	Tmr							
Tair	28	30	32	34	36	38	40	42
26	58.06	64.13	70.20	76.27	82.34	88.41	94.48	100.55
28	62.47	68.55	74.62	80.69	86.76	92.83	98.90	104.97
30	66.89	72.96	79.03	85.10	91.18	97.25	103.32	109.39
32	71.31	77.38	83.45	89.52	95.59	101.66	107.73	113.81
34	75.73	81.80	87.87	93.94	100.01	106.08	112.15	118.22
36	80.15	86.22	92.29	98.36	104.43	110.50	116.57	122.64
38	84.56	90.63	96.70	102.78	108.85	114.92	120.99	127.06
40	88.98	95.05	101.12	107.19	113.26	119.33	125.41	131.48

June – 16:00h

V= 0.2 m/s w=12 g/kg	Tmr							
Tair	28	30	32	34	36	38	40	42
26	58.06	64.13	70.20	76.27	82.34	88.41	94.48	100.55
28	62.47	68.55	74.62	80.69	86.76	92.83	98.90	104.97
30	66.89	72.96	79.03	85.10	91.18	97.25	103.32	109.39
32	71.31	77.38	83.45	89.52	95.59	101.66	107.73	113.81
34	75.73	81.80	87.87	93.94	100.01	106.08	112.15	118.22
36	80.15	86.22	92.29	98.36	104.43	110.50	116.57	122.64
38	84.56	90.63	96.70	102.78	108.85	114.92	120.99	127.06
40	88.98	95.05	101.12	107.19	113.26	119.33	125.41	131.48

June – 18:00h

V= 0.2 m/s w=12 g/kg	Tmr							
Tair	28	30	32	34	36	38	40	42
26	58.06	64.13	70.20	76.27	82.34	88.41	94.48	100.55
28	62.47	68.55	74.62	80.69	86.76	92.83	98.90	104.97
30	66.89	72.96	79.03	85.10	91.18	97.25	103.32	109.39
32	71.31	77.38	83.45	89.52	95.59	101.66	107.73	113.81
34	75.73	81.80	87.87	93.94	100.01	106.08	112.15	118.22
36	80.15	86.22	92.29	98.36	104.43	110.50	116.57	122.64
38	84.56	90.63	96.70	102.78	108.85	114.92	120.99	127.06
40	88.98	95.05	101.12	107.19	113.26	119.33	125.41	131.48

July – 12:00h

V= 0.2 m/s w=12 g/kg	Tmr							
Tair	28	30	32	34	36	38	40	42
26	58.06	64.13	70.20	76.27	82.34	88.41	94.48	100.55
28	62.47	68.55	74.62	80.69	86.76	92.83	98.90	104.97
30	66.89	72.96	79.03	85.10	91.18	97.25	103.32	109.39
32	71.31	77.38	83.45	89.52	95.59	101.66	107.73	113.81
34	75.73	81.80	87.87	93.94	100.01	106.08	112.15	118.22
36	80.15	86.22	92.29	98.36	104.43	110.50	116.57	122.64
38	84.56	90.63	96.70	102.78	108.85	114.92	120.99	127.06
40	88.98	95.05	101.12	107.19	113.26	119.33	125.41	131.48

July – 14:00h

V= 0.2 m/s w=12 g/kg	Tmr							
Tair	28	30	32	34	36	38	40	42
26	58.06	64.13	70.20	76.27	82.34	88.41	94.48	100.55
28	62.47	68.55	74.62	80.69	86.76	92.83	98.90	104.97
30	66.89	72.96	79.03	85.10	91.18	97.25	103.32	109.39
32	71.31	77.38	83.45	89.52	95.59	101.66	107.73	113.81
34	75.73	81.80	87.87	93.94	100.01	106.08	112.15	118.22
36	80.15	86.22	92.29	98.36	104.43	110.50	116.57	122.64
38	84.56	90.63	96.70	102.78	108.85	114.92	120.99	127.06
40	88.98	95.05	101.12	107.19	113.26	119.33	125.41	131.48

July – 16:00h

V= 0.2 m/s w=12 g/kg	Tmr							
Tair	28	30	32	34	36	38	40	42
26	58.06	64.13	70.20	76.27	82.34	88.41	94.48	100.55
28	62.47	68.55	74.62	80.69	86.76	92.83	98.90	104.97
30	66.89	72.96	79.03	85.10	91.18	97.25	103.32	109.39
32	71.31	77.38	83.45	89.52	95.59	101.66	107.73	113.81
34	75.73	81.80	87.87	93.94	100.01	106.08	112.15	118.22
36	80.15	86.22	92.29	98.36	104.43	110.50	116.57	122.64
38	84.56	90.63	96.70	102.78	108.85	114.92	120.99	127.06
40	88.98	95.05	101.12	107.19	113.26	119.33	125.41	131.48

July – 18:00h

V= 0.2 m/s w=12 g/kg	Tmr							
Tair	28	30	32	34	36	38	40	42
26	58.06	64.13	70.20	76.27	82.34	88.41	94.48	100.55
28	62.47	68.55	74.62	80.69	86.76	92.83	98.90	104.97
30	66.89	72.96	79.03	85.10	91.18	97.25	103.32	109.39
32	71.31	77.38	83.45	89.52	95.59	101.66	107.73	113.81
34	75.73	81.80	87.87	93.94	100.01	106.08	112.15	118.22
36	80.15	86.22	92.29	98.36	104.43	110.50	116.57	122.64
38	84.56	90.63	96.70	102.78	108.85	114.92	120.99	127.06
40	88.98	95.05	101.12	107.19	113.26	119.33	125.41	131.48

August – 12:00h

V= 0.2 m/s w=12 g/kg	Tmr							
Tair	28	30	32	34	36	38	40	42
26	58.06	64.13	70.20	76.27	82.34	88.41	94.48	100.55
28	62.47	68.55	74.62	80.69	86.76	92.83	98.90	104.97
30	66.89	72.96	79.03	85.10	91.18	97.25	103.32	109.39
32	71.31	77.38	83.45	89.52	95.59	101.66	107.73	113.81
34	75.73	81.80	87.87	93.94	100.01	106.08	112.15	118.22
36	80.15	86.22	92.29	98.36	104.43	110.50	116.57	122.64
38	84.56	90.63	96.70	102.78	108.85	114.92	120.99	127.06
40	88.98	95.05	101.12	107.19	113.26	119.33	125.41	131.48

August – 14:00h

V= 0.2 m/s w=12 g/kg	Tmr							
Tair	28	30	32	34	36	38	40	42
26	58.06	64.13	70.20	76.27	82.34	88.41	94.48	100.55
28	62.47	68.55	74.62	80.69	86.76	92.83	98.90	104.97
30	66.89	72.96	79.03	85.10	91.18	97.25	103.32	109.39
32	71.31	77.38	83.45	89.52	95.59	101.66	107.73	113.81
34	75.73	81.80	87.87	93.94	100.01	106.08	112.15	118.22
36	80.15	86.22	92.29	98.36	104.43	110.50	116.57	122.64
38	84.56	90.63	96.70	102.78	108.85	114.92	120.99	127.06
40	88.98	95.05	101.12	107.19	113.26	119.33	125.41	131.48

August – 16:00h

V= 0.2 m/s w=12 g/kg	Tmr							
Tair	28	30	32	34	36	38	40	42
26	58.06	64.13	70.20	76.27	82.34	88.41	94.48	100.55
28	62.47	68.55	74.62	80.69	86.76	92.83	98.90	104.97
30	66.89	72.96	79.03	85.10	91.18	97.25	103.32	109.39
32	71.31	77.38	83.45	89.52	95.59	101.66	107.73	113.81
34	75.73	81.80	87.87	93.94	100.01	106.08	112.15	118.22
36	80.15	86.22	92.29	98.36	104.43	110.50	116.57	122.64
38	84.56	90.63	96.70	102.78	108.85	114.92	120.99	127.06
40	88.98	95.05	101.12	107.19	113.26	119.33	125.41	131.48

August – 18:00h

V= 0.2 m/s w=12 g/kg	Tmr							
Tair	28	30	32	34	36	38	40	42
26	58.06	64.13	70.20	76.27	82.34	88.41	94.48	100.55
28	62.47	68.55	74.62	80.69	86.76	92.83	98.90	104.97
30	66.89	72.96	79.03	85.10	91.18	97.25	103.32	109.39
32	71.31	77.38	83.45	89.52	95.59	101.66	107.73	113.81
34	75.73	81.80	87.87	93.94	100.01	106.08	112.15	118.22
36	80.15	86.22	92.29	98.36	104.43	110.50	116.57	122.64
38	84.56	90.63	96.70	102.78	108.85	114.92	120.99	127.06
40	88.98	95.05	101.12	107.19	113.26	119.33	125.41	131.48

September – 12:00h

V= 0.2 m/s w=12 g/kg	Tmr							
Tair	28	30	32	34	36	38	40	42
26	58.06	64.13	70.20	76.27	82.34	88.41	94.48	100.55
28	62.47	68.55	74.62	80.69	86.76	92.83	98.90	104.97
30	66.89	72.96	79.03	85.10	91.18	97.25	103.32	109.39
32	71.31	77.38	83.45	89.52	95.59	101.66	107.73	113.81
34	75.73	81.80	87.87	93.94	100.01	106.08	112.15	118.22
36	80.15	86.22	92.29	98.36	104.43	110.50	116.57	122.64
38	84.56	90.63	96.70	102.78	108.85	114.92	120.99	127.06
40	88.98	95.05	101.12	107.19	113.26	119.33	125.41	131.48

September – 14:00h

V= 0.2 m/s w=12 g/kg	Tmr							
Tair	28	30	32	34	36	38	40	42
26	58.06	64.13	70.20	76.27	82.34	88.41	94.48	100.55
28	62.47	68.55	74.62	80.69	86.76	92.83	98.90	104.97
30	66.89	72.96	79.03	85.10	91.18	97.25	103.32	109.39
32	71.31	77.38	83.45	89.52	95.59	101.66	107.73	113.81
34	75.73	81.80	87.87	93.94	100.01	106.08	112.15	118.22
36	80.15	86.22	92.29	98.36	104.43	110.50	116.57	122.64
38	84.56	90.63	96.70	102.78	108.85	114.92	120.99	127.06
40	88.98	95.05	101.12	107.19	113.26	119.33	125.41	131.48

September – 16:00h

V= 0.2 m/s w=12 g/kg	Tmr							
Tair	28	30	32	34	36	38	40	42
26	58.06	64.13	70.20	76.27	82.34	88.41	94.48	100.55
28	62.47	68.55	74.62	80.69	86.76	92.83	98.90	104.97
30	66.89	72.96	79.03	85.10	91.18	97.25	103.32	109.39
32	71.31	77.38	83.45	89.52	95.59	101.66	107.73	113.81
34	75.73	81.80	87.87	93.94	100.01	106.08	112.15	118.22
36	80.15	86.22	92.29	98.36	104.43	110.50	116.57	122.64
38	84.56	90.63	96.70	102.78	108.85	114.92	120.99	127.06
40	88.98	95.05	101.12	107.19	113.26	119.33	125.41	131.48

September – 18:00h

V= 0.2 m/s w=12 g/kg	Tmr							
Tair	28	30	32	34	36	38	40	42
26	58.06	64.13	70.20	76.27	82.34	88.41	94.48	100.55
28	62.47	68.55	74.62	80.69	86.76	92.83	98.90	104.97
30	66.89	72.96	79.03	85.10	91.18	97.25	103.32	109.39
32	71.31	77.38	83.45	89.52	95.59	101.66	107.73	113.81
34	75.73	81.80	87.87	93.94	100.01	106.08	112.15	118.22
36	80.15	86.22	92.29	98.36	104.43	110.50	116.57	122.64
38	84.56	90.63	96.70	102.78	108.85	114.92	120.99	127.06
40	88.98	95.05	101.12	107.19	113.26	119.33	125.41	131.48

7.2.4 Heat load frequency

7.2.4.1 Met 1

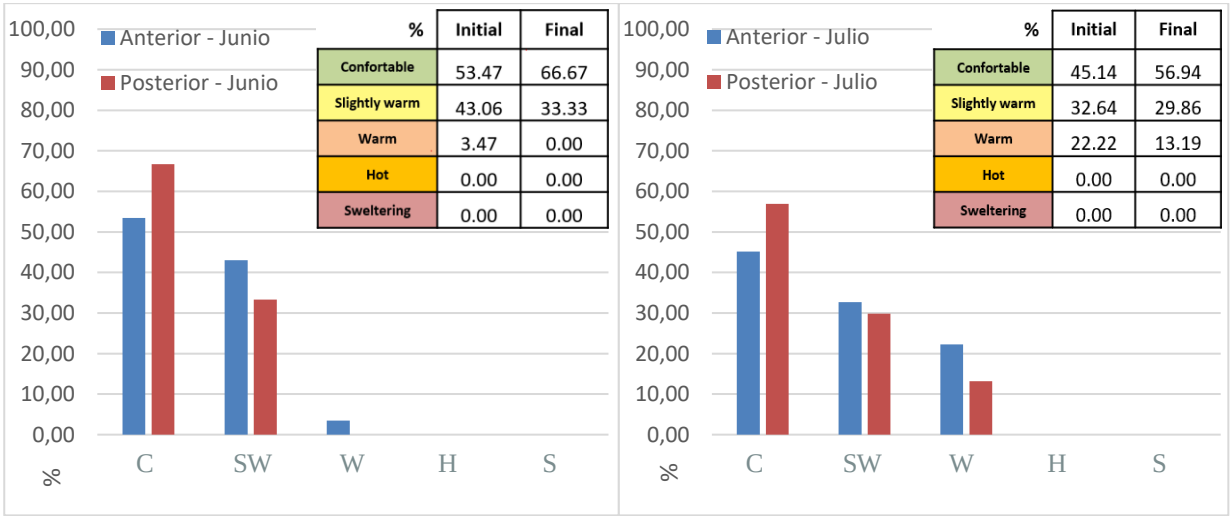

%	Initial	Final
Confortable	53.47	66.67
Slightly warm	43.06	33.33
Warm	3.47	0.00
Hot	0.00	0.00
Sweltering	0.00	0.00

%	Initial	Final
Confortable	45.14	56.94
Slightly warm	32.64	29.86
Warm	22.22	13.19
Hot	0.00	0.00
Sweltering	0.00	0.00

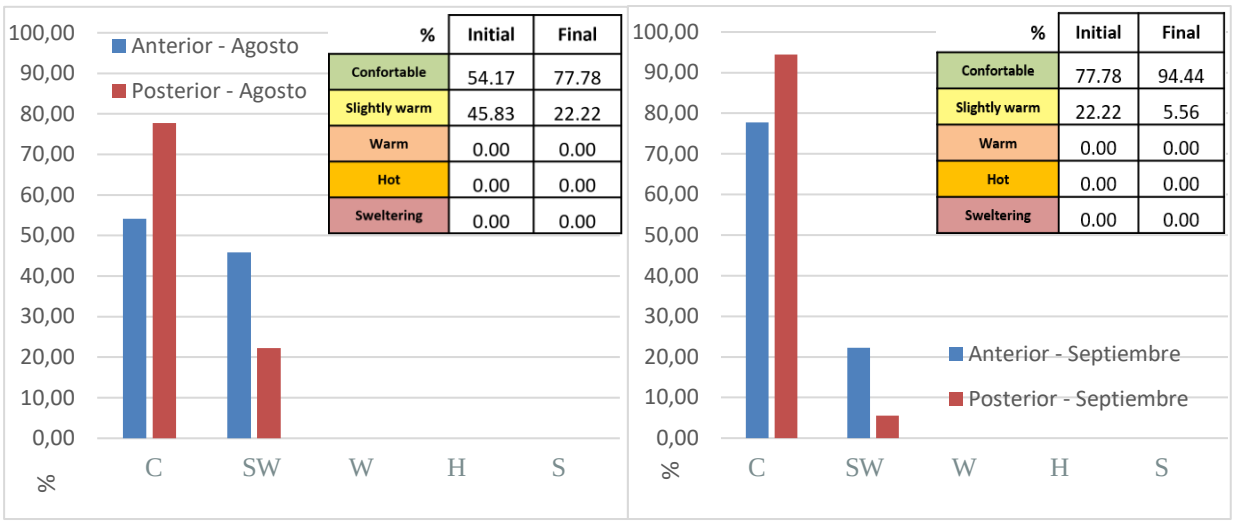
Anterior - Agosto
Posterior - Agosto
% Initial Final
Confortable 54.17 77.78
Slightly warm 45.83 22.22
Warm 0.00 0.00
Hot 0.00 0.00
Sweltering 0.00 0.00
% Initial Final
Confortable 77.78 94.44
Slightly warm 22.22 5.56
Warm 0.00 0.00
Hot 0.00 0.00
Sweltering 0.00 0.00
Anterior - Septiembre
Posterior - Septiembre
100,00 90,00 80,00 70,00 60,00 50,00 40,00 30,00 20,00 10,00 0,00
C SW W H S

7.2.4.2 Met 2

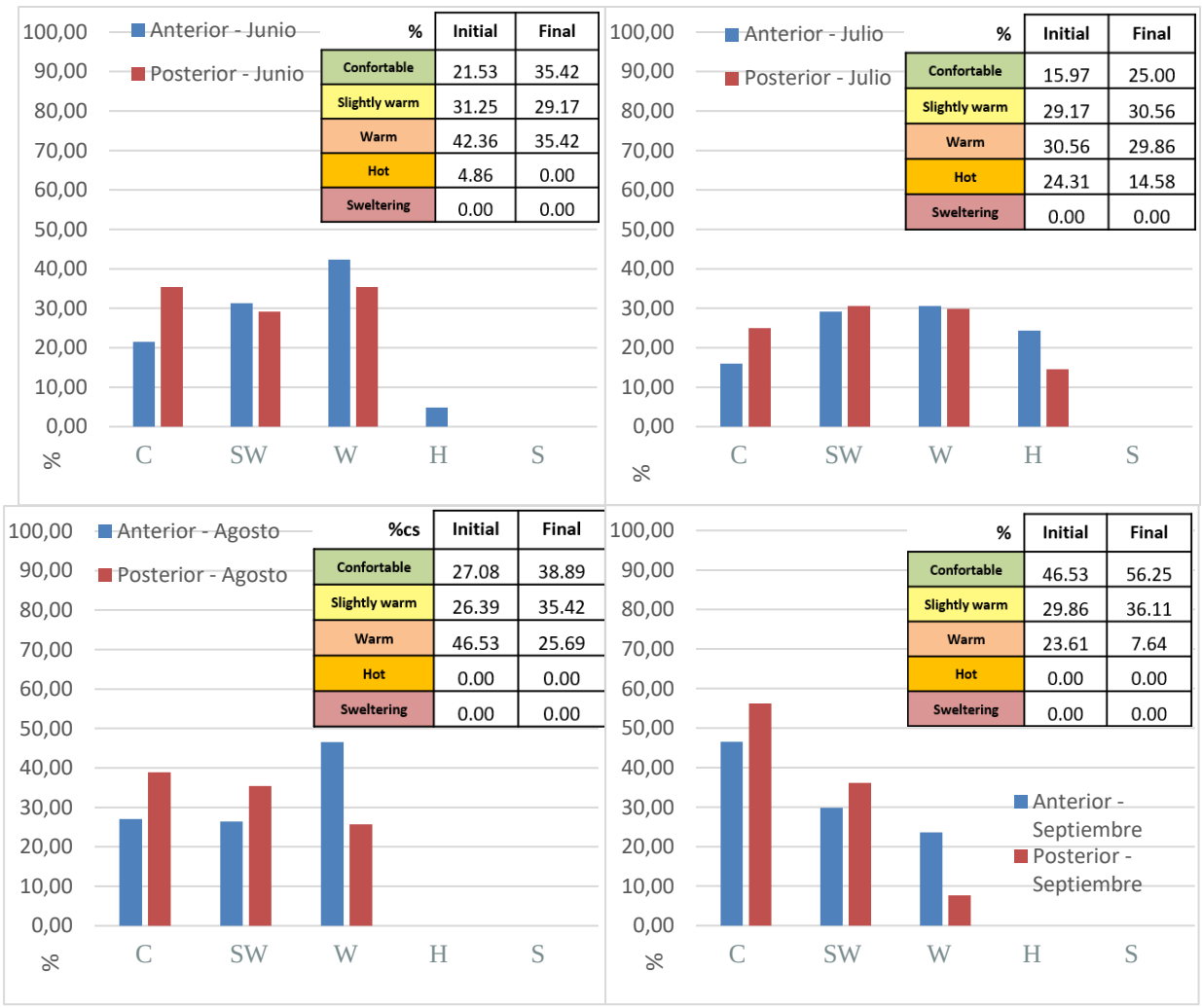
Anterior - Junio
Posterior - Junio
% Initial Final
Confortable 21.53 35.42
Slightly warm 31.25 29.17
Warm 42.36 35.42
Hot 4.86 0.00
Sweltering 0.00 0.00
Anterior - Julio
Posterior - Julio
% Initial Final
Confortable 15.97 25.00
Slightly warm 29.17 30.56
Warm 30.56 29.86
Hot 24.31 14.58
Sweltering 0.00 0.00
Anterior - Agosto
Posterior - Agosto
%cs Initial Final
Confortable 27.08 38.89
Slightly warm 26.39 35.42
Warm 46.53 25.69
Hot 0.00 0.00
Sweltering 0.00 0.00
% Initial Final
Confortable 46.53 56.25
Slightly warm 29.86 36.11
Warm 23.61 7.64
Hot 0.00 0.00
Sweltering 0.00 0.00
Anterior - Septiembre
Posterior - Septiembre
100,00 90,00 80,00 70,00 60,00 50,00 40,00 30,00 20,00 10,00 0,00
C SW W H S

7.2.5 Superficial temperature of the pavement

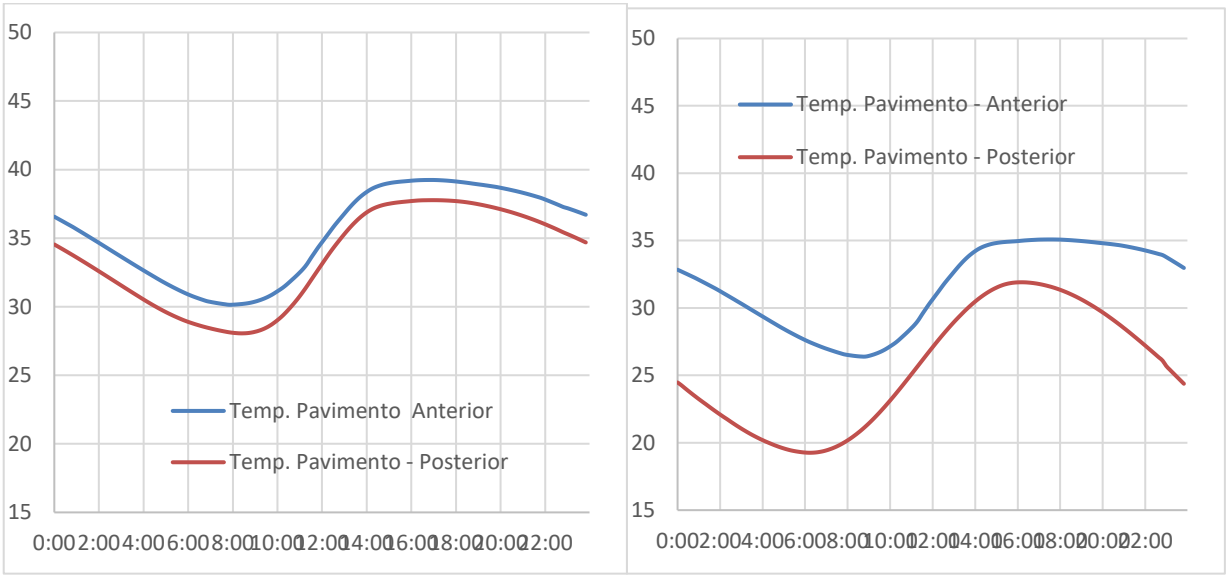

Superficial temperature evolution of the pavement (°C)

7.2.6 Radiations absorbed

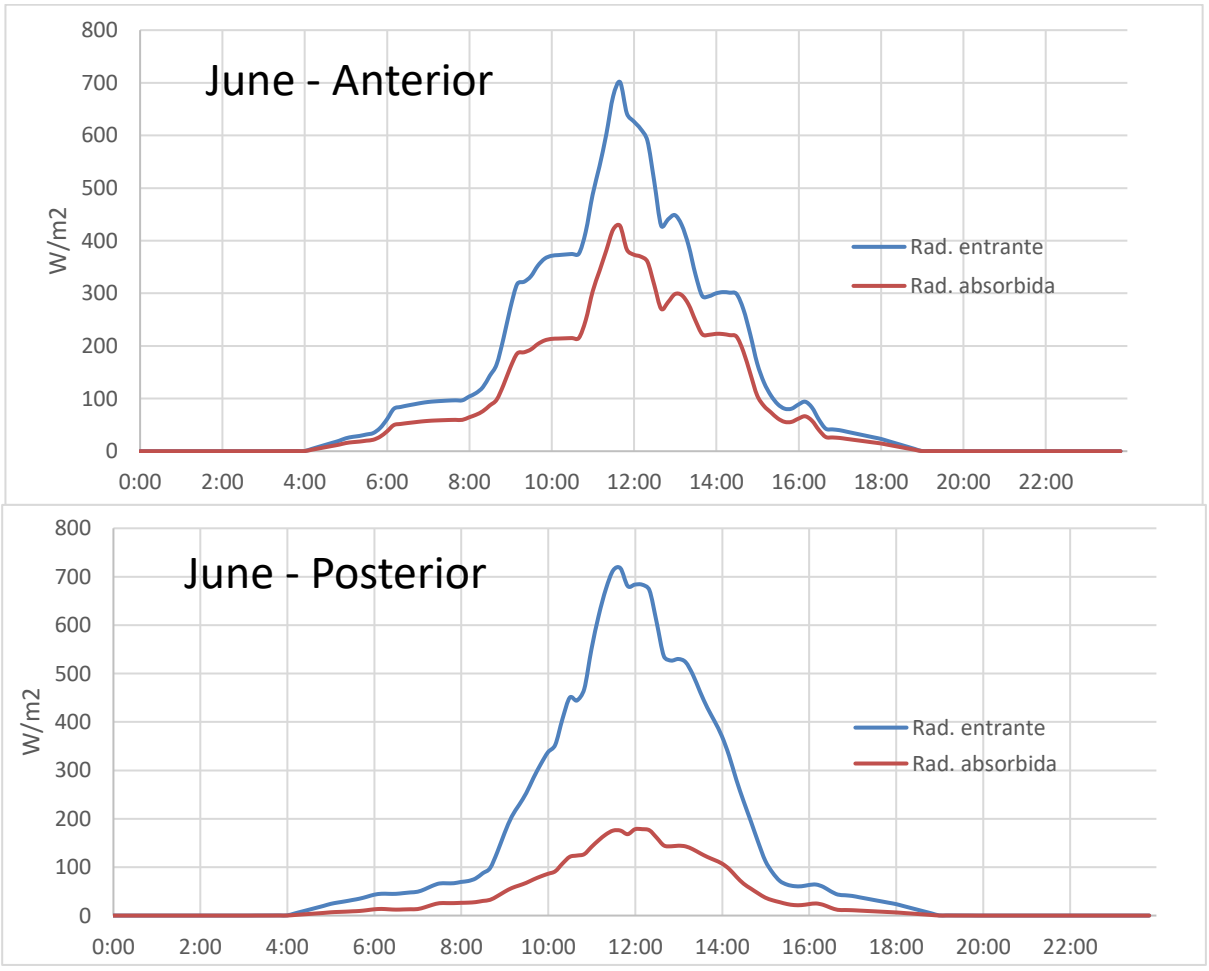

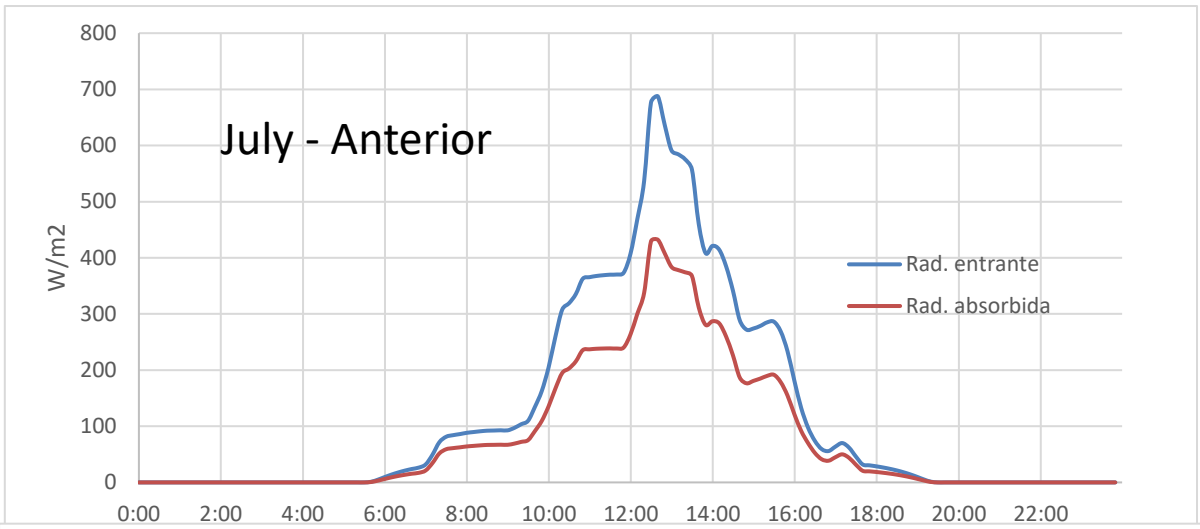
July - Anterior
W/m2
800
700
600
500
400
300
200
100
0
0:00
2:00
4:00
6:00
8:00
10:00
12:00
14:00
16:00
18:00
20:00
22:00
Rad. entrante
Rad. absorbida

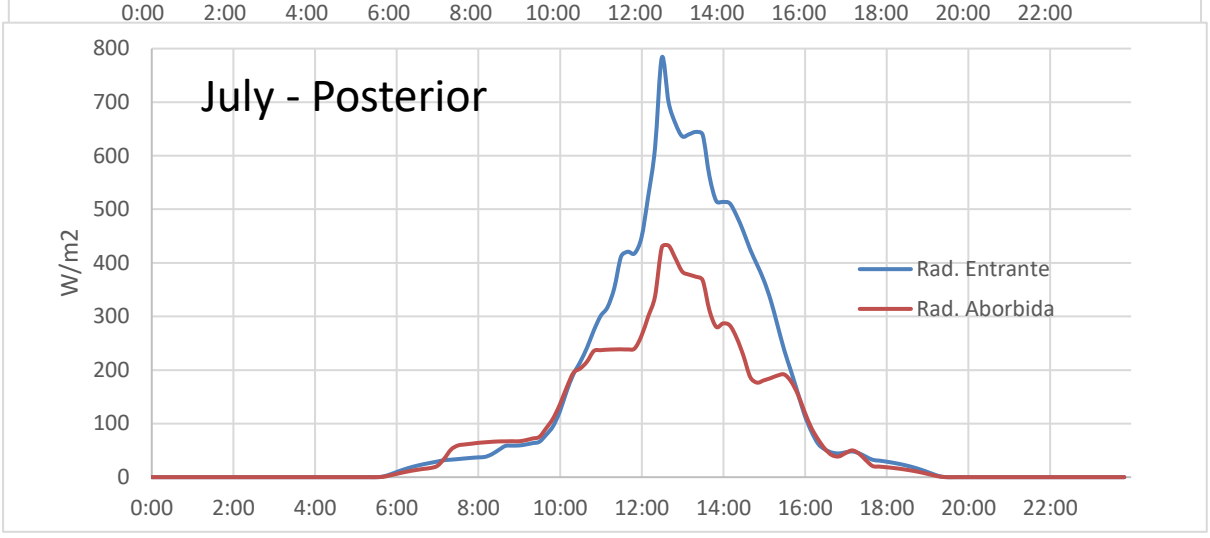
July - Posterior
W/m2
800
700
600
500
400
300
200
100
0
0:00
2:00
4:00
6:00
8:00
10:00
12:00
14:00
16:00
18:00
20:00
22:00
Rad. Entrante
Rad. Aborbida

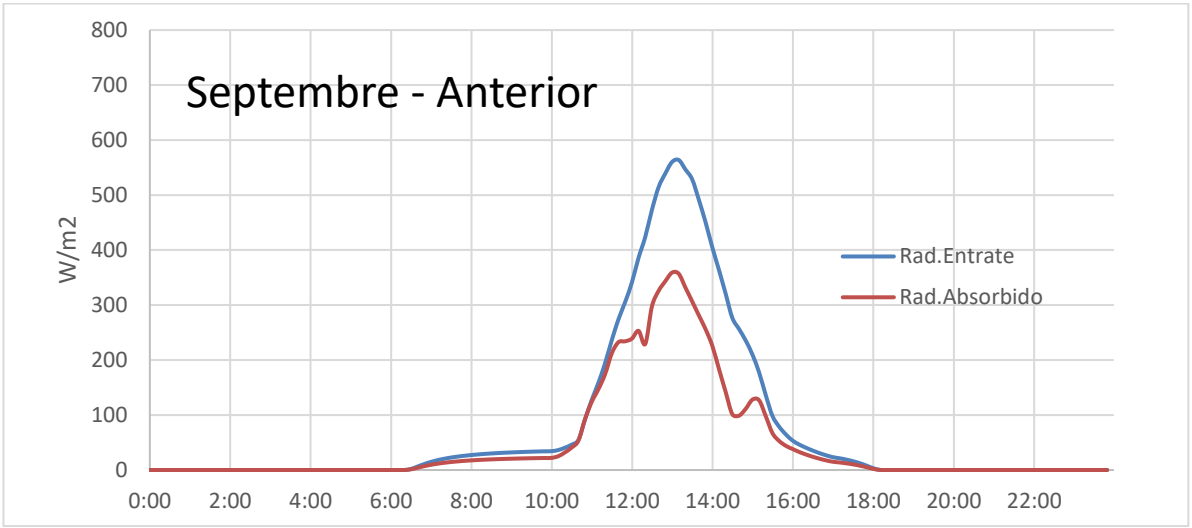
Septembre - Anterior
W/m2
800
700
600
500
400
300
200
100
0
0:00
2:00
4:00
6:00
8:00
10:00
12:00
14:00
16:00
18:00
20:00
22:00
Rad.Entrate
Rad.Absorbido

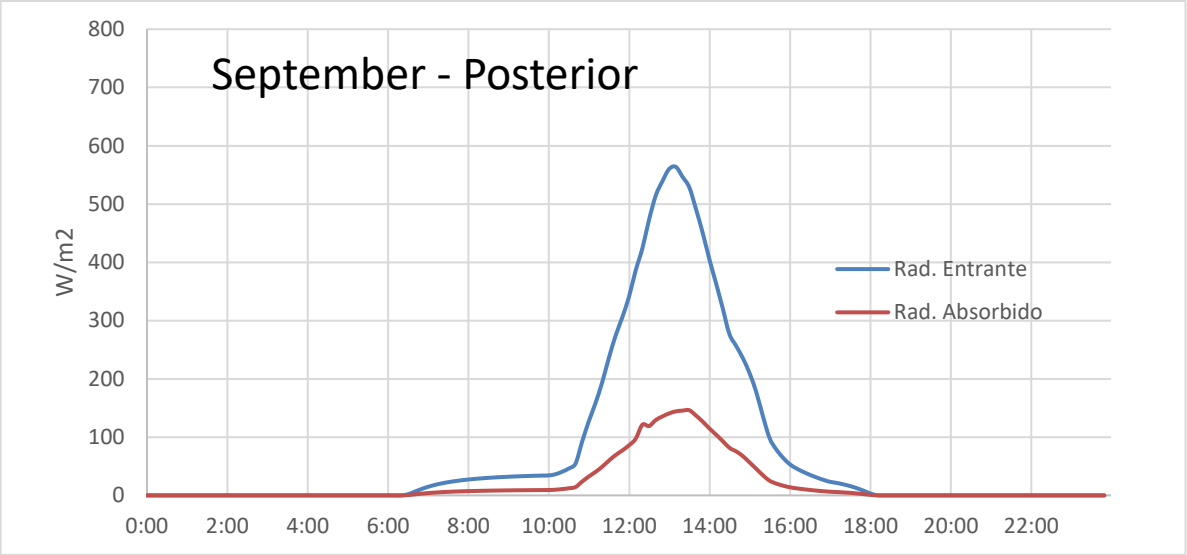

Evolution of radiations absorbed (W/m²)

10 BIBLIOGRAPHY

[1] National Public Radio (NPR). Rachel Treisman. Heat waves in Europe killed more than 61,600 people last summer, a study estimates. (July 12, 2023). Last accessed 17/07/2023. https://www.npr.org/2023/07/12/1187068731/heat-waves-europe-deaths-study

[2] Yee Yong Lee, Mohd Fadhil Md Din, Mohanadoss Ponraj, Zainura Zainon Noor, Kenzo Iwao, Shreeshivadasan Chelliapan. Overview of urban heat island (UHI) phenomenon towards human thermal comfort. In Environmental Engineering and Management Journal. (2017)

[3] Global climate and weather data. Wordclim. Last accessed 08/07/2023. https://www.worldclim.org/data/index.html

[4] Grupo de Termotecnia, Departamento de Ingeniería Energética. Paula Zbikowski Silveira. (2021). Confort térmico en espacios abiertos: modelado y leyes. University of Seville.

[5] ASHRAE (American Society of Heating and Refrigeration Engineers) Fundamentals (SI Edition) Chapter 9. Thermal Comfort. (2017). In *ASHRAE Handbook* (SI Units ed., pp. 180-212).

[6] Brown, R. D., & Gillespie, T. J. (1986). Estimating outdoor thermal comfort using a cylindrical radiation thermometer and an energy budget model. International Journal of Biometeorology, 30(1), p43-52.

[7] Urban Climates, 2017. Oke, T.R., Mills, G., Christen, A., & Voogt, J.A. Cambridge University

[8] Mayer, H. and Höppe, P.: Thermal Comfort of Man in Different Urban Environments, Theor. Appl. Climatol., 38, 43–49, (1987)

[9] J. Pickup, R. de Dear, An outdoor thermal confort index (OUT_SET*) – part 1- the model and its assumptions. In: Biometeorology and urban climatology at the turn of the millennium. De Dear, Kalma, Oke and Auliciems (Eds.) World Meteorological Organization.

[10] Tanabe, S. et al. (1993). Estimation of thermal sensation using PMV and SET* under high air movement conditions. J. Therm. Biol. 18(5/6): 551-554.

[11] International Organization for Standardization UNE-EN ISO 7933. Ergonomía del ambiente térmico: Determinación analítica e interpretación del estrés térmico mediante el cálculo de la sobrecarga térmica estimada. (2005)

[12] A. Sato. N. Ito. Research on the wind variation in the urban area and its effects in environmental engineering.

[13] Conference proceeding by ASHRAE. N. Ito. A field experiment study on the convective heat transfer coefficient on exterior surface of a building. (1972)

[14] Grupo de Termotecnia, Departamento de Ingeniería Energética y Mecánica de Fluidos. Guerra Macho, J.J., Álvarez Domínguez, S., Molina Félix, J.L., & Velázquez Vila, R. (1994). *GUÍA BÁSICA PARA EL ACONDICIONAMIENTO CLIMÁTICO DE ESPACIOS ABIERTOS* (1.a ed.). University of Seville.

[15] Grupo de Termotecnia, Departamento de Ingeniería Energética. Teresa Rocío Palomo Amores. (2020). Protocolo de evaluación del impacto de la iluminación natural para gestión energética. University of Seville.